CYR61 PROTECTS PHOTORECEPTORS IN THE RD1 MOUSE MODEL OF RETINITIS PIGMENTOSA THROUGH ACTIVATION OF RETINAL MÜLLER GLIA AND PIGMENT EPITHELIUM CELLS

Dissertation

der Mathematisch-Naturwissenschaftlichen Fakultät

der Eberhard Karls Universität Tübingen

zur Erlangung des Grades eines

Doktors der Naturwissenschaften

(Dr. rer. nat.)

vorgelegt von

Joanna Magdalena Kucharska

aus Warschau, Polen

Tübingen

2014

Tag der mündlichen Qualifikation:	28.01.2015
Dekan:	Prof. Dr. Wolfgang Rosenstiel
1. Berichterstatter:	Prof. Dr. Robert Feil
2. Berichterstatter:	Prof. Dr. Marius Ueffing

Niniejszą pracę dedykuję moim Rodzicom

I dedicate this work to my Parents

Table of Contents

Abbreviations

α-SMA - alpha smooth muscle actin
AAV - adeno-associated virus
ABC - ammoniumbicarbonat
ACN - acetonitrile
AIF - apoptosis inducing factor
AMD - age-related macula degeneration
ANG - angiogenin
APS - ammonium persulfate
AR - amphiregulin
BCA - bicinchoninic acid
BDNF - brain-derived neurotrophic factor
BNGF - beta-nerve growth factor
BP – beam pass
cAMP - cyclic adenosine monophosphate
cDNA - complementary DNA
cGMP - cyclic guanosine monophosphate
CCL2/JE - chemokine (C-C motif) receptor 2
CD105 - endoglin
CFH - complement factor H
CHAD - chondroadherin
CID - collision induced dissociation
CNTF - ciliary neurotrophic factor
COL3A1 - collagen type III, alpha I
CRALBP - cellular retinaldehyde binding protein
CREB-1 - cAMP responsive element binding protein 1
CRG-2 - chemokine (C-X-C motif) ligand 10
cSLO - confocal scanning laser ophthalmoscopy
Cp - crossing point
CT - carboxyl-terminal
CX3CL1 - fractalkine
CXCL10 – chemokine (C-X-C motif) ligand 10
Cyr61 - cysteine rich protein 61
CYTM - cystatin E/M
DAPI - 4',6-diamidino-2-phenylindole
DIV – days in vitro
DMEM - Dulbecco's Modified Eagle's Medium
DPBS - dulbecco`s phosphate buffered saline
dT - deoxy-thymine nucleotides
eGFP - enhanced GFP
EDTA - ethylenediaminetetraacetic acid
EGF-R - epidermal growth factor receptor
ER - endoplasmic reticulum
ERG - electroretinography
ERKs - extracellular signal-regulated kinases
ET-1 - endothelin-1
FAM3C - family with sequence similarity 3
FASP - filter aided sample preparation

FBS - fetal bovine serum
FCS - fetal calf serum
FGF-1 – fibroblast growth factor 1
FGF-2 - fibroblast growth factor 2
GAP - GTPase- activating proteins
GAPDH - glyceraldehyde 3-phosphate dehydrogenase
GC – ganglion cells
GCAPs - guanylate-cyclase-activating proteins
GCL – ganglion cell layer
GDNF - glial cell-derived neurotrophic factor
GDP -
GFAP - glial fibrillary acidic protein
GFRα1 - GDNF receptor α-1
GM-CSF - granulocyte–macrophage colony-stimulating factor
GS - glutamine synthetase
GTP -
HB-EGF - heparin-binding EGF-like
HPLC - high-performance liquid chromatography
HSPG - heparin sulfate proteoglycans
ICC - immunocytochemistry
IGF-1 - insulin-like growth factor-1
IGFBP-1 - insulin-like growth factor-binding protein 1
IGFBP-2 - insulin-like growth factor-binding protein 2
IGFBP-3 - insulin-like growth factor-binding protein 3
IGFBP-5 - insulin-like growth factor-binding protein 5
IHC - immunohistochemistry
IL-6 - interleukin-6
IL-8 - interleukin-8
IL-1β – interleukin-1β
INL – inner nuclear layer
IP-10 – chemokine (C-X-C motif) ligand 10
IPL – inner plexiform layer
IR - infrared reflectance
IS – inner segment
JAK - janus kinase
LC-MS/MS - liquid chromatography – tandem mass spectrometry
LEDGF - lens epithelium-derived growth factor
LIF - leukemia inhibitory factor
M cells – magni, large cells
MAPK - mitogen-activated protein kinase
MATN4 – matrilin 4
MCP-1 - chemokine (C-C motif) receptor 2
MitoQ - antioxidant MSO10
MMP-3 - matrix metallopeptidase 3
MMP-8 - matrix metallopeptidase 8
mRMG – mouse retinal Müller glial cells
mRNA - messenger RNA
OB - leptin
ONL – outer nuclear layer
OPL - outer plexiform layer

OS – outer segment
P – parvi, small cells
PAR - poly ADP-ribose
PARP - poly ADP-ribose polymerase
PB - phosphate buffer
PBS - phosphate-buffered saline
PDE6 - phosphodiesterase
PDGF - platelet-derived growth factor
PDGF-AA - platelet-derived growth factor alpha polypeptide
PDGF-AB - platelet-derived growth factor beta polypeptide
PEDF - pigment epithelium-derived factor
PFA - paraformaldehyde
PGF-2 - placental growth factor 2
PI - propidium iodide
PI3K - phosphoinositide 3-kinase
PKG - cGMP-dependent protein kinase
PN – postnatal day
PR – photoreceptors
PVDF - polyvinylidene fluorie
qPCR - quantitative Polymerase chain reaction
RCS - Royal College of Surgeons
RdCVF - rod-derived cone viability factor
RF - reflectance imaging
RIPA - radioimmunoprecipitation assay buffer
RLBP1 - retinaldehyde binding protein 1
RMG – retinal Müller glial cells
RP – retinitis pigmentosa
RPE - retinal pigment epithelium
RPGR - retinitis pigmentosa GTPase regulator
RT – room temperature
RT-PCR - reverse transcriptase- polymerase chain reaction
SDS - sodium dodecyl sulphate
SDS-PAGE - SDS-polyacrylamide
SEM - standard error of measurements
streptavidin-HRP - horseradish peroxidase labelled streptavidin
TBS - Tris-buffered saline
TBST - Tris-buffered saline Tween
TEMED - tetramethylethylenediamine
TF – tissue factor
TFA - trifluoroacetic acid
TGF-β - transforming growth factor-β
TIMP1 - tissue inhibitor of matrix metalloprotease 1
TNF-α - tumor necrosis factor α
TSR - trombospondin type I repeat
TUNEL - terminal deoxynucleotidyl transferase dUTP nick end-labeling
UA - urea
VEGF - vascular endothelial growth factor
VEGF-R1 - VEGF receptor 1
VEGF-R2 - VEGF receptor 2
vWC - von Willebrand factor type C

Summary

The term retinitis pigmentosa (RP) describes a group of retinal degenerations, in which inherited mutations lead to disturbed physiological functions of photoreceptors (PR) or retinal pigment epithelium (RPE) cells and progressive visual loss. Although gene therapy of RP can prevent loss of vision, the high heterogeneity of gene mutations restricts one gene therapy only to a subset of patients. In contrast, trophic factor delivery cannot be curative for RP, but protects PR irrespective of the underlying gene defect, leading to a significant delay in PR death and temporally maintaining residual vision. In experiments on rodent models of RP, subretinally injected glial cell line-derived neurotrophic factor (GDNF) significantly preserved morphology and function of rod cells. This neuroprotective effect is postulated to be indirect through retinal Müller glial (RMG) cells, which release a variety of factors upon GDNF stimulation. These factors in turn bind to receptors on the PR membrane to stimulate signal transduction pathways, which are crucial for their survival.

Encouraged by very promising results of GDNF's indirect prosurvival action in many studies of rodent retina, we focused on the investigation of the neuroprotective potential of RMG cells. To achieve this aim, primary mouse RMG cells were stimulated with GDNF and seven secreted factors were found to be highly upregulated. Out of this group, cysteine-rich heparin-binding protein 61 (Cyr61), a molecule with proved prosurvival activity in the context of cancer cells, was chosen for further investigation. As anticipated, Cy61 did indeed increase PR survival in *ex vivo* experiments on short-term and long-term rd1 mouse retinal explants, , confirming its neuroprotective activity.

Subsequently, we focused on the mechanism of Cyr61's prosurvival action on PR. Stimulation of the whole retinal tissue revealed activation of mitogen-activated protein kinase (MAPK)/Erk and janus kinase (JAK)/Stat pathways, but not phosphoinositide 3-kinase (PI3K)/Akt. Furthermore, analysis of very pure PR cultures treated with Cyr61 showed no activation of any of mentioned pathways, suggesting lack of a direct prosurvival effect of Cyr61. In contrast, stimulations of primary porcine RMG cells showed an increase in phosphorylation of all investigated proteins: Erk1/2, Stat3 and Akt. These results uncovered a positive feedback loop of Cyr61 action on RMG, implying at the same time an indirect mechanism for Cyr61 mediated neuroprotection. Investigation of Cyr61 treatment of primary porcine RPE cells demonstrated a very strong activation of MAPK/Erk and PI3K/Akt but not JAK/Stat3, suggesting indirect protection of PR also through RPE cells stimulation. Treatments of the human RMG and RPE cell lines MIO-M1 and ARPE19 with Cyr61 additionally revealed nuclear translocation of activated MAPK/Erk.

To determine the consequences of MAPK/Erk, JAK/Stat and PI3K/Akt pathways stimulation in RMG cells, we focused on Cyr61 induced secretome changes. Secretome

analysis using LC-MS/MS based quantitative proteomics showed an increase in the secretion of several proteins involved in extracellular matrix organization. The upregulation of two of these proteins - collagen, type III alpha 1 (COL3A1) and family with sequence similarity 3, member C (FAM3C), at the transcriptional level was confirmed by qPCR.

Finally, we investigated whether Cyr61 could protect PR *in vivo* in an RP rodent model. To this end we used the S334ter-3 rat model. Preliminary data form intravitreal injections of Cyr61 showed substantial changes in vascularization of the retina and lack of neuroprotective action on PR. Furthermore, Cyr61 significantly increased the percentage of TUNEL positive cells in the inner nuclear layer (INL). It remains to be determined whether alterations in the retinal vasculature may be a factor, which diminishes the neuroprotective potential of Cyr61

Taken together, the presented results introduce Cyr61 as a novel neuroprotective agent prolonging PR survival in an indirect way through stimulation of RMG and RPE cells. Further investigations may confirm Cyr61's neuroprotective effect *in vivo* and describe molecular basis of its indirect action in more detail.

Zusammenfassung

Eine bestimmte Gruppe von erblichen Retinadegenerationen wird unter dem Begriff retinitis pigmentosa (RP) zusammengefasst. Dieser Gruppe ist gemein dass die unterschiedlichen Mutationen letztlich zu einer Störung der physiologischen Funktionen der Photorezeptoren (PR) oder retinalen Pigmentepithelzellen (RPE) führen und damit einem fortschreitenden Verlust des Sehvermögens verursachen. Obwohl dieser Verlust durch Gentherapie verhindert werden kann, beschränkt die große Heterogenität der Genmutationen einen Gentherapieansatz auf nur eine Untergruppe der Patienten. Im Gegensatz dazu kann die Behandlung mit einem trophischen Faktor unabhängig vom jeweiligen Gendefekt für die symptomatische Behandlung eingesetzt werden. Durch diesen Ansatz kann das Absterben der PR verlangsamt und das verbliebene Sehvermögen länger erhalten werden.

Verschiedene Studien in Nagermodellen von RP haben bisher gezeigt, dass subretinale Injektion des neurotrophen Faktors glial cell line-derived neurotrophic factor (GDNF) die Morphologie und Funktion der PR erhält. Es wird postuliert daß dieser neuroprotektive Effekt indirekt durch eine Stimulation der retinalen Müller Gliazellen (RMG) bewirkt wird, welche nach GDNF Stimulation verschiedene andere neurotrophe Faktoren sekretieren. Diese Faktoren scheinen das Überleben der PR durch Aktivierung mehrerer Signaltransduktionswege zu fördern.

In Anbetracht der Wirksamkeit von GDNF, wurde in dieser Arbeit das neuroprotektive Potential von RMG untersucht. Zu diesem Zweck wurden primäre murine RMG mit GDNF stimuliert und es wurden sieben stark GDNF induzierte Faktoren identifiziert, von denen Cysteine-rich heparin-binding protein 61 (Cyr61) zur weiteren Untersuchung ausgewählt wurde, da für dieses Molekül bereits eine überlebensfördernde Wirkung aus der Krebsforschung bekannt war.

Eine neuroprotektive Aktivität von Cyr61 ließ sich tatsächlich nachweisen, da Cyr61 in *ex vivo* Retinaexplantaten von rd1 Mäusen das Überleben der PR verlängern konnte. Daher wurde das Wirkungsspektrum von Cyr61 in der Retina auf Zelltyp- und Singaltransduktionsebene untersucht um den molekularen Mechanismus des neuroprotektiven Effektes genauer zu charakterisieren. Stimulation der intakten Retina zeigte Aktivierung der mitogen-activated protein kinase (MAPK)/Erk und janus kinase (JAK)/Stat Transduktionswege, allerdings keine Stimulation des phosphoinositide 3-kinase (PI3K)/Akt Weges.

Allerdings zeigte die Analyse von hochreinen PR Kulturen, dass Cyr61 keinen der obigen Transduktionswege in diesen Zellen aktivierte, was gegen einen direkten Einfluss von Cyr61 auf die PR sprach. Im Gegensatz dazu reagierten primäre Schweine-RMG auf Cyr61 Stimulation mit einer Aktivierung aller drei Transduktionwege - Erk1/2, Stat3 und Akt. Diese Ergebnisse zeigen einen positiven Rückkopplungsmechanismus von Cyr61

auf RMG und implizieren gleichzeitig einen indirekten Mechanismus des neuroprotektiven Effekts von Cyr61.

Die Untersuchung des Einflusses von Cyr61 auf RPE zeigte außerdem eine sehr starke Aktivierung der MAPK/Erk und PI3K/Akt Signalwege, allerdings keine Aktivierung des JAK/Stat3 Weges. Daher ist ein indirekter Mechanismus des neuroprotektiven Effekts über RPE ebenfalls plausibel. Weiterhin konnte gezeigt werden dass Behandlung der humanen RMG und RPE Zelllinien MIO-M1 und ARPE19 mit Cyr61 zur Aktivierung und nukleären Translokation von Erk und Akt führte.

Um die weiteren Folgen der Aktivierung der MARK/Erk, JAK/Stat und PI3K/Akt Transduktionswege in RMG zu bestimmen, wurden Cyr61 induzierte Änderungen im Sekretom dieser Zellen mittels LC-MS/MS basierter Proteomik untersucht Dies zeigte Sekretionsinduktion mehrerer Proteine die in der Organisation der Extrazellulären Matrix involviert sind. Diese Induktion wurde für zwei Proteine – Kollagen Typ III alpha 1 (COL3A1) und family with sequence similarity 3, member C (FAM3C) auch auf der transkriptionellen Ebene mittels qPCR bestätigt.

Schließlich wurde das therapeutische Potential von Cyr61 in dem Ratten RP Model S334ter-3 untersucht. Vorläufige Daten zeigten allerdings keinen neuroprotektiven Effekt nach intravitrealer Injektion von Cyr61. Paradoxerweise erhöhte Cyr61 Behandlung den Anteil TUNEL positiver Zellen in der inneren nukleären Schicht der Retina. Ungeklärt bleibt, ob Änderungen in der Vaskularisierung der Retina, die zusätzlich beobachtet wurde, dieses Ergebnis verursacht haben könnten.

Insgesamt charakterisieren die Ergebnisse dieser Arbeit Cyr61 als einen neuen neuroprotektiven Faktor der das Überleben von PR durch einen indirekten Mechanismus über Aktivierung von RMG und RPE verlängern kann. Weitere Erforschung des neuroprotektiven Effekts von Cyr61 wird die Frage seiner Wirksamkeit *in vivo* klären und dessen molekulare Grundlage tiefergreifend aufklären.

I. INTRODUCTION

Chapter One: The human retina and its physiology

The visual perception is a fascinating sense giving us important information from the surrounding environment. Light that enters the cornea is focused by the lens and passes through the vitreous body to fall on the receptive tissue of the vision sense – the retina. Here, neuronal cells collect the light photons and pass the registered signal through optic nerve to the higher centres of the brain where it is further processed to eventually create an image of the surrounding scene. Retinal degenerations, attributable to genetic disturbances, may lead to the preliminary death of neuronal or supporting cells causing vision disorders leading even to total blindness.

The introduction is divided into three parts. Chapter one describes retinal histological structure (1.1) with focus on the role of individual cell types - photoreceptors (PR, 1.1.1), retinal ganglion cells (GC, 1.1.2), retinal Müller glial (RMG, 1.1.3) cells and retinal pigment epithelium (RPE, 1.1.4) cells - in the process of vision. These types of cells will be the main focus of the research presented in this thesis. In addition, the development of a healthy retinal vasculature will be described, as some results are better appreciated with knowledge of the subtle structure of the retinal blood supply (1.2).

1.1 Structure of the retina

The retina is located at the back of an eye to process the image projected by the lens into electrical impulses and send them further to the visual cortex to create an image in our brain. Five types of neuronal cells are involved in this process: PRs detect signals from photons and pass them to horizontal and bipolar cells through synaptic connections. Horizontal cells probably feed the signal back to PR (to inhibit them) or pass the stimulation to bipolar cells. Bipolar cells send the signal to GC, in a direct way, or indirectly, through amacrine cells. Ganglion cells then further process the signals and send them to the brain through the optic nerve.

The neuronal cells and RMG cells are anatomically organised into layers creating the retinal tissue (Fig. 1). The innermost layer is composed of GC and is followed by the inner plexiform layer (IPL) created from GC axons together with axons of amacrine and bipolar cells. The following inner nuclear layer (INL) consists of nuclei of neuronal cells: bipolar, amacrine and horizontal cells together with nuclei of RMG cells. The penultimate outer plexiform layer (OPL) is easy to distinguish histologically as it contains the processes of bipolar, horizontal and PR cells. The final, outermost, layer is composed of PR cells, whose nuclei are densely organized creating the outer nuclear layer (ONL). The sensory part of the retina is embedded in the retinal pigment epithelium, whose RPE cells

contact the PR on their apical side and are firmly attach to choroid layer of the eye through their basal side (Wright *et al.* 2010).

Besides neuronal cells the human retina consists of three types of glial cells: RMG cells (described in 1.1.3), microglial cells and astrocytes. Microglial cells are immune cells, derived from blood and responsible for the initiation of inflammatory processes as well as defence against invading pathogens. Microglia activation in the retina can also be closely related to PR cell death and retinal degeneration (Karlstetter *et al.* 2010). Astrocytes influence the development of the superficial and deep layers of retinal vasculature by secretion of vascular endothelial growth factor (VEGF). Moreover, they accompany as well as stabilize the developing blood vessels, becoming a part of the blood-retinal barrier, and regulate blood flow within the retinal tissue (Gardner *et al.* 1997, Kur *et al.* 2012).

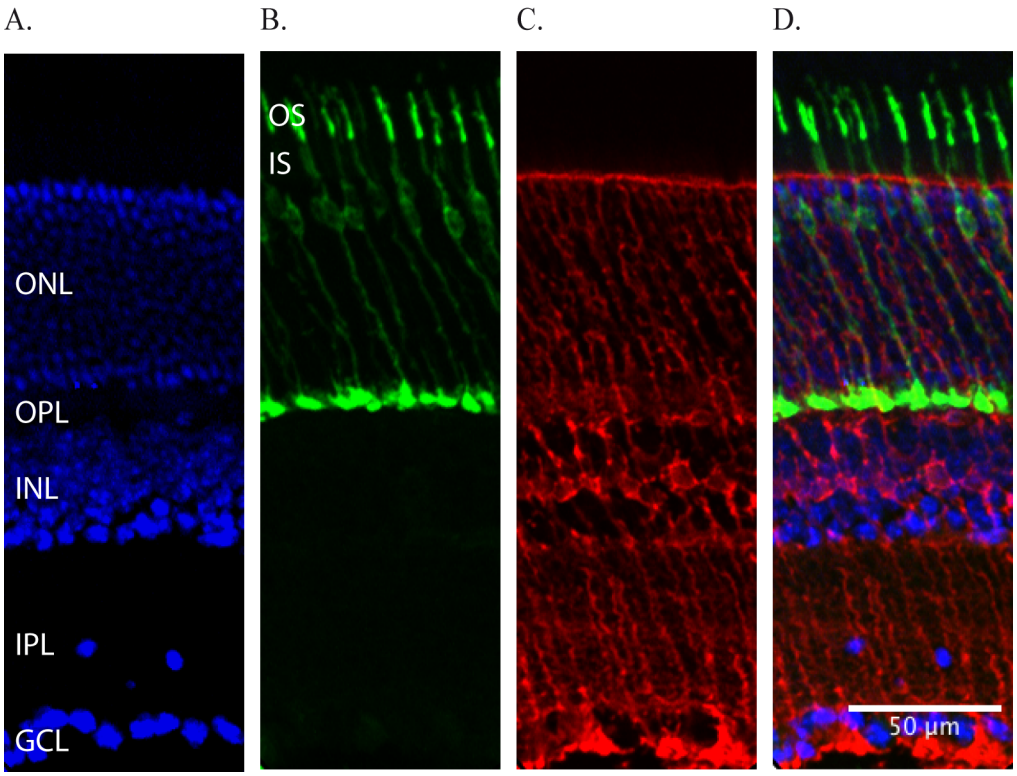

Figure 1. Histological structure of porcine retina.
Retinal tissue consists of five different layers: ganglion cell layer (GCL), inner plexiform layer (IPL), inner nuclear layer (INL), outer plexiform layer (OPL) and outer nuclear layer (ONL). Blue – DAPI for nuclei, green - arrestin for cones, red – glutamine synthetase for RMG, inner segments (IS), outer segments (OS).

1.1.1 Photoreceptors

Photoreceptors are located in the outermost layer of the retinal tissue, in the longest distance from the lens, right before RPE cells. This requires the light to travel through all other retinal layers before reaching the PR outer segments. To facilitate the light to reach the PR without being highly scattered, the axons of neuronal cells in the plexiform layers of the retina are unmyelinated, making these layers relatively transparent (Kandel *et al.*

2000). Additionally, RMG possess features of optical fibres, allowing light to be transmitted to PR with only minimal loss (Franze *et al.* 2007).

Photoreceptors respond to light with gradual changes in their membrane potential, where the amplitude of hyperpolarization increases monotonically as a function of decreasing light intensity till achieving saturation (Fu 2010). The vision system gains information from two types of photoreceptor cells with complementary specialization in order to collect more information from the surrounding environment.

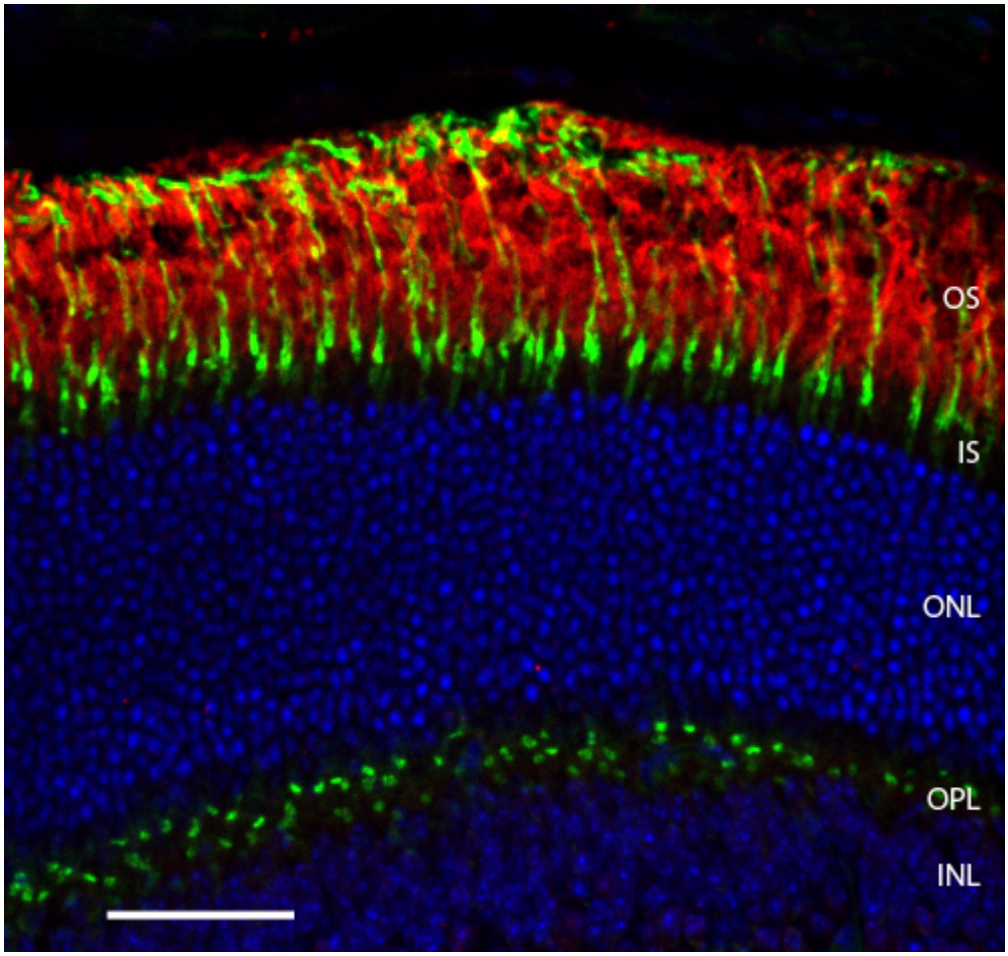

Figure 2. Photoreceptor inner and outer segments.
Rods and cones were stained on mouse retina. Rods outer segments (OS) were stained with anti-rhodopsion (red). Cones were stained with peanut agglutinin (green). OS, inner segments (IS) and synaptic endings in outer plexiform layer (OPL) of cones are indincated on the right. Nuclei were stained with DAPI (blue) to show outer nuclear layer (ONL) and inner nuclear layer (INL). Scale bar – 50µm.

Cones (Fig. 1, 2, 4) are specialized for vision in daylight and are characterised by a high acuity of vision (Kandel et al. 2000). They are concentrated in the fovea centralis and become less abundant toward the periphery of the retina. They have high temporal resolution (short integration time and fast response) and they are more sensitive to direct axial rays than rods. The cone system is chromatic, because there are three subgroups of these cells, which can detect light of a different wavelength, depending on the visual pigment they contain (Fu 2010). Cones expressing L–opsin are sensitive to the

electromagnetic spectrum in the red region, cones filled with M-opsin register light from green region and S-opsin cones detect parts of the blue spectrum of light. Each of these cones is connected to one bipolar cell. As a result, the brain obtains colour information from comparison of the responses from the three types of cones. On the other hand, lower signal amplification makes them less sensitive to photons than rods. Cone response to photons is much faster than that of rods and they can detect flickering light of frequencies higher than 55Hz (Kandel et al. 2000). Cones are the main receptive cells of the vision sense and people with cone dysfunction are legally blind.

Rods are responsible for night and peripheral vision and their special distribution as well as physiological adaptations serves this function. They are located on the whole retinal tissue except for the fovea centralis (Curcio *et al.* 1990). Their light reception is achromatic, because they posses only one type of pigment activating phototransduction cascade - rhodopsin. Rhodopsin belongs to the super family of G-protein coupled receptors. It consists of the protein opsin with the reversibly covalently bound ligand, 11-cis-retinal (Khorana 1992). Thanks to its stability rhodopsin can be densely packed in the rod discs. Additionally, many rods create synapses with the same target bipolar cell, strengthening the light signals initiated in any single cell and raising the retina's ability to detect dim light (Kandel et al. 2000). These features give rods light sensitivity much greater compared to cones, allowing them to detect even single photons. The disadvantage of this is the rod's slow response to light, with a 100ms interval, because the effects of the photons absorbed during this time need to be summed together (Kandel et al. 2000). As a result, their temporal resolution is low, leading to long integration times and slow responses. This also prevents them from resolving light in time laps shorter than 12Hz (Kandel et al. 2000). Furthermore, since many rods connect to the same bipolar cell, they create a large unit of resolution, which decreases the acuity of vision in comparison to cones. Loss of rods results in tunnel vision and night blindness.

Four major functional compartments in rods and cones can be distinguished (Wright et al. 2010). From outside to inside, relative to the layers of the retina, the first compartment - outer segment (OS), is characterized by intracellular stacked membrane inclusions. Light sensitive visual pigment molecules are embedded in these stacks, making this region responsible for phototransduction. The second compartment is the inner segment (IS), which is densely packed with most of biosynthetic cell machinery, consisting of microtubules, mitochondria, endoplasmic reticulum and the Golgi complex. The third compartment contains the nucleus and is followed by the fourth one comprised of synaptic ending forming connections with interneurons - horizontal and bipolar cells (Kandel et al. 2000, Wright et al. 2010).

1.1.1.1 Phototransduction in rod photoreceptors

The light absorption by the visual pigments in photoreceptors stimulates a cascade of changes that leads to hyperpolarization of the PR membrane through reduced membrane

conductance for cations (Na^+ and Ca^{2+}) (Fu 2010). Phototransduction in rods is the best-characterized sensory transduction pathway. The key molecule in their phototransduction cascade is the second messenger cyclic guanosine 3'-5' monophosphate (cGMP). Cyclic GMP governs ionic fluxes by opening cGMP-gated ion channels, which leads to Na^+ and Ca^{2+} ion inward currents.

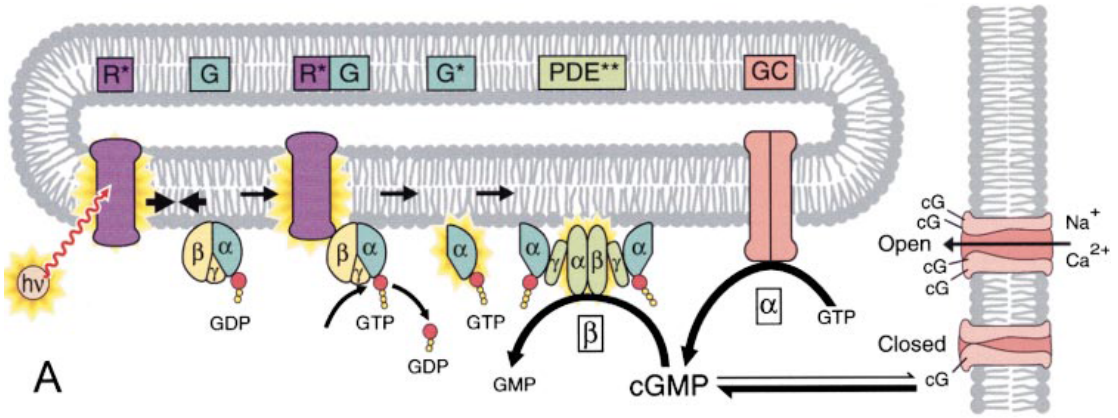

Figure 3. Rod visual phototransduction.
Photons (hv) fall on a rhodopsin molecule R, embedded in the rod outer segment membrane, which induces isomerization of 11-cis retinal to all-trans retinal within the molecule, and activates rhodopsin (R*). Each excited R* contacts molecules of transducin (G), catalyzing the exchange of GDP for GTP on their α subunit (G*). Activated G*, dissociate from transducin and binds to the γ subunit of phosphodiesterase (PDE). When two G* molecules bind to the PDE holomer, PDE α and β subunits are released from inhibition of γ subunits and PDE is activated (PDE**). Next, PDE** reduces cytoplasmic cGMP concentration through hydrolysis. This causes closure of cGMP-gated channels in the membrane. The rate constant of PDE** hydrolysing cGMP is indicatd by β and the rate of guanyl cyclase (GC) synthetising cGMP is indicated by α. Reprinted by permission from Elsevier (Leskov *et al.* 2000)

In darkness, cytoplasmic concentrations of cGMP are elevated, keeping cGMP-gated ion channels open. The resulting inward current of Na^+ ions through open cGMP-gated channels exceeds an outward current of K^+ through non-gated K^+ selective channels. This net inward current, also called dark current, keeps PRs in a partly depolarized state (-35mV), in the absence of light (Moriondo *et al.* 2001). In darkness, rhodopsin is in an inactive state, because of 11-cis retinal that blocks free opsin from activating the transduction cascade. When photons fall on the OS discs of rod PR (Fig. 3), it is absorbed by 11-cis retinal. This causes retinal isomeration from the 11-cis to all-trans configuration. As a result, the interaction of the all-trans retinal molecule with the amino acid side chains in the opsin-binding site forces a conformational change of rhodopsin into the unstable metarhodopsin II (Khorana 1992). Next, metarhodopsin II activates transducin, by catalyzing the exchange of GDP for GTP in its α subunit. This exchange enables the transducin α subunit to dissociate from the β and γ subunits and to bind to the γ subunit of phosphodiesterase (PDE6) (Norton *et al.* 2000). This sterically displaces the subunit and releases the PDE α and β subunits from inhibition. Subsequently, activated PDE6 lowers cGMP concentration through its hydrolysis to GMP, which leads to closure of Na^+/ Ca^{2+} selective cGMP-gated ion channels. The persisting K^+ outward current

causes PR hyperpolarization, increasing the membrane potential to 30mV, followed by closure of voltage-gated Ca^{2+} channels (Moriondo et al. 2001). Since calcium is essential for the fusion of neurotransmitter vesicles with their presynaptic membranes, this results in decreased release of the excitatory neurotransmitter glutamate from PR. Subsequently, decreased glutamate release from PR causes activation (depolarization) of rod On bipolar cell or inhibition (hyperpolarization) if it is an OFF bipolar cell. Bipolar cells then transmit the signal directly or indirectly (through amacrine cels) to the GC, which then passes the information to the neurons in the brain (Kandel et al. 2000, Nelson 2007).

Recovery of the rod is essential after light activation and requires inactivation of the phototransduction cascade components: metharhodopsin II, transducin and PDE6. Recoverin, a calcium-binding protein, is activated by the decrease in intracellular calcium concentration and dissociates from rhodopsin kinase. Activated rhodopsin kinase phosphorylates metarhodopsin II thus decreasing its affinity for transducin. The phosphorylated metarhodopsin II is then bound by arrestin, which completely deactivates it (Fu 2010). Eventual all-trans retinal disconnect from the unstable metarhodopsin II and is transported to RPE cells, where it is converted back to 11-cis retinal and is send back to the PR to regenerate light receptive rhodopsin (Sakamoto & Khorana 1995, McBee *et al.* 2001).

Inactivation of transducin proceeds by hydrolysis of bound GTP through its intrinsic GTPase activity. This process is accelerated by the interaction with the GTPase activation protein, GTPase- activating proteins (GAP) complex: R9AP-RGS9-1-Gβ5L. The RGS9-1 subunit of this complex facilitates the hydrolysis of GTP to GDP. Dissociation of the α subunit of GDP leads to inactivation of PDE6 (Fu 2010).

In addition to the inactivation of the main signalling pathways proteins, there is a second very important event that must occur – cGMP restoration. The concentration of a free cGMP is dependent not only on the hydrolysing activity of PDE6 but also on guanylate cyclase (GC), which can synthetise cGMP. Activity of GC is dependent on guanylate-cyclase-activating proteins (GCAPs) and the Ca^{2+} concentration. In darkness, GCAPs are bound to Ca^{2+}, but after activation of phototransduction, Ca^{2+} concentration is low, which causes the ions to dissociate from GCAPs. GCAPs released from Ca^{2+} can bind to GC, activating it, returning the cGMP basal concentration within a short time. Finally, the dark current is restored and PR again release neurotransmitters (Fu 2010).

1.1.2 Retinal ganglion cells

Ganglion cells constitute the innermost layer of the retina (Fig. 1) and their axons form the optic nerve, which then projects to the thalamus and other targets in the brain. Ganglion cells transmit information as a series of action potentials and they report contrast in light, rather than the absolute light intensity (Nelson 2007). The reason for this property lies in the receptive field organization of GCs, which is the area of PR that is

monitored by one GC. Receptive fields are characterised by two important features: they are circular and in most cases divided into two parts: a circular centre zone (receptive field centre) and the surrounding area of the field. The main classes of ganglion cells can be distinguished based on this organization. On-center gangion cells are stimulated when light falls on the centre of their receptive field. Light that falls on the surrounding area inhibits the GC. In contrast, off-center ganglion cells are inhibited by light in the central zone of the receptive field and excited when light falls on the area surrounding the receptive field. Both type of GC are equal in abundance and the size of the receptive fields is dependent on their localization in different areas of the retina (Kandel et al. 2000). In the fovea centralis region, where the acuity of vision is the greatest, the receptive fields are small while in the periphery the fields are larger. Parallel functioning of on-center and off-center ganglion cells also improves the visual system's sensitivity to rapid changes in light intensity (Nelson 2007). On-center ganglion cells perceive rapid increase in light intensity while off bipolar cells signal rapid decrease in light. Moreover, the centre-surrounding structure of GC receptive fields gives more information about brightness and colour of objects since this react mainly to changes in contrast, rather than on the absolute amount of light, giving more information about brightness and colour of objects (Nelson 2007). In general, gangion cells can be divided into two functional groups (each containing on- and off-center GC): the M (magni or large) type and the more abundant P (parvi or small) type (Kolb 2011). M cells have large dendritic arbors, reflective of their large receptive fields, and respond temporally to sustained illumination. They detect big features of objects and can follow fast changes in the light stimulus – its movement (Kandel et al. 2000). On the other hand, P cells have small receptive fields and respond to particular wavelengths, making them more perceive for form and colour (Kandel et al. 2000, Nelson 2007).

1.1.3 Retinal Müller glial cells

Retinal Müller glial cells stretch through all layers of the retina and enclose all retinal neuronal cells (Fig. 1 and 4). RMG introduce a great functional support and their proper activity is essential for the normal functioning of the tissue and correct vision. As their physical structure is similar to that of optical fibers, they can participate in low-loss light transfer through the whole retinal tissue to the PR (Franze et al. 2007). RMG cells greatly support the histological structure of the retina (Willbold *et al.* 1997) and constitute an anatomical link for retinal neurons to exchange molecules with the vitreous body and blood vessels (Reichenbach *et al.* 1993, Newman & Reichenbach 1996). They maintain pH, ion and water homeostasis within the retinal tissue (Newman & Reichenbach 1996, Bringmann *et al.* 2006), control the retinal blood flow (Paulson & Newman 1987) and take part in formation and maintenance of the blood-retinal barrier (Tout *et al.* 1993). Furthermore, RMG are involved in glucose tissue homeostasis, and provide neurons with nutrients (eg. lactate/puryvate) essential for neuronal oxidative metabolism (Poitry-Yamate *et al.* 1995, Tsacopoulos & Magistretti 1996). Moreover, they provide precursors

of neurotransmitters, which they also take up and recycle later on. This role in neurotransmitter recycling makes them important regulators of the physiological processes in neuronal signalling (Bringmann et al. 2006). In addition, RMG secrete vasoactive factors like VEGF (Eichler *et al.* 2000), pigment epithelium-derived factor (PEDF) (Eichler *et al.* 2004), transforming growth factor-β (TGF-β) (Ikeda *et al.* 1998), as well as neurotrophic factors like ciliary neurotrophic factor (CNTF), brain-derived neurotrophic factor (BDNF), lens epithelium-derived growth factor (LEDGF) (Seitz *et al.* 2010), leukemia inhibitory factor (LIF) (Agca *et al.* 2013), fibroblast growth factor 2 (FGF-2, bFGF) (Hauck *et al.* 2006b) and glial cell-derived neurotrophic factor (GDNF) (Zhu *et al.* 2012). Finally, RMG have been found to influence neuronal excitability (Newman & Zahs 1998, Stevens *et al.* 2003).

In contrary to retinal neuronal cells, which are susceptible to injury by different perturbations, RMG cells are highly resistant to hypoglycemia or disturbed blood supply leading to ischemia or anoxia within the tissue (Bringmann et al. 2006). This difference in robustness can induce a disproportional RMG proliferation leading to gliosis, which exacerbates retinal degeneration and PR death (Bringmann *et al.* 2009). RMGs display a stereotypic response to injury independent of different noxious conditions, which includes upregulation of glial fibrillary acidic protein (GFAP) (Bringmann & Reichenbach 2001) and activation of extracellular signal-regulated kinases (ERKs) (Geller *et al.* 2001). However, specific responses have also been described. One example for a specific response is the regulation of glutamine synthetase (GS) expression. While it decreases after PR degeneration caused by light damage (Grosche *et al.* 1995), it increase after hepatic retionopathy, when it is necessary to detoxify the tissue from elevated levels of ammonia (Reichenbach *et al.* 1995). Similarly, neurotrophic factors like LIF are secreted by RMG after light injury to protect PR from premature death (Agca et al. 2013).

The wide range of RMG functions within the retina and their resistance to different injury conditions make RMG an important therapeutic target. Many investigations in the last 20 years have focused on the influence of Müller glial-derived prosurvival factors as a potential therapy for retinal degenerations, including retinitis pigmentosa. Neurotrophic factors like BDNF, CNTF, GDNF or LIF whose receptors are present on RMG but not on PR were shown to prolong PR survival in different animal models of retinal degenerations (Faktorovich *et al.* 1990, Di Polo *et al.* 1998, LaVail *et al.* 1998, Frasson *et al.* 1999a, Kirsch *et al.* 2010).

1.1.4 Retinal pigment epithelium cells

Retinal pigment epithelium cells form a single epithelial layer on the inside of the choroid. They contact PR outer segments on their apical side. Interactions between PR and RPE cells play an important role in retinal metabolism and recycling (Wright et al. 2010). Since PR do not have the necessary enzymes, all-trans retinol is transported from PR to RPE cells and re-isomerised to 11-cis retinal, essential for the light reactions in

phototransduction (see 1.1.1.1), and send back to PR (Wright et al. 2010). In addition, RPE cells contain melanosomes - the pigment granules that absorb stray light falling into the eye, which improves the quality of the PR light perception (Kandel et al. 2000).

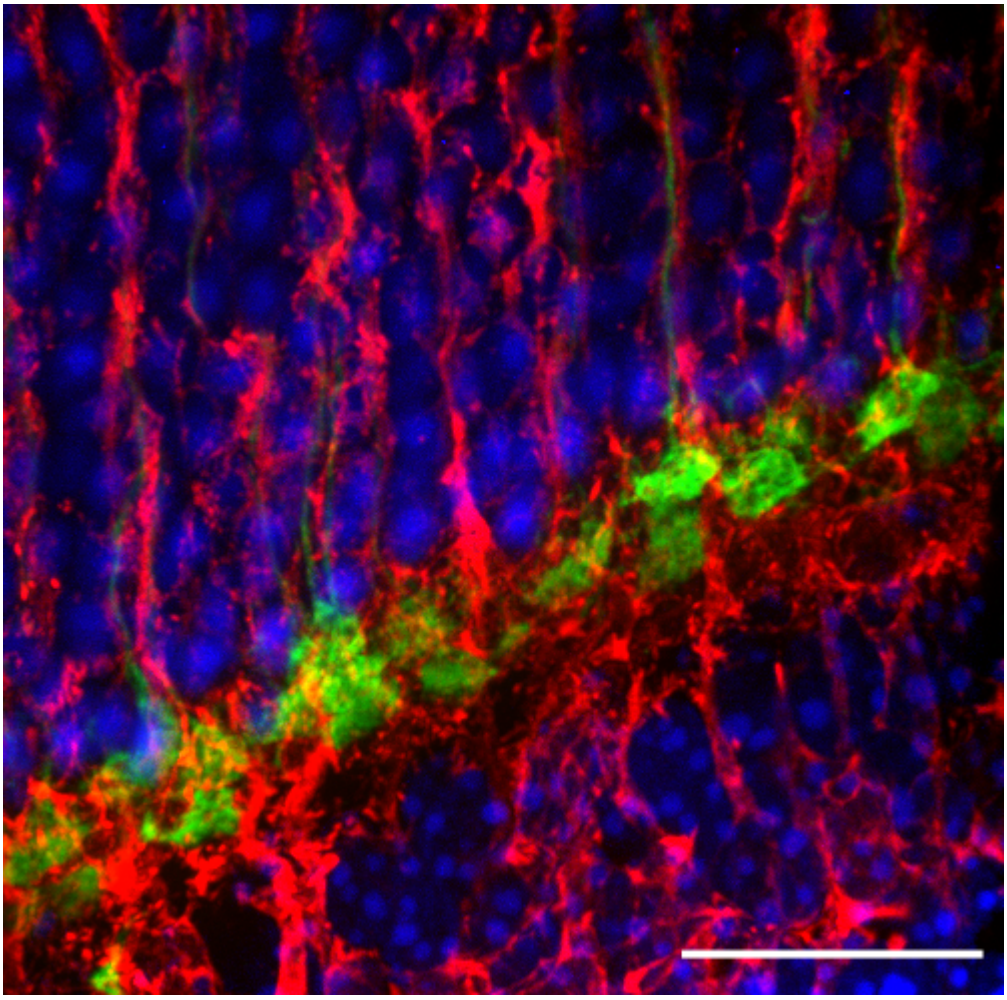

Figure 4. Retinal Müller glial cells surround neuronal retinal cells.
Retinal Müller glial cells were visualized by immunohistochemistry on mouse retina with glutamine synthetase (red). Cone axons and synaptic endfeet were stained with peanut agglutinin (green). DAPI was used to visualise nuclei (blue) Scale bar 10µm.

Furthermore, studies on genetically inherited retinal degenerations reveal a strong dependence of PR and RPE from each other. On one hand PR degeneration is followed by RPE cell atrophy in some patients with RP as well as in the rd1 and rd10 mouse model of RP (Mitamura *et al.* 2012, Pennesi *et al.* 2012, Samardzija *et al.* 2012). On the other hand, RPE cells secrete many factors like CNTF, BDNF, FGF-2, VEGF, GDNF, LIF, PEDF, TGF-β2, beta-nerve growth factor (BNGF), insulin-like growth factor-binding protein 1 (IGFBP-1) (Li *et al.* 2011), LEDGF (Matsui *et al.* 2001), insulin-like growth factor-1 (IGF-1) (Savchenko *et al.* 2001), platelet-derived growth factor (PDGF) (Campochiaro *et al.* 1994) and tissue inhibitor of matrix metalloprotease 1 (TIMP1) (Padgett *et al.* 1997). These molecules influence not only PR survival (Ahuja *et al.* 2001), PR outer segment regeneration and the phototransduction machinery (Wen *et al.* 2012)

but also the endothelium of blood vessels in the eye (Lambooij *et al.* 2003). The basolateral side of the RPE, together with Bruch's membrane and choriocapilars, forms an outer part of blood-retina barrier (Hamilton & Leach 2011). Therefore, RPE cells have the additional function of controlling ion homeostasis as well as the epithelial transport into the eye. Specifically, they supply PR with nutrients (e.g. glucose and ω-3 fatty acids), and mediate the retrograde transport of metabolic end-products back to the circulation (Kandel et al. 2000).

RPE cells are constantly at risk of very intense oxidative stress, since they have the task of clearing PR outer segments damaged by excessive photo oxidation through phagocytosis. On the basal side RPE adjoin choroid tissue characterised by a strong oxygen blood perfusion (Shadrach *et al.* 2013). To survive in such a highly photo-oxidative environment with a high amount of free radicals, RPE cells possess the ability to detoxify peroxidized lipids, proteins and DNA through high concentrations of enzymatic and non-enzymatic anti-oxidant systems (Kandel et al. 2000).

Finally, RPE cells are a part of the immunological defence system of the eye. The RPE contributes to these defences through formation of a physical barrier that separates the blood stream from the inner space of the eye. Additionally, they secrete immune modulatory factors like interleukin-8 (IL-8) and IL-6 (Li et al. 2011), cyclin A (Kaestel *et al.* 2005) and complement factor H (CFH) (Mandal & Ayyagari 2006). Interestingly, RPE express toll-like receptors (Kumar *et al.* 2004), and under certain circumstances even MHC class II receptors (Makhoul *et al.* 2012), which are thought to enable them to participate in pathogen recognition.

1.2 Vasculature of the retina

Development of the retinal blood vessels is similar in rat and mouse (Cairns 1959, Ritter *et al.* 2005). During fetal development blood vessels sprout at the head of optic nerve and spread radially from the centre of the retina to the peripheral parts. At birth the retina of a rat is avascular and the hyaloid system of vessels nourishes the lens and the retina. Hyaloid vessels originate from the optic disc, cross the vitreous body and pass close to the surface of the retina. This arrangement persists between postnatal day (PN) PN0-PN5. At around PN6, the hyaloid vessels start to regress, and at PN9 only a small residue of the vessels, crossing the vitreous body, is left. The eventual atrophy of the hyaloid vessels is observed between PN15-PN22 (Cairns 1959).

The development of the main retinal vessels starts after birth at the innermost side of the retina and progress outward in the direction of the choroid (Fig. 5). Four to eight arterioles spring from the central retinal artery and symmetrically radiate out in the optic nerve fiber layer. First capillaries bud from these radiating arterioles between PN1 and PN2 and form the superficial plexus. These capillaries avoid the immediate proximity of the artery, but not the vein. Its development is almost complete by PN8-PN10, except for

minor maturation of the retina in the periphery until PN16 (Cairns 1959, Engerman & Meyer 1965). The deep capillary plexus, which will supply the inner retina, springs from the superficial plexus between PN6-PN8 (Cairns 1959, Engerman & Meyer 1965). The capillary network penetrates deeply into the inner nuclear layer but not further than the outer plexiform layer. Large collecting veins that arise from the plexus perforate the inner nuclear layer. The deep capillary plexus fully develops, draining the peripheral area, by PN15-PN16, at which time the hyaloid vessels are basically gone (Cairns 1959).

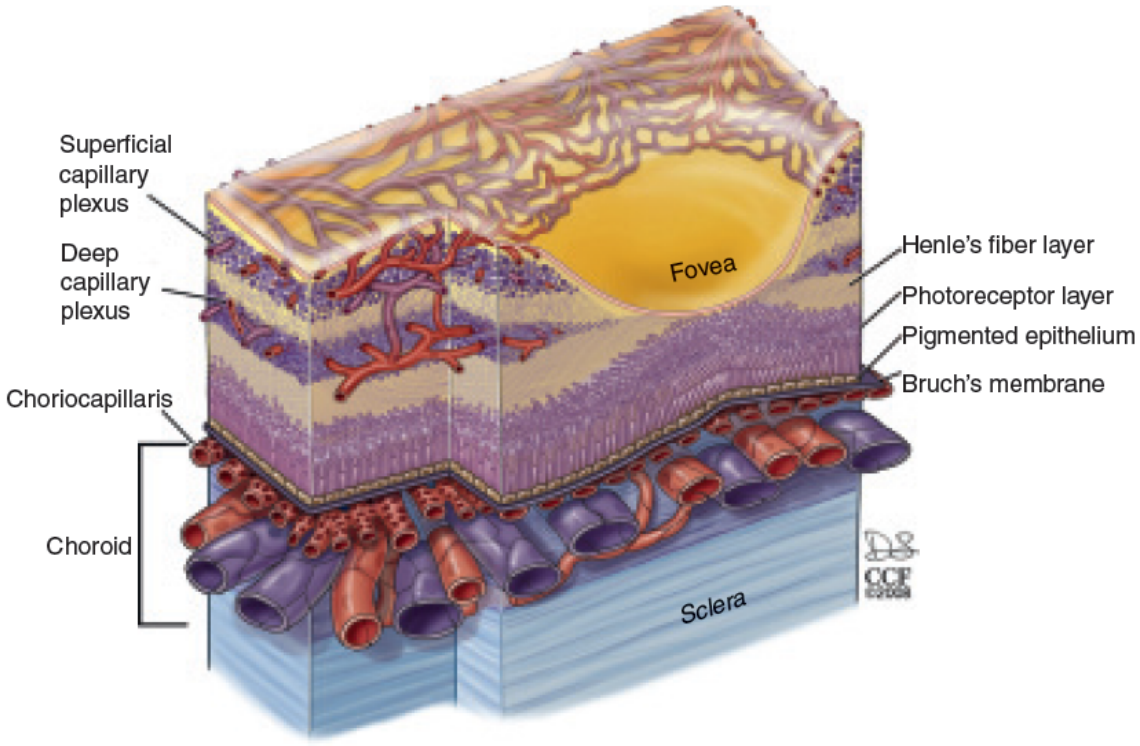

Figure 5. Vasculature of an adult human eye.
The picture presents the retinal vasculature, penetrating the retina from the inner side as well as the choroidal vasculature surrounding the RPE (subretinal vasculature). Reprinted by permission from Elsevier (Anand-Apte & Hollyfield 2010).

In human retina hyaloid vessels are present in the embryonic and fetal stages of development. It is fully developed at the ninth week and starts to regress right afterwards. By the sixth month of gestation, hyaloid vessels are gone and only the Cloquet canal, spreading from the optic disk to the posterior surface of the lens, remains. The retinal vascular network starts to develop during the fourth month of gestation, when first vessels form a first primitive central retinal arterial system. The vessels then extend from the optic nerve to the periphery of the retina, so by the time of delivery the whole retina is surrounded. Human retina achieves the vasculature pattern of an adult by the fifth month after birth (Anand-Apte & Hollyfield 2010).

Chapter Two: Retinal pathology

Chapter two focuses on retinal pathology caused by genetic mutations. It shortly presents inherited retinal degenerations (2.1), focusing on symptoms and retinal changes in patients with retinitis pigmentosa (RP, 2.1.1), the disease that is the focus of the experimental part of the thesis. The chapter is closed by the descriptions of retinitis pigmentosa animal models (2.2) – *Pde6b*^{rd1} (rd1) mouse (2.2.1) and S334-ter-line 3 (S334ter-3) rat (2.2.2), which were used in this study.

2.1 Inherited retinal degenerations

Genetically inherited mutations leading to disorders of photoreceptor or supporting cells are a common reason for impaired vision. Some of them, like Leber congenital amaurosis (Perusek & Maeda 2013), or Batten disease (Rakheja *et al.* 2007) affect vision from early childhood. Others like Stargardt disease starts in patients before they are 20 years old (Nentwich & Rudolph 2013). Similarly, the age of onset for the disease investigated in this study, retinitis pigmentosa, ranges from childhood to early adulthood (Hartong *et al.* 2006).

2.1.1 Retinitis pigmentosa

Retinitis pigmentosa is a collective term for a group of hereditary retinal progressive diseases, in which the genes affected by mutations lead to rod, cone or RPE cell degeneration (van Soest *et al.* 1999). Around 1 in 4000 individuals is affected by this disease worldwide (Hartong et al. 2006). This translates to around one million patients in total. Due to a severely constricted visual field most RP patients are legally blind by the age of 40 (Hartong et al. 2006).

Retinitis pigmentosa can be inherited in an autosomal dominant, autosomal recessive or X-linked way. Today, 57 genes and loci responsible for the disease have been identified (RetNet: https://sph.uth.edu/RetNet/sum-dis.htm). Autosomal recessive RP accounts for 50 – 60% of cases, out of which mutations in α or β subunits of rod phosphodiesterase are one of the most common with 9% of total cases. Mutations in both subunits of PDE6 are found at about equal proportions in patients. Autosomal dominant RP accounts for 30-40% of cases and within this group, mutations of rhodopsin make up the lion's share with 25% of cases. X-linked mutations are responsible for only a minor fraction (5-15%) of RP cases. Interestingly, – only one gene accounts for 70 -80% of X-linked RP cases - GTPase regulator (*RPGR*) (Hartong et al. 2006). Retinitis pigmentosa occurs in patients from childhood to adulthood and is usually limited to the eyes. Nevertheless, around 20-30% of patients are afflicted by additional non-ocular manifestation caused by their respective gene defects. Examples of these cases are Usher's syndrome or α-tocopherol transport protein deficiency, although more than 30 other forms have been described (Hartong et al. 2006).

The symptoms and disease progression of retinitis pigmentosa are highly variable. Some patients lose sight in childhood, while others in mid-adulthood. In most of the patients, the rods are the first cells to be affected, which causes night blindness followed by loss of peripheral vision and finally tunnel vision. Patients with end-stage retinits pigmentosa often present with an almost complete loss of central vision by the age of 60 (Hartong et al. 2006). However, retinitis pigmentosa can start with cone rather than rod degeneration in a subgroup of patients, leading to impaired central vision, impaired visual acuity and defective colour vision (Birch *et al.* 1999). Symptoms may also include refractive error in the eye and patients may develop myopia (mostly X-linked RP, (Fishman *et al.* 1988)) or hyperopia (mostly dominant RP, (Hartong et al. 2006)). RP can remain undiagnosed for long periods of time, if patients live in environments that are electrically illuminated during the night. Moreover, during daily tasks no subjective difficulties will arise even if the visual field is reduced to around 50 degrees in diameter (compared to 180 degrees for a healthy person). Even more striking is the fact that patients can lose 90% of cones in the fovea centralis before realising a reduction in visual acuity (Geller & Sieving 1993). Furthermore, patients with electroretinogram amplitude 50 times smaller than normal can still have ambulatory vision (defined as an ability to move around using only visual information) and read newspapers (Andreasson *et al.* 1988). Taken together, by the time patients notice visual disturbances the disease may already be in very advanced stages.

The disease is diagnosed by measurements of colour vision, dark adaptation and contrast sensitivity as well as fundus observations. In addition, the electrical responses of the photoreceptors to the flashes of light are measured using electroretinography (ERG). Patients affected by RP have delayed rod and cone response with reduced amplitude during ERG measurements (Hartong et al. 2006). Similarly, atrophy of retinal vessels together with intraretinal pigmentation in the periphery of the tissue is found in almost all cases (Fig. 6). For some patients, images of the fundus autofluorescence reveal increased concentrations of the age-related pigment lipofuscin in the RPE. These regions also have decreased ERG amplitudes (Popovic *et al.* 2005, Robson *et al.* 2006). Around 50% of patients develop posterior subscapular cataracts (Heckenlively 1982, Fishman *et al.* 1985). Additionally, the head of the optic nerve can have a pale colour (optic-disc pallor) (Fig. 6). Furthermore, changes in the retinal morphology, like thickness, structure of the PR layer and presence of macular oedema, have been described using non-invasive optic coherence tomography (Jacobson *et al.* 2000, Ko *et al.* 2005, Sandberg *et al.* 2005).

2.2 Animal models of retinitis pigmentosa

RP research currently utilizes a large number of different animal models to investigate different therapeutic approaches. The rd1 mouse and S334ter line 3 (S334ter-3) rat animal models of RP, used in this study, will be described below, together with a short description on validated therapies.

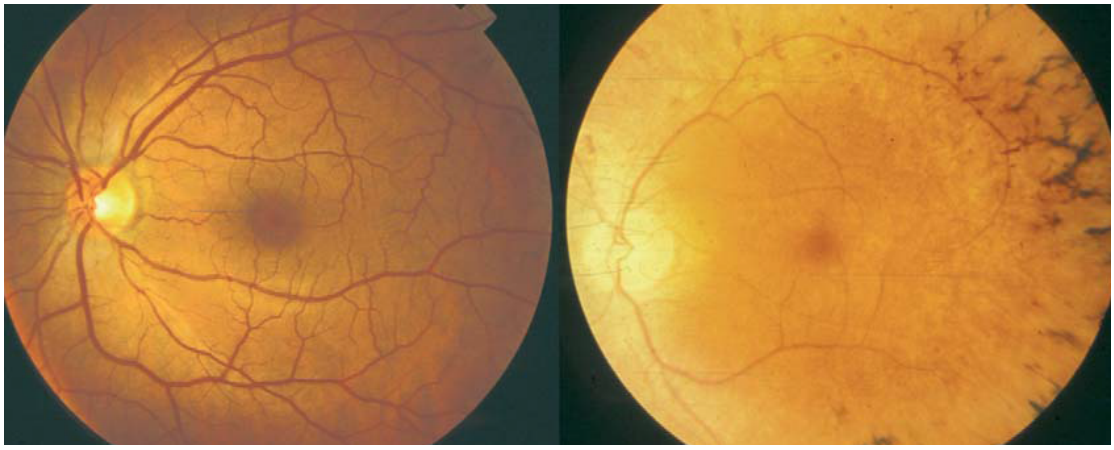

Figure 6. Morphological alterations in the fundus of a retinitis pigmentosa patient.
Healthy retinal vasculature (on the left side) versus vasculature of an RP patient (on the right side) was assessed by funduscopy. RP retina shows vascular atrophy, peripheral pigment deposits as well as a pale optic disc. Reprinted by permission from Elsevier (Hartong et al. 2006).

2.2.1 rd1 mouse

The retinal degeneration (*Pde6b*^{rd1}, rd1, C3H/HeJ) mouse, firstly described as the "rodless retina" (*r*) (Keeler 1924), is currently the best characterized animal model for RP. In these animals degeneration of the retina is caused by a mutation on chromosome 4 and in exon 7 of the β-subunit of PDE6 (Fig. 3), which leads to production of a non-functional protein (Bowes *et al.* 1990, Pittler & Baehr 1991). This mutation has been also found in human patients affected with autosomal recessive RP (see 2.1.1). The retina of rd1 mice shows first signs of PR abnormality already from the day of birth - increased activity of anaerobic glycolysis and increased production of lactate (Acosta *et al.* 2005). In the next stage (PN4) retarded growth of photoreceptor inner segments can be observed (Caley *et al.* 1972, Sanyal & Bal 1973), followed by swollen mitochondria of the rod inner segments at PN8 (Farber & Lolley 1974). Subsequently, increased uptake of oxygen, utilization of higher amounts of glucose as well as lactic acid production followed by the rapid decrease of these parameters at PN12 takes place for the whole rd1 retinal tissue (Bowes et al. 1990). Moreover, although cellular integrity and thickness of ONL in PN10 rd1 retina is comparable to the wild type retina, outer segment disks show signs of disruption (Carter-Dawson *et al.* 1978). This phenomenon is accompanied by pyknotic nuclei and the beginning of rods degeneration (Sanyal & Bal 1973). At PN11, the rate of rod degeneration starts to increase progressively, but the rods are still present and the general number of PR is not yet significantly decreased in comparison to wild type (Portera-Cailliau *et al.* 1994, Hauck *et al.* 2006a). The peak of degeneration is around PN12-PN14 (Fig. 7) (Sanyal & Bal 1973, Carter-Dawson et al. 1978) and no rods are left in the central retina by PN36 and in the periphery by PN65 (Carter-Dawson et al. 1978). Cones, although not affected by the mutation, degenerate secondarily within the first six postnatal months although residual nuclei can occasionally be found at the age of 18 months (Carter-Dawson et al. 1978).

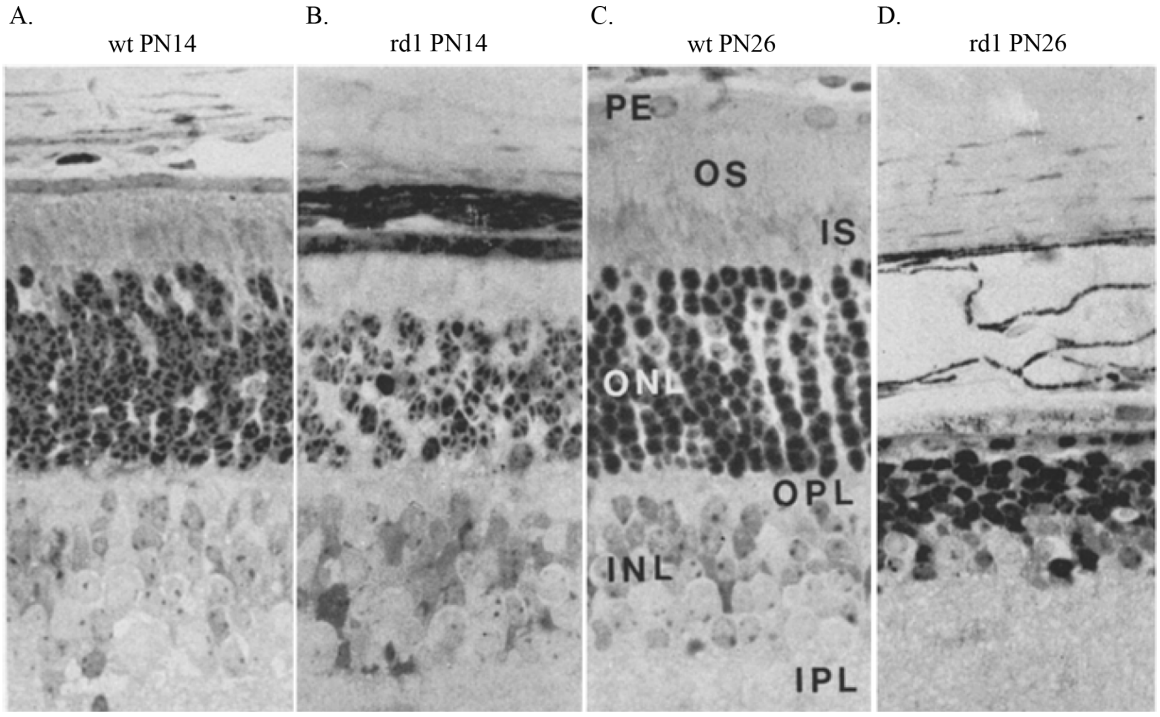

Figure 7. The peak of rd1 retinal degeneration occurs between PN12 and PN14.
Ultrastructural comparison between wild type (Balb/c) and rd1 mice. Wildtype control retinas at PN14 (A) and PN26 (C) are shown for comparison. Photoreceptor loss is observable at PN14 (B) and pronounced at PN26 (D) in rd1 mice. On the pictures are indicated: retinal pigment epithelium (PE), outer segments (OS), inner segments (IS), outer nuclear layer (ONL), outer plexiform layer (OPL), inner nuclear layer (INL), inner plexiform layer (IPL). Magnification 500x Reprinted by permission from Springer (Sanyal & Bal 1973).

On the cellular level, the PR degeneration process in the rd1 mouse retina is difficult to classify since it does not conform to the characteristics of either classical apoptosis or necrosis (Leist & Jaattela 2001, Edinger & Thompson 2004). On one hand, Apoptosis inducing factor (AIF) and caspase-12 - two markers of apoptosis – were shown to translocate to the nucleus of degenerating PR (Sanges *et al.* 2006). Similarly, elevated Ca^{2+} level and swollen mitochondria indicate induction of PR death through apoptosis (Lipton & Nicotera 1998). On the other hand, the degeneration happens without activation of initiator caspases (-8, -9) or downstream effector caspases (-2, -3, -7) and without release of cytochrome c (Holcik & Korneluk 2001, Doonan *et al.* 2003, Zeiss *et al.* 2004). Moreover, although there is massive death of PR cells within a short timeframe, there is no evidence for necrosis or an inflammatory reaction (Portera-Cailliau et al. 1994). The fact that between PN10 and PN14 activated microglia cells migrate to the degenerating PR is another mosaic piece in the degeneration of the rd1 retina (Zeiss & Johnson 2004, Zeng *et al.* 2005). Taken together, the rd1 PR degeneration appears to be caused by a type of apoptosis, which deviates from the textbook definition in some regards, the missing cytochrome c release, for instance.

Many therapeutic strategies were already applied in the rd1 RP animal model. Impairment of the β-subunit of PDE6 leads to accumulation of cGMP (Farber & Lolley 1974), which

causes an constant influx and eventual overload of calcium and sodium through cGMP-gated sodium channels. The excessive Ca^{2+} influx into PR cell together with upregulation of CaM kinase II is visible between PN5 - PN10 (Fox *et al.* 1999, Doonan *et al.* 2005, Hauck et al. 2006a, Sanges et al. 2006) and causes mitochondria depolarization and energy collapse (Doonan et al. 2005) as well as endoplasmic reticulum (ER) stress (Yang *et al.* 2007). As this mechanism is reminiscent of the induction of neuronal death through overstimulation with excitatory neurotransmitters and resulting calcium overload (excitotoxicity) (Lipton & Nicotera 1998), many experiments applying calcium channel inhibitors were performed. D-cis diltiazem is a competitive antagonist of L-type calcium and cyclic nucleotide-reglated channels, clinically used in cardiology (Koch & Kaupp 1985, Haynes 1992). In one *in vivo* study on rd1 mice it partially rescued PR from preliminary death (Frasson *et al.* 1999b). On the other hand, other studies on D-cis diltiazem could not confirm its neuroprotective effect (Tawara *et al.* 1989, Pawlyk *et al.* 2002, Fox *et al.* 2003, Takano *et al.* 2004). Another L-type antagonist of calcium channels, nivadipine, was effective in preserving PR morphology, but not function, in *in vivo* studies on rd1 mice (Takano et al. 2004). Application of pharmacological inhibitors of cGMP-dependent protein kinase (PKG) into rd1 mouse eye resulted in a strong decrease in PR death (Paquet-Durand *et al.* 2009).

Interestingly, increased activity of the Ca^{2+} dependent protease - calpain has been found in TUNEL positive rd1 PR after PN11. This increase has been linked to phosphorylated cAMP responsive element-binding protein (CREB-1) dependent downregulation of calpastatin, an endogenous inhibitor of calpain (Paquet-Durand *et al.* 2006). Since calpain activation can be connected to neuronal degeneration (Sakamoto *et al.* 2000, Arataki *et al.* 2005), different calpain inhibitors were tested. Intravitreal injections of a calpastatin peptide resulted in decreased PR cell death (Paquet-Durand *et al.* 2010). Furthermore, intravitreal injections with calpain inhibitor I and II inhibited activation of two markers of apoptosis - AIF and caspase-12 and decreased PR cell death (Sanges et al. 2006). On the other hand, *in vivo* experiments performed only with calpain inhibitor I failed to show reduction of PR cell death in rd1 mouse retina (Doonan et al. 2005).

Calcium overload in neuronal cells also results in mitochondrial depolarization and subsequent reactive oxygen species production (Lipton & Nicotera 1998). Severe mitochondrial oxidative stress is already observable after the first week of life in rd1 mice (Farber & Lolley 1974, Vlachantoni *et al.* 2011). Consistent with a role of oxidative stress in rd1 PR cell death, seven days of hypoxia could prolong PR survival in rd1 retinal explants. However, treatment of rd1 mice with the antioxidant MSO10 (MitoQ) failed to increase PR survival (Vlachantoni et al. 2011). Another strategy, injections of different antioxidants between PN18 and PN35, resulted in the reduction of cone oxidative damage, increased survival rate and partially preserved cone function (Carter-Dawson et

al. 1978). This last result is in line with the hypothesis that cone death is caused by oxidative stress arising after rod cell death (Carter-Dawson et al. 1978).

2.2.2 S334ter line 3 pigmented rat

Multiple missense mutations at the C-terminus (Pro347Ser, Pro347Leu, Pro437Gln, Val345Leu, Val345Met and Q344ter) (Sung *et al.* 1991, Sung *et al.* 1993, Jacobson *et al.* 1994, Sandberg *et al.* 1995) were found in human cases of RP (Fig. 8). The C-terminus contains the rhodopsin-sorting signal, responsible for targeting the protein to the PR outer segments. Mutations in this region cause the most severe symptoms in RP patients (Sandberg et al. 1995).

Mutant rhodopsin transgenic S334ter rats were developed in the laboratories of the University of California in San Francisco in 1996 (http://www.ucsfeye.net/mlavailRDratmodels.shtml). The S334ter mutation causes premature termination of rhodopsin translation resulting in a C-terminally truncated rhodopsin protein lacking the last 15 amino acid residues. As a consequence, almost all of the phosphorylation sites of the molecule are missing (Mendez *et al.* 2000, Concepcion *et al.* 2002). Five lines (line -3, -4, -5, -7, - 9) of S334ter rats with the same mutation but different rates of PR degeneration were obtained. The S334ter-3 line shows, after S334-ter-7 rats, the second most severe phenotype (Pennesi *et al.* 2008, Martinez-Navarrete *et al.* 2011).

In the S334ter-3 retina, the first pycnotic nuclei can be found in the proximal half of the ONL at PN4 and PN6 followed by occasional degenerating PR observed from PN8 until PN11 (Liu *et al.* 1999, Pennesi et al. 2008, Martinez-Navarrete et al. 2011). Next, between PN11 and PN12, caspase-3 activation increases and rods undergo rapid degeneration, causing more than 50% of them to die (Liu et al. 1999, Martinez-Navarrete et al. 2011). At PN15, 65% of PRs are lost (Pennesi et al. 2008). This is accompanied by a significant increase of endoplasmic reticulum stress markers (Kroeger *et al.* 2012). The next day, the PR layer declines to two or three rows. At PN20 – PN30 only one or two rows remain with residual inner segments (Liu et al. 1999, Martinez-Navarrete et al. 2011) and at PN60 only cones are left (Martinez-Navarrete et al. 2011). Increased expression of GFAP by RMG as a reaction to PR degeneration begins around PN21. The RMG cells form a seal between PR and RPE starting at PN60 (Ray *et al.* 2010). Rod outer segments never develop in the heterozygous S334ter-3 rats (Liu et al. 1999, Martinez-Navarrete et al. 2011) while cone outer segments are shorter and distorted in comparison to normal rats (Martinez-Navarrete et al. 2011, Ji *et al.* 2012). After rod degeneration, cones start to lose their outer segments, and within two months start to die (Li *et al.* 2010) Nevertheless, cone degeneration does not lead to complete cone loss even at PN600 (Ji et al. 2012). In the early stages of the degeneration cones without outer segments are viable and capable to regenerate the outer segments. (Li et al. 2010).

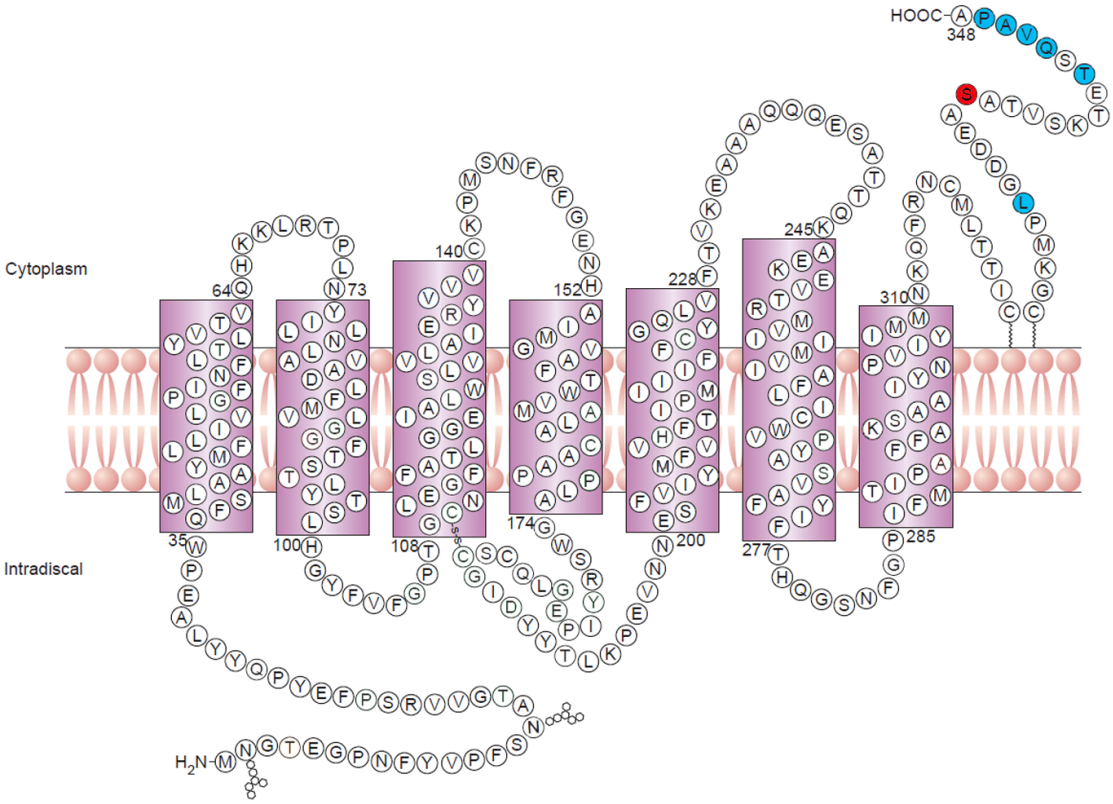

Figure 8. Mutations in the rhodopsin C-terminus lead to retinitis pigmentosa.
A mutation on the cytoplasmatic C-terminus of rhodopsin causes the most severe symptoms in patients with retinitis pigmentosa. The S334ter mutation (red) shortens the C-terminus by 15 amino acids, which deprive the protein of most of its phosphorylation sites (blue). Reprinted by permission from Elsevier (Mendes *et al.* 2005)

In contrast to the rd1 mouse model, apoptosis of rods is accompanied by activation of the canonical pathway with increased activity of caspase-9, caspase-3 and cytochrome c release (Kaur *et al.* 2011). Moreover, the irreversible caspase-3 inhibitor z-DEVD-fmk inhibits PR degeneration (Liu et al. 1999). Calpastatin downregulation, strong activation of calpain and poly ADP-ribose polymerase (PARP) together with increased oxidative DNA damage and poly ADP-ribose (PAR) polymer accumulation heavily imply the canonical apoptosis pathway in the death of PR in the S334ter model (Kaur et al. 2011).

S334ter-3 retinas undergo an interesting secondary modification concomitant with PR degeneration. Both PR types form circular structures around dying cells as rods start to degenerate at PN10-PN15 (Fig. 9). These structures are spread throughout the whole retina by PN90 (Ji et al. 2012, Zhu *et al.* 2013). They are very regular and consistent structures, with respect to cone spatial arrangement as well as orientation. Their formation is probably modulated by RMG (Lee *et al.* 2011, Zhu et al. 2013). At PN180, the circular structures start to loose their form, the cones lose their specific orientation and start to die (Ji et al. 2012). Activated microglia invade the space left by dead PR and are replaced later by remodelled RMG processes (Zhu et al. 2013).

Rapid rod death forces changes in other neurons. The first cells undergoing cellular modifications are rod bipolar and horizontal cells, followed by amacrine cells (Ray et al. 2010, Martinez-Navarrete et al. 2011). Bipolar cells show retraction of dendrites, form clusters along the outer plexiform layer at PN11-13 and by PN60 their number deteriorate to half their original number in the central retina (Ray et al. 2010, Martinez-Navarrete et al. 2011). The decrease continues afterwards, affecting about one-third of the bipolar cells in the healthy retina (Ray et al. 2010). Horizontal cell processes appear thinner and less complex around PN11-PN21 (Ray et al. 2010, Martinez-Navarrete et al. 2011), leading to gaps in the outer plexiform layer. Between PN60 and PN90 around half of the horizontal cells are lost and almost no terminal tips can be observed in the remaining horizontal cells (Ray et al. 2010, Martinez-Navarrete et al. 2011). Additionally, the density of horizontal cells in whole mount retina at PN60 and PN90 is significantly reduced in the central, but not the peripheral retina (Ray et al. 2010). Amacrine cells are affected as well and their mislocalization toward the INL at PN180 and PN600 has been reported (Ray et al. 2010). One study showed indications for apoptosis in inner retinal neurons and within ganglion cells after PR degeneration (Martinez-Navarrete et al. 2011), which had not been observed in an earlier study (Ray et al. 2010). Surprisingly, ganglion cells ON and OFF responses were recordable even from three-month-old homozygous S334ter-3 rats (An *et al.* 2002).

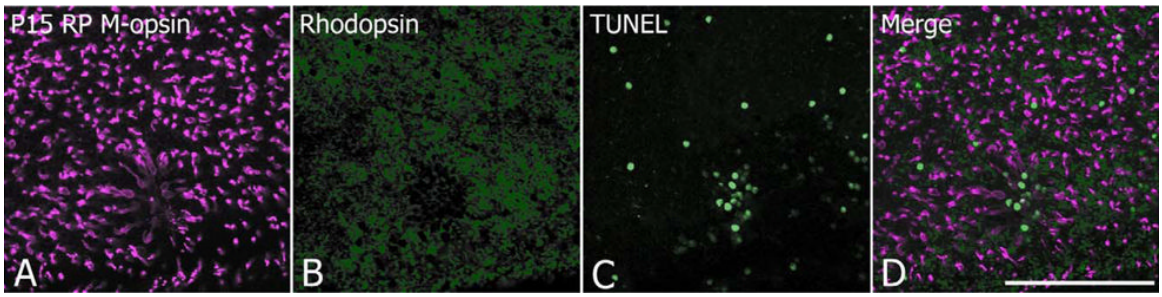

Figure 9. Photoreceptors form circular structures around dying cells in the degenerating S334ter-3 rat retina.
Confocal images of the whole-mount retina prepared from PN15 rats. During rod degeneration around cones (M-opsin, violet) and rods (rhodopsin, green) arrange themselves in circular structures around TUNEL positive cells (green). Scale bar 100µm Reprinted by permission from John Wiley and Sons (Ji et al. 2012).

Early rod degeneration also negatively influences retinal blood vessel development. The deep capillary plexus in rat retina is mature by PN15, but in S334ter-3 65% of PRs are gone by this time. As a consequence, capillaries do not develop properly and their number reaches only 6-7% relative to wild type retinas at this time point. This effect is permanent and even after one year no increase in vascularization of the deep capillary plexus could be found (Pennesi et al. 2008).

Chapter three: Therapeutic strategies against retinitis pigmentosa

Chapter three briefly summarizes novel therapeutic strategies against RP (3.1) and reviews neuroprotective factors that are currently under investigation (3.2). Additionally, it provides the rationale for more detailed studies on GDNF neuroprotective action (3.2.1), presenting a wide spectrum of successful research conducted on different animal models of RP. Eventually, cysteine rich protein 61 (Cyr61/CCN1), the molecule whose neuroprotective potential was chosen for investigation in the presented thesis, is described in detail (3.2.2).

3.1 Experimental therapies for retinitis pigmenotsa

Many different treatment strategies are investigated to treat RP. These include gene therapies, transplantation of whole retinas or stem cell therapy, implantation of electrical devices, pharmacological treatment with vitamin supplementation, or factor application. Each of them has advantages as well as disadvantages.

Gene therapy, so far the most successful, is dependent on the type of mutation and aims to induce the local production of the missing or mutated protein. This therapy must be tailored specifically to each individual patient (Jacobson et al. 2000, Acland *et al.* 2005, Bi *et al.* 2006). Transplantation of fetal retinal sheets has proven a rescue in cases where PR and RPE cells had already degenerated, but because of difficulties with tissue supply and ethical issues, it cannot be assumed as a universal therapy (Seiler *et al.* 2008, Seiler & Aramant 2012). Stem cell therapy using pluripotent or multipotent adult stem cells are already under investigation and could be an alternative to transplantation of retinas from fetuses (Borooah *et al.* 2013, Bharti *et al.* 2014, Kamao *et al.* 2014). A different approach originates from the developing field of electrical devices that are able to stimulate the optic nerve, retina or visual cortex and may also be an option for patients with already degenerated PR (Chow *et al.* 2004, Brelen *et al.* 2005, Pezaris & Eskandar 2009, Zrenner *et al.* 2011). Another therapeutic strategy employs vitamin A supplementation which was shown to be beneficial in patients with mutations of genes responsible for retinoid recycling in the visual cycle (Perusek & Maeda 2013). Finally, the application of a neuroprotective factor has never been shown to be fully curative, but has the advantage of being more universal, as this strategy is focused on intervening at the level of cellular pathways leading to PR death (Van Hooser *et al.* 2000) which in many cases proceeds independently of a specific mutation (Kaur et al. 2011). Neurotrophic factors may have the potential to slow down PR death in retinal degenerations of various origins and preserving the patient's residual vision for an extended period. While not curative in nature, this approach could offer a significant reduction in suffering and increase life quality for patients.

3.2 Neuroprotective factors

In 1990 Faktorovich and co-workers published their pioneering work showing prolonged PR survival in the PR degeneration model Royal College of Surgeons (RCS) rat, after FGF-2 injection (Faktorovich et al. 1990). Since that time, many other successful studies on a variety of neurotrophic factors have been conducted in several animal models of RP (Thanos & Emerich 2005). These include BDNF (Zhang *et al.* 2009), CNTF (Li et al. 2010, Lipinski *et al.* 2011), LEDGF (Baid *et al.* 2013), PEDF (Cayouette *et al.* 1999), granulocyte–macrophage colony-stimulating factor (GM-CSF) (Schallenberg *et al.* 2012) and rod-derived cone viability factor (RdCVF) (Yang *et al.* 2009). Since GDNF is one of the subjects of this thesis, its neuroprotective function in different models of retinal degeneration are reviewed in more detail in the following.

3.2.1 GDNF in retinitis pigmentosa research

GDNF, together with neurturin, artemin and persephin, is a member of the transforming growth factor-β-related neurotrophic factor family. It was first purified and described in 1993, and was shown to promote neuronal survival from the embryonic stage in the central and peripheral nervous system (Lin *et al.* 1993, Homma *et al.* 2000, Sariola & Saarma 2003). Two of its receptors, GDNF receptor α-1 (GFRα1) and GFRα2, were shown to be present in the central nervous system as well as in spinal cord neurons (Jing *et al.* 1996, Yu *et al.* 1998, Liu & Rask-Andersen 2014). Furthermore, GFRα1 was found on neurons of the olfactory system (Marks *et al.* 2012).

In the retina, GDNF is expressed already from the first weeks of embryonic life (Hellmich *et al.* 1996, Nosrat *et al.* 1996). Postnatal, GDNF is synthetized by RMG (Harada *et al.* 2003) and by RPE cells (Ming *et al.* 2009) and its receptors are expressed on RMG (Harada et al. 2003, Hauck et al. 2006b), ganglion cells and PR (Jomary *et al.* 2004, Rothermel *et al.* 2004), although some available data contradict the presence of GDNF receptors on PR (Harada et al. 2003, Hauck *et al.* 2006b).

For the first time, Frasson and coauthors validated GDNF's neuroprotective effect *in vivo* in animal model of RP in 1999. Subretinal injection of GDNF into eyes of rd1 mice achieved spectacular effects in regard to prolonged survival but also function of PR. Moreover, no angiogenic activity or macrophages migration was diagnosed (Frasson et al. 1999a). Since that time many investigations on GDNF's neuroprotection were conducted, investigating different animal models of RP as well as different ways of trophic factor delivery. Overexpression of GDNF in PR or RPE of transgenic rd10 mice, showed significant increase in PR survival as well as function for up to 40 days (Ohnaka *et al.* 2012). First attempts to use adeno-associated virus (AAV) gene transfer to deliver GDNF to the retina were conducted on the S334-ter-4 rat. Subretinal injections of AAV delayed PR cell death for at least 45 day and increased ERG amplitudes (McGee Sanftner *et al.* 2001). A prolonged effect of GDNF rescue on the same rat model was achieved in following studies, injecting a special variant of AAV, capable of efficiently and

selectively transducing RMG. This therapy led to sustained functional PR rescue for more than five months (Dalkara *et al.* 2011). Moreover, combination of AAV neurotrophic factor delivery with gene replacement therapy brought further interesting results suggesting that the combination of both therapies may yield better results than gene therapy of factor application alone. AAV-mediated delivery of GDNF in addition to the X-chromosome linked inhibitor of apoptosis gene delivered to eyes of Prph2Rd2/Rd2 mice and RCS rats prolonged PR survival and preserved their function for up to three and two months, respectively (Buch *et al.* 2006). Non-viral GDNF gene delivery was performed using GDNF-encoding plasmids transferred with electrical devices through ciliary muscles into the eyes of RCS rats. Its expression was confirmed for at least seven months, but PR survival as well as function was preserved for around 50 days (Touchard *et al.* 2012). Another GDNF based approach was intravitreal delivery of embryonic stem cells engineered to secrete GDNF. Tests on S334-ter-4 rats significantly prolonged PR survival for at least three months. Although no immunosuppression was required, several adverse effects, like lens opacities and total retinal detachment, were reported. At the same time, GDNF was increased 10-12 fold in serum samples, raising the danger of systemic negative effects, attributable to long-term exposure to GDNF (Gregory-Evans *et al.* 2009).

Taken together, GDNF seems to be a powerful neurotrophic factor and investigation of its mode of action can shed more light on the molecular pathways leading to PR survival.

3.2.2 Cyr61

Cysteine-rich heparin-binding protein 61 (Cyr61, CCN1, IGF-binding protein 10) is a member of the CCN extracellular matrix protein family and was first investigated in studies on a mouse fibroblast cell line. The Cyr61 gene encodes a 379-amino-acid protein containing 38 cysteine residues (O'Brien *et al.* 1990). Cyr61 is classified as an immediate-early gene, as its mRNA is synthesized within minutes after serum or growth factor (PDGF, FGF2, TGF-β1) stimulation and peaks at 60 - 90 minutes, after which the level of mRNA decreases by transcriptional repression and rapid degradation (Lau & Nathans 1987, O'Brien et al. 1990, Jun & Lau 2011). The protein is synthetized within one to two hours after stimulation and is associated after secretion with the cell surface as well as the extracellular matrix, but it is not detectable in the conditioned medium of stimulated cells (O'Brien et al. 1990, Yang & Lau 1991). Intracellular and cell surface associated Cyr61 has a half-life of around 30 minutes (Lau & Nathans 1987, O'Brien et al. 1990, Yang & Lau 1991) while it has a half-life longer than 24 hours when associated with the extracellular matrix (Yang & Lau 1991).

Cyr61 consists of four domains (Fig. 10). The first domain starts from an N-terminal secretory peptide and shares sequence homology with the N-terminal region of the insulin like growth factor-binding protein (IGFBP) domain. The second domain, von Willebrand factor type C (vWC), is followed by a variable or hinge region, which is highly charged

and does not contain any cysteines. The third domain is designated trombospondin type I repeat (TSR), based on homology. The fourth domain, containing a cysteine knot motif carboxyl-terminal (CT), resembles the CT domains of some other extracellular proteins and is believed to mediate protein-protein interaction. The first three domains are well preserved within the CCN family, while the CT domain varies between the family members (Lau & Lam 1999, Lau 2011).

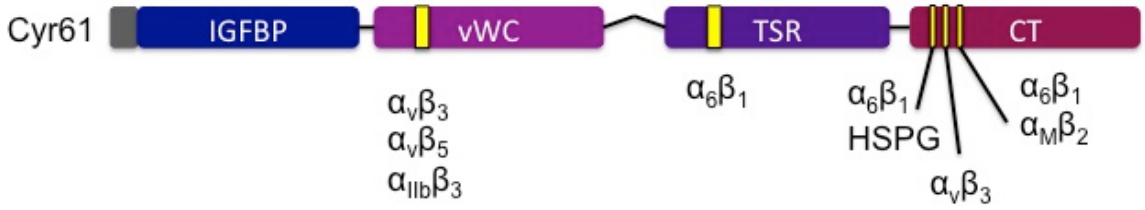

Figure 10. Schematic structure of Cyr61.
Cyr61 consists of four domains: insulin like growth factor-binding protein (IGFBP), von Willebrand factor type C (vWC), trombospondin type I repeat (TSR) and carboxyl-terminal (CT). Binding sides for integrins have been localized on three of the domains. After (Lau 2011).

Expression of *cyr61* is induced as a result of a wide range of different stimuli like serum growth factors (O'Brien et al. 1990), PDGF and FGF-2 (Lau & Nathans 1987), TGF-β1 (Brunner *et al.* 1991), estrogen (Csoregh *et al.* 2009), hypoxia (Shun *et al.* 2011), VEGF (Athanasopoulos *et al.* 2007), UV light (Quan *et al.* 2006), mechanical stretch (Chaqour & Goppelt-Struebe 2006) and inflammatory cytokines such as IL-1 and tumor necrosis factor α (TNF-α) (Gashaw *et al.* 2008).

Cyr61 mediates different cellular responses by binding to a wide range of integrins and heparin sulfate proteoglycans (HSPGs) (Yang & Lau 1991, Lau 2011). Possible binding regions for some of the different Cyr61 integrin receptors have been identified in three of its domains (Fig. 10). Depending on a specific receptor type, Cyr61 promotes different cellular responses. For instance, binding of Cyr61 to $\alpha_v\beta_3$ integrin on endothelial cells (Leu *et al.* 2002) and breast cancer cells (Menendez *et al.* 2005) increases their survival, while binding of Cyr61 to $\alpha_6\beta_1$ and syndecan4 on fibroblasts can initiate apoptosis (Todorovic *et al.* 2005). By virtue of it's binding to other integrins, Cyr61 can also influence cell adhesion ($\alpha_6\beta_1$ and HSPGs, $\alpha_v\beta_3$), migration ($\alpha_v\beta_5$), differentiation ($\alpha_v\beta_3$), invasiveness ($\alpha_v\beta_3$, $\alpha_v\beta_5$) and senescence ($\alpha_6\beta_1$ and HSPGs) (Leask & Abraham 2006, Lau 2011). Interestingly, Cyr61 was also shown to induce MMP13 expression in chondrosarcoma cells, implying possible effects on extracellular matrix organization (Tan *et al.* 2009).

Cyr61 is highly upregulated during mouse embryogenesis and is associated with neuronal, skeletal and cardiovascular development (O'Brien & Lau 1992). It is also essential for proper placental development as well as vascular integrity (Mo *et al.* 2002). Consequently, disruption of Cyr61 gene is embryonically lethal (Mo et al. 2002). Cyr61 can exert strong angiogenic properties (Brigstock 2002, Harris *et al.* 2012) and elevated

Cyr61 levels are associated with retinal vascular alterations in diabetic retinopathy (You *et al.* 2009, You *et al.* 2010, You *et al.* 2012). On the other hand, in an animal model of retinopathy of prematurity, overexpression of Cyr61 improved retinal vascularization and was suggested as a potential therapeutic factor (Hasan *et al.* 2011). Moreover, Cyr61 supported proper perfusion of the vasculature in peripheral ischemic disease, making it a possible option for ischemia therapy development (Fataccioli *et al.* 2002, Rayssac *et al.* 2009).

In the prosurvival context, Cyr61 strong antiapoptotic capacities were shown on a variety of tumour cells (Menendez et al. 2005, Yoshida *et al.* 2007, Sabile *et al.* 2012, Zhang *et al.* 2012c), but at this point Cyr61 had not been investigated as a potential neuroprotective factor. Sparse information in the neuronal context reveals that *cyr61* is expressed in primary neurons and glial cells in response to estrogen treatment (Csoregh et al. 2009) as well as in a hippocampal cell line in response to FGF-2 (Chung & Ahn 1998). On the other hand, downregulation of Cyr61 was observed during infantile Batten disease, characterised by neuronal cell degeneration including retinal degeneration (Haltia 2006, Qiao *et al.* 2007). Cyr61 was also shown to have an influence on the development of the proper dendritic branching pattern of neuronal cells (Malik *et al.* 2013).

Taken together, not much is known about Cyr61 a possible player in neuroprotection, which made it a fascinating factor to study in this context.

II. MATERIALS AND METHODS

A. Materials

A.1 Chemicals, reagents, commercial kits, factors and enzymes

In this study dH2O is referred to deionized water, ddH2O is referred to ultra-pure water (Milli-Q Biocel, Millipore, Billerica, MA, USA). The chemicals were bought from Sigma, Steinheim, Germany, if not stated otherwise.

Name	Manufacturer
2-Iodacetamid (IAA)	Merc, Darmstad, Germany
Acrilamide	Serva, Heidelberg, Germany
Agaroze	Biozym, Olderdorf, Germany
BCA protein Assay	Thermo Scientific, Waltham, USA
Blotting grade milk powder	BioRad, Munich , Germany
Bovine serum albumin (BSA, lyophilized)	Sigma, Steinheim, Germany
Bradford Reagent	Bio-Rad, Munich , Germany
Calcein	Invitrogen, Carlsbad, USA
Complete protease inhibitor cocktail	Roche, Mannheim, Germany
1,4-Dithiothreit (DTT)	Merc, Darmstad, Germany
4',6-Diamidino-2-Phenylindole, Dihydrochloride (DAPI)	Life Technologies, Carlsbad, USA
DNase	Sigma, Steinheim, Germany
Endoproteinase Lys-C	Sigma, Steinheim, Germany
Glycerol	Merc, Darmstad, Germany
Hoechst 33342	Life Technologies, Carlsbad, USA
High-performance liquid chromatography (HPLC) water	Merc, Darmstad, Germany
Hydroxypropyl methylcellulose (Methocel™ 2%)	OmniVision, Puchheim, Germany
NaCl	Merc, Darmnstad, Germany
NE-PER Nuclear and Cytoplasmic Extraction Reagents Kit	Thermo Scientific, Waltham, USA
Nonidet-P40 (NP-40)	Roche, Mannheim, Germany
Normal goat serum (NGS)	Invitrogen, Carlsbad, USA
Orange G	Sigma, Steinheim, Germany
Papain	Worthington, Lakewood, USA
Paraformaldehyde (PFA)	Sigma, Steinheim, Germany
Peanut agglutinin	Vector Laboratiories, Peterborough, UK
Phosphatase inhibitor cocktail P2, P3	Sigma, Steinheim, Germany
Propidium iodide	Life Technologies, Carlsbad, USA
Proteinase K	MP Biomedicals, Santa Ana, California, USA
Recombinant Human Cysteine-rich angiogenic inducer 61 (Cyr61/CCN1)	R&D Systems, Minneapolis, MN USA
Recombinant Human Glial-Derived	Peprotech, Princeton, USA

Neurotrophic Factor, ATF-1 (GDNF)	
RevertAid First Strand cDNA Synthesis Kit	Thermo Scientific, Waltham, USA
RNaseZap® RNase decontamination solution	Life Technologies, Carlsbad, USA
Serva Clear Stain	Serva, Heidelberg, Germany
Sodium dodecyl sulfate (SDS)	Serva, Heidelberg, Germany
Sucrose	Merc, Darmstad, Germany
Trypsin	Sigma, Steinheim, Germany
Tris-(hydroxymethyl)-aminomethan (Tris)	Serva, Heidelberg, Germany
Triton X-100	Merck, Darmnstad, Germany
tropicamide eye drops (Mydriaticum Stulln™)	Pharma Stulln, Germany
TRIzol®	Life Technologies, Carlsbad, USA
Urea	Merc, Darmstad, Germany
Purisept	PuriCore Labcaire Systems, Clevedon, UK

A.2 Consumables

Name	Manufacturer
96 well plates	BD Bioscience, San Jose, USA
96 well plates 4titued®	4titued®, Berlin, Germany
Cell culture plates 6cm Ø	Thermo Scientific, Waltham, USA
Cell culture plates 6-well, 12-well and 3cm Ø	BD Bioscience, Heidelberg, Germany
Cell scraper 25 cm	Sarstedt, Nümbrecht, Germany
Cover glass 24 x 50mm; No. 1.5	VWR Interrnational, Darmstadt, Germany
Disposal bags (sterile)	Carl Roth, Karlsruhe, Germany
ECL+ enhanced chemiluminescence films	GE Healthcare, Buckinghamshire, UK
Falcon conical tubes	BD Bioscience, Heidelberg, Germany
Flasks T-25, T-75, T-175	Greiner, Frickenhausen, Germany
Fluoro Save Reagent	Calbiochem, Merc, Darmstad, Germany
Microscope slides Super Frost Plus®	Menzel, Braunschweig, Germany
Nanosep® Centifugal Devices	Pall Life Sciences, New York, USA
Needels, sterile, Sterican®	Braun, Melsungen, Germany
Neubauer Chamber Cell Counting	Celeromics, Grenoble, France
Nitril gloves, powder-free	Exceed, The Hauge, The Netherlands
PVDV membrane	GE Healthcare, Buckinghamshire, UK
Petri dishes	Greiner, Frickenhausen, Germany
Pipetboy	Eppendorf, Hamburg, Germany
Pipetman 2µl 10µl, 20µl, 100µl, 200µl, 1000µl	Eppendorf, Hamburg, Germany
Pipette tipps 10µl, 20µl, 200µl, 1000µl	StarLab, Hamburg, Germany
Plastic pipettes, Cellstar® 2ml, 5ml, 10ml, 25ml, 50ml	Greiner bio-one, Kremsmünster, Austria
Polycarbonate membranes Costar	Corning Incorporated, Corning, NY, USA
Polypropylene conical tube, Falcon 15ml, 50ml	BD Bioscience, Heidelberg, Germany
Protein LoBind Tubes	Eppendorf, Hamburg, Germany
Proteome ProfilerTM Mouse Angiogenesis Array	R&D Systems, Minneapolis, MN USA

Tissue-Tek	Sakura, staufen, Germany

A.3 Laboratory equipment

Instrument	Manufacturer
78 diopter double aspheric lens (Volk Optical™)	Mentor, Ohio, USA
Agfa Curix 60 Developer	Agfa, Mortsel, Belgium
Autoclave Tuttnauer Systec 5075 ELV	Systec, Wettenberg, Germany
Camera Easy 400K	Herolab, Wiesloch, Germany
Cell incubator	Sanyo Scientific, San Diego, USA
Centrifuge 3-18K	Sigma Laborzentrifugen, Osterode, Germany
Centrifuge 5415R	Eppendorf, Hamburg, Germany
Centrifuge 5430R	Eppendorf, Hamburg, Germany
Cryotome CM 180	Leica Microsystems, Wetzlar, Germany
Dissection microscope	Leica Microsystems, Wetzlar, Germany
Fluorescent microscope DM IRE2	Leica Microsystems, Wetzlar, Germany
Laminar flow hood	BDK, Sonnenbühl-Genkingen, Germany
LightCycler© 480 System	Roche, Mannheim, Germany
Liquid Nitrogen Tank Chronos	Messer, Sulzbach, Germany
Inlab micro pH Electrode	Mettler-Toledo, Greifensee, Switzerland
Inverse fluorescence microscope DMIRE2	Leica Microsystems, Wetzlar, Germany
Magnetic stirrer RH basic	IKA Labortechnik, Staufen, Germany
Mass spectrometer Orbitrap XL	Thermo Fisher Scientific, Waltham, USA
Milli-Q Biocell	Millipore, Billerica, USA
Mini Trans Blot Electrophoretic Transfer Cell	BioRad, Munich , Germany
Mr. Frosty Freezing Container, Nalgene™	Thermo Scientific, Waltham, USA
NanoDrop™	Thermo Fisher Scientific, Waltham, USA
PCR machine Peqstar	Peqlab, Erlangen, Germany
Power supply PowerPac 300	Bio-Rad, Freiburg, Germany
Power supply PowerPac HC	Bio-Rad, Freiburg, Germany
Scanner Epson Perfection 1240V	Epson, Suwa, Japan
Shaker Duomax 1030	HeidolphInstruments, Schwabach, Germany
Shaker KS260 basic	IKA Labortechnik, Staufen, Germany
Synergy HT microplate reader	Biotek, Bad Friedrichshall, Germany
Thermomixer comfort	Eppendorf, Hamburg, Germany
Ultra-low temperature freezer (-80°C)	Sanyo Scientific, San Diego, USA
Ultrasonic bath Transsonic 310/H	ElmaUltrasonic, Singen, Germany
Ultraspec 3300 pro UV/Vis photometer	GE Healthcare, Buckinghamshire, UK
UV transilluminator UVT-40M	Herolab, Wiesloch, Germany
Vortex Genius 3	IKALabortechnik, Staufen, Germany
Spectralis HRA+OCT™, scanning-laser ophthalmoscope	Heidelberg Engineering, Heidelberg, Germany

A.4 qPCR Primers

Name	Sequence (5'-3')	Tm*
Collagen type III, alpha I (COL3A1)_Forward	AATGATGGTGCCCGAGGAAG	60°C

Collagen type III, alpha I (COL3A1)_Reversed	AGCAGGACCCATTTCACCTT	60°C
family with sequence similarity 3 (FAM3C)_Forward	GTGGGGAGGAAATGTGGCT	70°C
family with sequence similarity 3 (FAM3C)_Reversed	TCAGTCTTGCTTCTGGGGGA	70°C
vascular endothelial growth factor (VEGF)_Forward	CCACCATGCCAAGTGGTCC	60°C
vascular endothelial growth factor (VEGF)_Reversed	CACTCCAGACCTTCGTCGTT	60°C

* Tm – melting temperature

A.5 Antibodies for immunofluorescence and for western blotting

Antibody	Species	Dilution	Number	Supplier
pStat3	rabbit	1:2000	9145	Cell Signaling, Massachusetts, USA
pStat3	rabbit	1:1000	9131	Cell Signaling, Massachusetts, USA
Stat3	rabbit	1:2000	4904	Cell Signaling, Massachusetts, USA
pAkt	rabbit	1:2000	4060	Cell Signaling, Massachusetts, USA
Akt	rabbit	1:2000	4691	Cell Signaling, Massachusetts, USA
pErk1/2	rabbit	1:2000	4370	Cell Signaling, Massachusetts, USA
Erk1/2	rabbit	1:1000	9102	Cell Signaling, Massachusetts, USA
α-tubulin	rat	1:10000	T6074	Abcam, Cambridge, England
b-Actin	mouse	1:10000	A-5441	Sigma, Steinheim, Germany
PARP	mouse	1:2500	NB100-64828	Novus Biologicals, Colorado, USA
Glutamin Synthetase (GS)	mouse	1:1000	610517	BD Transduction Lab, Heidelberg, Germany
Cone arrestin	rabbit	1:10000	AB15282	Millipore, Billerica, USA
Recoverin	rabbit	1:3000	AB5585	Millipore, Billerica, USA
Alexa fluor 488	rabbit	1:1000	A12379	Life Technologies, Carlsbad, USA
Alexa fluor 568	mouse	1:1000	F24630	Life Technologies, Carlsbad, USA

A.6 Animals, primary cell cultures and cell lines used in the study

The day of birth was defined as postnatal day (PN) 0. Animals were maintained with free access to water and food in an air-conditioned room on a 12-h light–dark cycle.

All experiments were carried out in accordance with applicable German laws, with the European Council Directive 86/609/EEC, and with ARVO Statement for the Use of Animals in Ophthalmic and Vision Research.

Cell/tissue type	Culture type	Species	Supplier
ARPE19	Cell line	Human retinal pigment epithelium cell line	LGC Standards GmbH, Wesel, Germany
MIO-M1	Cell line	Human Retinal Müller glial cell line	kindly provided by Astrid Limb (Moorfields Hospital, London)
Mouse retinal Müller glial cells (mRMG)	Primary cell culture	hGFAP-eGFP transgenic mice on C57BL6 background	kindly provided by Magdalena Götz (Institute of Stem Cell Research, Helmholtz Zentrum München, Germany)
Photoreceptors (PR)	Primary cell culture	Pig	local slaughterhouse
Retinal pigment epithelial cells (RPE)	Primary cell culture	Pig	local slaughterhouse
Retinal Müller glial cells (RMG)	Primary cell culture	Pig	local slaughterhouse
Retinal explants	Organotypic retinal culture	C3H/HeJ ($Pde6b^{rd1}$) mice	Jackson Laboratories, Bar Harbor, USA
Eyes	*In vivo* studies	S334ter rats	Xenogen Biosciences, San Francisco, USA

A.7 Media, buffers and standard solutions

A.7.1 Media and antibiotics for cell and tissue culture

Medium	Components
Medium for cell lines: ARPE19 and MIO-M1	Dulbecco's modified Eagle's medium (DMEM) (Gibco, Paisley, UK)
Medium for primary mRMG, porcine RMG and porcine RPE cells	10 % Fetal bovine serum (FBS) (Gibco, Paisley, UK) 1% penicillin/streptomycin (Pen Strep) (Gibco, Paisley, UK)
Medium for porcine RMG for analysis on Orbitrap XL	Dulbecco's modified Eagle's medium (DMEM) without phenol red (Gibco, Paisley, UK)
Medium for primary PR	Dulbecco's Modified Eagle Medium: Nutrient Mixture F-12 (DMEM/F12) (Gibco, Paisley, UK) 10% FBS 1% penicillin/streptomycin
Medium for retinal explant culture (R-16 serum-free medium)	R-16 medium (Gibco, Paisley, UK) 0.1µg/ml Biotin

List of supplements to R-16 serum-free medium (supplemented medium)	1µg/ml Ethanolamine 40nM $NaSeO_3$ x $5H_20$ 5nM $MnCl_2$ x $4H_20$ 20nM $CuSO_4$ x $5H_20$ 32.5mM $NaHCO_3$ 0.2% BSA 10µg/ml transferrin 0.0063µg/ml progesteron 2µg/ml insulin 0.002µg/ml thyroid hormone T3 0.02µg/ml corticosterone 2.77µg/ml thiaminHCl (vitamin B_1) 0.31µg/ml vitamin B_{12} 0.045µg/ml α-LipoicAcid =Thiotic Acid 0.1µg/ml retinol 0.1µg/ml retinyl acetate 1µg/ml DL-tocopherol 1µg/ml tocopherylacetat 1µg/ml linoleic acid 1µg/ml linolenic acid 7.09µg/ml L-cysteineHCl 1µg/ml glutathione 50µg/ml Na-puryvate 25µg/ml glutamine 100µg/ml vitamin C
Serum-free medium for RMG and RPE	DMEM 1% penicillin/streptomycin
Serum-free medium for PR	DMEM/F-12 1% penicillin/streptomycin
Trypsinization	Tripsin (Gibco, Paisley, UK)
Washing	Dulbecco's Phosphate-Buffered Saline (DPBS) (Gibco, Paisley, UK) ddH_20 autoclaved

A.7.2 Buffers and reagents for primary cell isolation

Name	Components
Dissociation buffer for porcine RPE	1mM Ethylenediaminetetraacetic acid (EDTA) in DPBS 260 mM L-Cys 100 µg/ml BSA 2.86 units of activated papain
Ringer's solution for porcine and mouse RMG	125.4mM NaCl 3.6mM KCl 1.2mM $MgCl_2$ 22.6mM $NaHCO_3$ 0.1mM NaH_2PO_4 0.4mM $NaHPO_4$ 1.2mM Na_2SO_4 10mM Glucose 2.5mM EGTA

Activating solution for papain	pH 7.4 1.1mM EDTA 5.5mM cystein 0.067mM β-mercaptoethnol pH 6.2

A.7.3 Solutions for histology and immunofluorescence methods

Solution	Components
4% paraformaldehyde (PFA)	4g of PFA 50ml ddH_2O 50ml 0.2 PB
0.2M Phosphate Buffer (PB)	86.84g Na2HPO4.7H20 10.48g NaH2PO4.H2O up to 2 litters (L) of dH_2O 10M HCl to acquire pH7.4
Blocking solution for ICC	10% NGS 0.5% Triton X DPBS
Blocking solution for IHC	10% NGS 1% BSA 0.5% Triton X 0.1M PB (pH7.4)
ICC primary antibody buffer	10% NGS 0.5% Triton X DPBS
ICC secondary antibody buffer	3% NGS 0.5% Triton X DPBS
IHC antibody buffer	3% NGS 1% BSA 0.5% Triton X 0.1M PB (pH7.4)
Permeabilization solution for TUNEL	0.1% Trition X 0.1% sodium citrate,
DPBS-Triton X	0-5% Triton X DPBS

A.7.4 Buffers and standard solutions for protein biochemistry

Lysis buffers

Name	Components
Lysis buffer I	1% DM in 1% TBST
Lysis buffer II	50mM Tris, pH 7.4 250mM NaCl 25mM EDTA 1% NP-40 10% glycerol
Radioimmunoprecipitation assay buffer (RIPA) buffer	50mM Tris-Hcl pH 7.4 150mM NaCl 0.1% SDS

	0.5% Sodium Deoxycholate 1% NP-40

Solutions for SDS gels

Gel solution for SDS separating gel (10 ml)	**10%**
ddH_2O	4 ml
Acrylamide:bisacrylamide (37.5%:1%)	3.3 ml
1.5 M Tris-HCl pH 8.8	2.5 ml
10% SDS	100 µl
10% APS	50 µl
TEMED	20 µl
Gel solution for SDS stacking gels (5 ml)	**4%**
ddH_2O	3.5 ml
Acrylamide:bisacrylamide (37.5%:1%)	700 µl
1.5 M Tris-HCl pH 6.8	700 µl
10% SDS	50 µl
10% APS	50 µl
TEMED	20 µl

Buffers for SDS-Page and Western Blotting

5x SDS sample buffer	5 % SDS 250 mM Tris-HCl pH 6.8 500 mM β-Mercaptoethanol 50 % Glycerol 0.4 % Bromphenol blue
Blocking soultuion for immunoblotting	TBST 5 % Milk powder
Blotting buffer	12 mM Tris base 96 mM Glycine 20 % Methanol
SDS Electrophoresis buffer	50 mM Tris base 384 mM Glycine 0.2 % SDS
Stripping buffer	100mM 2-Mercaptoethanol 2% SDS 62.5mM Tris-HCl pH6.7
Tris-buffered saline (TBS)	6.05g Tris 8.76g NaCl fill up to 1L with dH_2O
Tris buffer saline Tween (TBST) 1%	50 mM Tris-HCl pH7.5 150 mM NaCl 5% of Tween-20

Buffers for FASP digestion

Urea (UA) buffer	8M urea in 0.1M Tris/HCl pH 8.5
Ammoniumbicarbonat (ABC) buffer	50mM ABC in HPLC water

A.7.5 Buffers and solutions for molecular biology

TBE	89mM Tris 89mM boric acid 2mM EDTA
1% agarose gel	3g agarose 300ml TBE buffer 9µl Serva Clean Stain
6x loading buffer	0 mM Tris-HCl 0.15% Orange G 60% Glycerol 60mM EDTA

A.8 Software and databases

Software	Supplier
Adobe Illustrator CS	Adobe Systems, San Jose, USA
Adobe Photoshop CS5	Adobe Systems, San Jose, USA
EndNote	Thomson Reuters
GraphPad Software	Statcon
ImageJ (Fiji)	W. Rasband
LightCycler© 480 software	Roche
Mascot 2.4	Matrix Science, Boston, USA
MS Office 2003 (Word, Excel, Powerpoint)	Microsoft
Progenesis LC-MS	Non-Linear Dynamics, Newcastle, UK
Proteome discoverer 1.3	Thermo Fisher Scientific, Waltham, USA

Database	Link
NCBI	http://www.ncbi.nlm.nih.gov/
NCBI Blast	http://blast.ncbi.nlm.nih.gov/Blast.cgi
NCBI Nucleotide	http://www.ncbi.nlm.nih.gov/entrez/query.fcgi?db=nucleotide
NCBI Protein	http://www.ncbi.nlm.nih.gov/entrez/query.fcgi?db=protein
NCBI PubMed	http://www.ncbi.nlm.nih.gov/entrez/query.fcgi
Swiss-Prot	http://us.expasy.org/sprot/
GenCards®	http://www.genecards.org/

B. Methods

B.1 Preparation and maintenance of primary retinal cell cultures

B.1.1 Mouse retinal Müller glial cells

Mouse RMG (mRMG) cells were isolated from GFAP-eGFP/C57BL6 eyes, as described before (Hauck *et al.* 2008) with modifications. The mice were sacrificed and their eyes were enucleated shortly after the animals' death. Eyeballs were disinfected with 80% ethanol and replaced into DPBS for dissection. Next, retinas were placed in an eppendorf tube washed two times with Ringer's solution and treated with 2.2 units of activated papain (30min at 37˚C in activation solution) for 45min at 37˚C. Thereafter, the papain was stopped with DMEM medium containing 10% FBS and 150 units of DNAse and the tissue was carefully triturated into single cells. Then, cells were centrifuged (150 x g for 5min), resuspended in fresh medium DMEM containing 10% FBS and 1% penicillin/streptomycin, plated on 12 well plates and cultured for 7 days (d7) in 5% CO_2 at 37°C.

Before stimulation, cells were washed and starved in the serum-free medium for 24h. Next, new medium containing 0,1µg/ml GDNF, or medium without supplementation (for control cells) was applied for an additional 24h. Following stimulation, supernatants were collected and filtered (cut-off 0.2µm) to remove large cellular debris and residual cells (supernatant samples). Cells were lysed in 100µl of lysis buffer, including complete protease inhibitor cocktail and phosphatase inhibitor cocktails 2 and 3 (cell lysates samples). Supernatants and cell lysates were stored at -80°C until further analyses.

B.1.2 Porcine retinal cells

The porcine eyes were enucleated within 5min after death of the animals and kept on ice in CO_2-independent medium until further use. The eyeballs were disinfected in 80% ethanol followed by Purisept, by immersion in each of them for 5min, than the eyeballs were placed in a fresh, sterile CO_2-independent medium. Subsequently, the eyeballs were cut around the iris and the vitreous body was discarded. The retina was dissected for further isolation of photoreceptors (PR) and retinal Müller glial cells (RMG) while obtained eyecup served to isolate retinal pigment epithelium (RPE) cells.

To control purity of each type of cell culture, representative samples from PR, RMG and RPE isolation were analysed by western blot. Marker proteins for each cell type were assessed by immuodetection: recoverin for PR, vimentin for RMG and RPE65 for RPE (Fig. 11). Given that different cultivation periods were used for each cell type (PR – 2 days in culture, RMG – 8-11 days in culture, RPE – up to 5 days in culture) vimentin was chosen over glutamine synthetase (GS) for RMG identification. This stems from the fact that RMG in culture drastically decrease GS expression, while vimentin stays at around the same level (Hauck *et al.* 2003). On the presented picture (Fig. 11), RPE fraction 1 did

not achieve purity demands (too high RMG input in relation to RPE cells) and was excluded from further analysis.

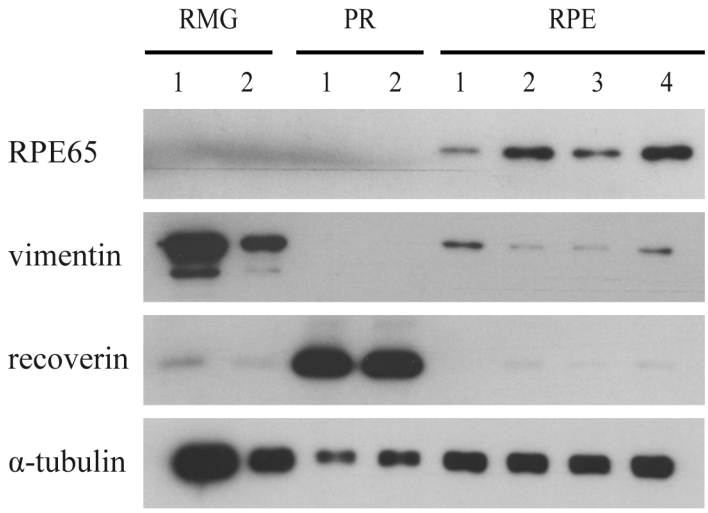

Figure 11. Three retinal primary cell types: RMG, PR and RPE, could be prepared in high purity.
Representative aliquots (10µg) from each primary cells isolation were blotted using wet transfer onto one membrane and protein markers for retinal Müller glial cells (RMG; vimentin), photoreceptors (PR; recoverin) and retinal pigment epithelium (RPE; RPE65) were visualized by immunodetection. α-tubulin serves as a loading control.

B.1.2.1 Photoreceptors

Primary porcine photoreceptor cultures were prepared according to two protocols. The first protocol (protocol I) was following protocol published before (Hauck et al. 2008). The second protocol (protocol II) was a modification of protocol I with the objective of increasing purity of PR preparations, as published recently (Kucharska *et al.* 2014).

The major blood vessels were dissected from obtained retinal tissue, and the remaining tissue was cut into small pieces and distributed into 15ml falcon tubes (1,5 eyeball per falcon tube). Than retina was washed two times with 1ml of Ringer's solution. For retinal dissociation, the tissue was incubated with 250µl Ringer's solution containing 2.86 units of activated papain for 12min at 37˚C. Next, the digestion was stopped with 1ml of DMEM Nut MixF12 containing 10% FCS. Subsequently, 150 units of DNAse in activation solution were applied to the tissue and the whole falcon tube was shaken 20 times to release PR. Then, the falcon tubes were left for 5min to sediment only partly dissociated tissue and eventually the supernatant containing the floating PR was collected into a new 50ml falcon tube. Only this first fraction was used for protocol II. In contrast, protocol I included a second isolation step to increase the yield of PR isolation at the cost of purity. Specifically, 1ml of medium enriched in serum was added to the partly dissociated tissue in falcon tubes and the tissue was mechanically dispersed, by aspirating it once through a fire-polished glass Pasteur pipette. The resulting second supernatant with floating PR was collected as a second fraction and added to the first PR fraction.

The PR cells collected into 50ml falcon tube (following protocol I or II), were pelleted by centrifugation (150 x g for 5min), resuspended in fresh DMEM/F-12 medium containing 1% penicillin/streptomycin and 2% FCS (according to the protocol I) or 10% FCS (according to the protocol II), counted and between $16*10^5$ and $22.4*10^5$ cells were plated onto coated 6cm dishes (see B.1.2.1.1). Additionally, 6cm dishes were prepared, to control viability as well as purity of PR fractions. The remaining tissue in 15ml falcons was used to obtain RMG (see B.1.2.2).

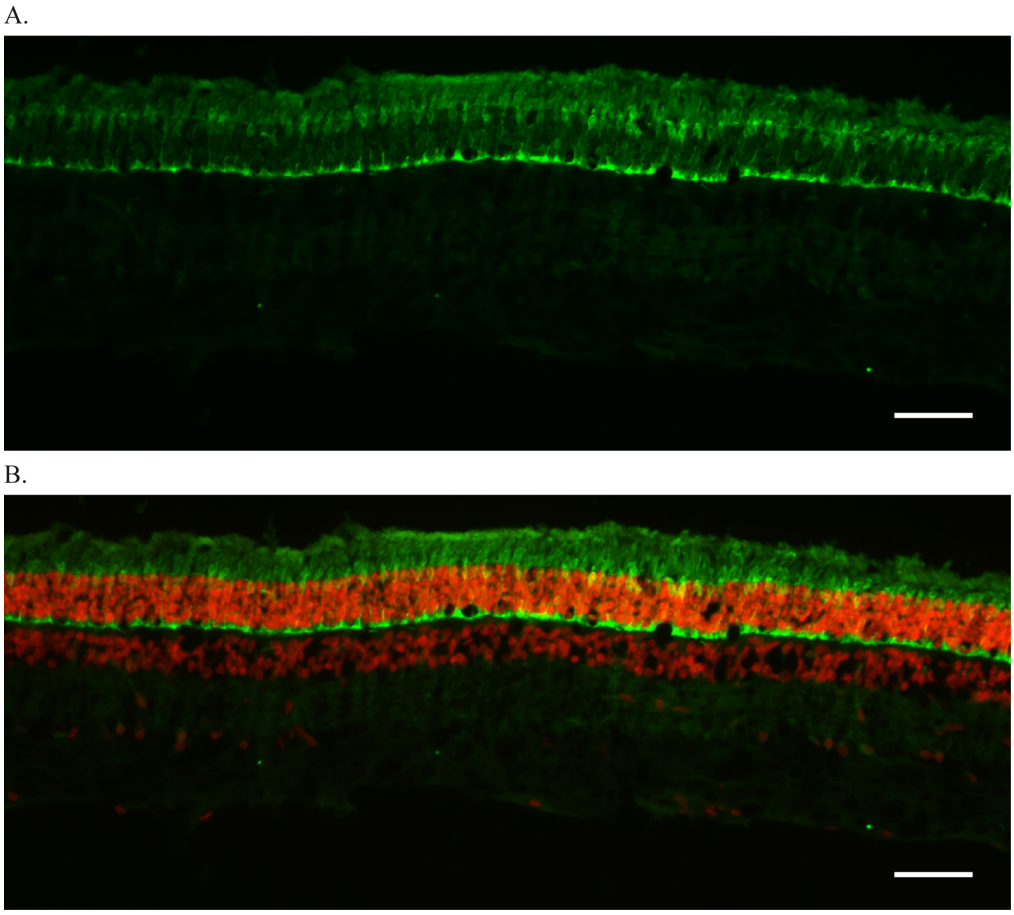

Figure 12. Specificity of recoverin to stain photoreceptors in porcine retinal tissue.
Porcine cryosections were stained with recoverin to visualize PR (green, panel A). Panel B shows overlay of panel A and nuclei visualized with Hoechst 33342 (red). Scale bars 100µm

Isolated PRs were serum starved for 2h or 24h, for protocols II and I, respectively. Afterwards, cells were stimulated with 1µg/ml Cyr61 for the indicated time points.

Subsequently, the medium was discarded and cells were lysed with RIPA buffer supplemented with complete protease inhibitor cocktail and phosphatase inhibitor cocktails 2 and 3. The samples were kept on ice with occasional vortexing. Lysates were centrifuged at 16000 x g for 30min and supernatants transferred to fresh eppendorf tubes. Total protein content was determined using the BCA protein assay before samples were stored at -80˚C until further use.

The viability of PR, obtained with protocol II, was controlled two times: the first time right after the isolation (using a cell counting chamber) and the second time at the day of the experiment (staining of the cells on 6cm dishes). To observe the amount of living and dead cells, PR were incubated with calcein, which stains living cells, or propidium iodide (PI), which stains dead cells. These two probes can be distinguished based on their different excitation/emission characteristics. In this way, high viability of PR preparation could be shown (Fig. 19).

In addition, the purity of PR fraction obtained with protocol II was controlled in two ways: by western blotting (see Fig. 11) and by immunocytochemistry (ICC) using the marker proteins recoverin (for PR) and GS or vimentin (for RMG). Recoverin was used as a PR maker, as in porcine retina it is only present in PR (Fig. 12) (Guduric-Fuchs *et al.* 2009, Ghosh & Arner 2010, Johansson *et al.* 2010). For ICC, at the day of the experiment, the cells were fixed with 4% PFA for 15min in RT, washed 3 times with DPBS and blocked for 1h at room temperature (RT) with blocking solution for ICC. Primary and secondary antibodies were diluted in ICC primary antibody buffer and ICC secondary antibody buffer, respectively, to visualize RMG cells and with Hoechst 33342 (to stain nuclei). Images were required at 100 or 200-fold magnification with a Leica DM IRE2 fluorescent microscope (Fig. 22).

Coating of 6 cm dishes for PR culture

For culturing PR it is crucial to prepare an appropriate coating of the culture dishes, otherwise the cells will not attach properly and will be washed with first changing of the medium. For effective coating, firstly, dishes were incubated with 2µg/cm^2 of p-Lysin for 3h at 37°C. Next, dishes were washed with 2ml of autoclaved ddH_2O and coated with 1µg/cm p-Laminin at 37°C overnight. Finally, the dishes were washed 3 times with 3ml of ddH_2O and left under UV light to dry out. Ready dishes were closed in sterile disposal bags and stored at 4°C for up to 2 weeks.

B.1.2.2 Retinal Müller glial cells

The remaining retina in 15ml falcon tubes after PR isolation (see B.1.2.1) was resuspended with DMEM containing 10% FCS and 1% penicillin/streptomycin and plated onto 10cm petri dishes. The next four days, non-attached cells were removed by agitation and changing the medium. Cells were cultured for up to 11 days to achieve confluence higher than 75%.

At the day of the experiment, cells were washed and starved for 2h in the serum-free medium. Next, cells were stimulated with medium supplemented with 1µg/ml Cyr61 for indicated periods of time. Afterwards, supernatant was discarded and cells were lysed with RIPA buffer supplemented with complete protease inhibitor cocktail and phosphatase inhibitor cocktails 2 and 3. Next, lysates were kept on ice for 30min with occasional vortexing. Eventually, lysates were cleared by centrifugation (16000 x g for

30min) and the protein content was measured using bicinchoninic acid (BCA) protein assay. The samples were stored at -80˚C for further analysis.

B.1.2.3 Retinal pigment epithelium cells

The obtained eyecups (see B.1.2), with RPE still attached to the inner surface, were incubated with 1mM EDTA in DPBS for 15min at RT to discard residues of RMG and PR outer segments. Then, the eyecups were incubated with dissociation buffer for 25min in 37˚C. RPE cells were dissociated by gentle buffer agitation, collected, centrifuged (150 x g for 5min), resuspended and plated on 6-well dishes. Every day the non-attached cells were removed by mild agitation and medium changes. Cells were incubated up to 5 days to achieve >75% confluence.

Prior to experiments, cells were washed and starved in the serum-free medium for 2h followed by 1µg/ml Cyr61 medium supplementation for the indicated time periods. Next, the medium was discarded and cells were lysed with RIPA buffer supplemented with complete protease inhibitor cocktail and phosphatase inhibitor cocktails 2 and 3. Following, cells were incubated on ice for 30min with occasional vortexing. Finally lysates were cleared by centrifugation (16000 x g for 30 min) and stored at -80˚C for future analysis. The protein content was evaluated using BCA protein assay.

B.2 Maintenance and growth of retinal cell line cultures

The human RPE cell line - ARPE19 (Dunn *et al.* 1996) and the human RMG cell line - MIO-M1 (Limb *et al.* 2002) were grown in DMEM containing 10% FCS and 1% penicillin/streptomycin in 37˚C and 5% CO_2. Cells were split 1:5 upon reaching 80% or 100% confluence, for MIO-M1 or ARPE19, respectively First the old medium was removed and cells were washed with pre-warmed DPBS (at 37˚C). Then, 2ml of trypsin/EDTA (for a 10cm dish) were applied and cells were incubated at 37˚C for 5min. Finally, the trypsin activity was stopped by addition of 10ml DMEM containing 10% FCS and cells were collected by centrifugation at 150 x g for 3min at RT. The pellet containing cells was resuspended in 5ml of fresh medium and transferred into new culture dishes with fresh medium.

For the generation of cryo-stocks cells were harvested using trypsin/EDTA and centrifuged as described above. The pelleted cells were resuspended in FCS supplemented with 10% DMSO and 1ml of the suspension was distributed into cryo-tubes. Cryo-tubes were placed in Nalgene™ frosty freezing holder filled with isopropanol and left at -80˚C overnight. For long-term storage, cryo stocks were placed in a cryo tank filled with liquid nitrogen. To thaw the cells, cryo stocks were kept in a water bath (37˚C) with mild agitation. Shortly after thawing, a fresh medium containing serum and antibiotic was added and cells were plated onto a new culture dish.

B.2.1 Cell line stimulations

ARPE19 and MIO-M1 cells were seeded in 6 well plates (for experiments in which the whole cell lysate was analysed) or in 6cm dishes (for experiments in which nuclear and cytosolic fractions were analysed separately) und cultivated until confluence >75% was reached. Before each experiment, cells were washed and starved for 3h in the serum-free medium. Thereafter, cells were stimulated with 1µg/ml of Cyr61 for indicated periods of time. For preparation of whole cell lysates, supernatants were discarded and cells were lysed by adding 60-100µl of lysis buffer (1% DM in 1% TBS-T,) including complete protease inhibitor cocktail and phosphatase inhibitor cocktails 2 and 3. For separation into nuclear and cytosolic fractions, supernatant was discarded and cellular fractions were prepared with NE-PER Nuclear and Cytoplasmic Extraction Reagents Kit as described in the manufacturer's protocol. First, cells were trypsinized, resuspended in ice cold DPBS, transferred to 1.5ml eppendorf tubes and pelleted via centrifugation at 800 x g for 3min. Next, supernatant was discarded and 200µl cytoplasmic extraction reagent I supplemented with complete protease inhibitor cocktail and phosphatase inhibitor cocktails 2 and 3 was added to the pelleted cells. After vigorous vortexing, samples were incubated on ice for 10min. Subsequently, 11µl of cytoplasmic extraction reagent II was added to the samples and after 1min incubation on ice samples were centrifuged for 5min at 16000 x g. Cytoplasmic fractions (supernatant) were transferred to fresh eppendorf tubes and stored in -80°C until further analysis. The insoluble fraction was resuspended in 100µl ice-cold nuclear extraction reagent supplemented with complete protease inhibitor cocktail and phosphatase inhibitor cocktails 2 and 3 and kept on ice for 40min with very intense vortexing every 10min. Finally, samples were centrifuged (16000 x g for 10min) and the nuclear fraction (supernatant) was collected in fresh eppendorf tubes. Protein content of the lysates was determined using the Bradford assay. Samples were stored in -80°C until further analysis.

B.3 Organotypic retinal explant cultures

B.3.1 Organotypic retinal explant cultures preparation

Organotypic retinal explant cultures were performed as described before (Caffe *et al.* 2001, Del Rio *et al.* 2011) with slight modifications. $Pde6b^{rd1}$ (rd1) mice at postnatal day 5 (PN5, assuming the day of birth as PN0) were sacrificed and eyes enucleated. After disinfection in 80% ethanol, eyes were washed and incubated in R16 serum-free medium containing 36 units of proteinase K for 15min at 37°C. Afterwards, to stop proteinase K activity, the eyes were transferred to R16 medium containing 20% of FBS for 5min. Next, the anterior segment, sclera, choroids, lens and vitreous body were removed under a magnifying glass. The dissected retina, with attached RPE layer was cut at four edges and explanted on a polycarbonate membrane. Explants were incubated on polycarbonate membranes placed in R16 supplemented medium in the way, that the tissue was in a

separate compartment, over the medium in the culture well, in 5% CO_2 at 37°C (see Materials: A.7.1). The medium was exchanged every second day.

B.3.1.1 Short term and long term retinal explants

Short-term retinal explants were prepared by Patricia del Rio from Research Unit Protein Science, in Helmholtz Zentrum München, Germany. Prepared explants from five days old rd1 mice (PN5) were cultured for 6 days (DIV6). At the second day of culture (PN5 DIV2) medium was changed for R16 supplemented medium with addition of 0.5µg/ml Cyr61 (treated explants) or for only R16 supplemented medium (control explants). After 6 days in culture explants were fixed in 4% paraformaldehyde for 15 minutes and washed in 0.1 PB (Fig. 13). The tissue was cryoprotected with an increasing gradient of sucrose diluted in 0.1M PB with pH 7.4. Explants were incubated for one hour in 10% sucrose and for one hour in 20% sucrose at RT and in 30% sucrose overnight at 4°C. At the end, samples were embedded in Tissue Tek and cryosectioned using a Leica cryotome and collected on Super Frost Plus® slides. Sections were stored in -20°C for TUNEL analysis.

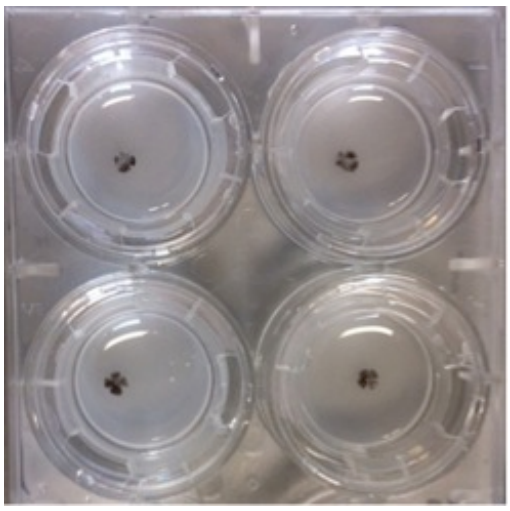

Figure 13. Mouse retinal explants PN5 DIV6 in 4% PFA on polycarbonate culture membranes.
Retinal explants were fixed in 4% PFA after 6 days in culture, followed by washing and cryopreservation. Sliced retina was stained according to the TUNEL assay protocol (see B.5).

Long-term retinal explants were prepared by Blanca Arango-Gonzalez from Institute of Ophthalmic Research, at University of Tübingen, Germany. Explants from PN5 rd1 mice were cultured in vitro for 12 days (DIV12). The R16 supplemented medium was exchanged for R16 supplemented medium with 1µg/ml Cyr61 (treated samples) at the second day of culture (PN7 DIV2). Explants serving as a control were supplied only with R16 supplemented medium. After 12 days in culture explants were fixed in 4% PFA, washed with 0.1M PB. For cryoprotection of the tissue, explants were incubated for one hour in 10% followed by one hour in 20% sucrose. Finally, explants were left in 30% sucrose at 4°C overnight. Thereafter, explants were embedded in Tissue Tek, sectioned on Super Frost Plus® slides using a cryotome and stored at -20°C for TUNEL analysis.

B.3.1.2 Stimulation of retinal explant cultures for Western blot analysis

The eyes of PN6 mice were enucleated and retinal explant culture was prepared as described above (see B.3.1). After placing dissected retinal explants on a polycarbonate membrane in R16 serum-free medium, tissue was left for 6h in 5% CO_2 at 37°C to recover. Afterwards, the membranes with retinas were transferred to R16 serum-free medium containing 1µg/ml Cyr61 for indicated periods of time. The tissue left in pure R16 serum-free medium served as a control. Next, explants were collected, put on ice, lysed in lysis buffer II, homogenized with sonification and centrifuged (16000 x g for 30min). Cleared lysates were stored in -80°C for further analysis.

B.4 Intraocular injection of Cyr61 into rat eyes

The *in vivo* validation of Cyr61 was conducted in cooperation with Blanca Arango-Gonzalez from Institute of Ophthalmic Research, at University of Tübingen, Germany. All experiments were carried out in accordance with applicable German laws, with the European Council Directive 86/609/EEC, with ARVO Statement for the Use of Animals in Ophthalmic and Vision Research and conformed to German law.

Intravitreal injections were performed as described elsewhere (Arango-Gonzalez *et al.* 2009). S334ter line 3 (S334ter-3) transgenic rats were anesthetized with ether and received a total of two intraocular injections at PN7 and PN10. Recombinant human Cyr61 (0.25 µg), dissolved in 1µl sterile phosphate-buffered saline (PBS; 0.05M, pH7.4), was injected with a fine glass microelectrode through the sclera into the vitreous body of the right eye at the level of the temporal peripheral retina. The contralateral eye received 1µl of vehicle solution and served as a control.

At PN12, after decapitation of the rats, the eyes were enucleated and the cornea and lens were removed. For radial sections, the remaining eye cup was immersed in 4% PFA in 0.1 M PB (pH 7.4) for 1h at 4°C. After fixation, the eye cups were washed several times in 0.1 M PB, cryoprotected for one hour in 10% as well as in 20% sucrose in 0.1M PB and in 30% sucrose eyes were incubated at 4°C overnight. Next, the tissue was embedded in Tissuetek and frozen in liquid nitrogen.

B.4.1 Visualization of rat retina vasculature

Retinal vasculature analyses were done in collaboration with Vinícius Monteiro de Castro from University of São Paulo, São Paulo, Brazil and Blanca Arango-Gonzalez from Institute of Ophthalmic Research, at University of Tübingen, Germany. Blood vessels in the eyes of Cyr61 or DPBS injected S334ter-3 rats were evaluated by *in vivo* angiography using confocal scanning laser ophthalmoscopy (cSLO) combined with detection algorithms. This method allows for observation of vasculature originating from inner limiting membrane and deeper layers within the retina as well as visualization of pathological intraretinal structures like macular cysts (Bartsch & Freeman 1994, Elsner *et*

al. 1996). All experiments were performed in accordance with the Association for Research in Vision and Ophthalmology statements on the care and use of animals in ophthalmic research. Throughout the examination process, a calm, quiet ambiance with dim illumination was maintained. Immediately after sacrifice, pupils were dilated with tropicamide eye drops before image acquisition. Hydroxypropyl methylcellulose and a custom-made contact lens were applied on the eye. The animals and device were manually held and aligned closely together.

The Spectralis HRA+OCT™ device is a digital cSLO equipped with three laser wavelengths (488, 785 and 815nm) with barriers filters for fluorescein (500nm) and indocyanine green (830nm) angiography. Appropriate barrier filters at 500nm and 830nm remove the reflected light with unchanged wavelength while allowing only the light emitted by the dye upon stimulation to pass through. To adapt the commercial system to the optics of the rat eye, a 78-dioptre double aspheric lens was added at the 40mm focal lens of the front objective and fixed directly to the outlet of the device. A custom-made contact lens with a focal length of 7mm was applied to the eye of the mouse with a drop of methylcellulose.

For the images, optic disc was placed in a centre of each picture. For each animal infrared reflectance (IR) imaging (excitation laser of 815nm) and red-free reflectance imaging (RF) (excitation laser of 488nm) was obtained with two angles of view, 30º and for a detailed view 20º. The focus was adjustable over a +40/-10 diopters range. The built in software was used for post-processing the images, including alignment, adjustment of contrast, construction of a mean image and/or of a composite image.

B.5 TUNEL staining

Sections from mouse retinal explant cultures (see B.3) and from rat eyes (see B.4) were evaluated for detection of cell death with the terminal deoxynucleotidyl transferase dUTP nick end-labeling (TUNEL) assay according to the manufacturer's instructions. First, slides were washed for 30min with DPBS followed by incubation with permeabilization solution for 2min on ice. Next, slides were washed with DPBS and TUNEL mixture reaction was applied on each slide (50µl enzyme solution mixed with 450µl of label solution). The slides were incubated in a humidified chamber for 60min in 37°C, in the dark. To ensure that the TUNEL mixture reaction spread homogeneously across the tissue and to avoid evaporation, the sections were covered with parafilm. Next, the slides were washed once with DPBS and incubated with Hoechst 33342 or DAPI diluted in DPBS (1:5000) for 8min. Finally, slides were washed 3 times with DPBS, dried out, embedded with antifade reagent and closed with cover glasses. For negative control, slides were incubated only with labeling solution, without terminal transferase. For positive control, prior to labeling procedures, sections were incubated for 30min with 100 units DNase I in 50mM Tris-HCl, pH 7.5, 1mg/ml BSA, to induce DNA double strand breaks. No labeling

was observed in the negative control sections while for the positive control sections, all retinal layers were stained (data not shown). To visualize TUNEL positive cells beam pass (BP) filter with excitation BP450/490 wavelengths and emission BP515/565 wavelengths was applied. The pictures of the retina were acquired at 200-fold magnification using fluorescent Axio Imager Z1 Zeiss microscope.

B.5.1 Image analysis and statistics for TUNEL staining

Subsets from each retinal section were defined and analysed with the Definiens 2 software (Definiens Enterprise Image Intelligence™ Suite, Definiens AG, Munich). To determine the total cell number in outer nuclear layer (ONL), the area of ONL was measured and then divided through the average cell size. To calculate the percentage of TUNEL positive cells the number of TUNEL positive cells was divided by the total cell number in ONL. Statistical comparisons among different groups were made with GraphPad Prism, using the one-tailed Mann Witney U test.

B.6 Immunofluorescence methods

B.6.1 Preparation of porcine tissue for immunohistochemistry

Porcine retina, dissected from an eyeball, or the mouse eyecup was fixed in 4% PFA for 30min. Next the tissue was washed three times with DPBS and cryoprotected by incubation for one hour in 10% and 20% sucrose in 0.1M PB – one hour in each of the solution at RT followed by overnight incubation in 30% sucrose in 0.1M PB at 4°C. Finally, the tissue was embedded in Tissue Teck and stored in -80°C. Ready cryoblocks of the tissue were cut on microscope slides using a Leica cryotome.

B.6.2 Immunohistochemistry

Slides with fixed sections of retinal tissue were 3 times washed with DPBS followed by incubation with blocking buffer for one hour at RT. Next, samples were incubated with primary antibody diluted in IHC antibody buffer (for dilutions see A.5) for overnight at 4°C. To avoid evaporation of the antibody solution, the slides were covered with parafilm. The next day the slides were washed three times for 5min with DPBS and incubated with secondary antibody diluted in IHC antibody buffer (for dilutions see A.5) for one hour at RT. Further, slides were incubated in Hoechst 33342 or DAPI diluted in DPBS (1:5000) for 8min. Finally, samples were washed three times for 5min with DPBS, dried out, embedded with antifade reagent and closed with cover glasses.

B.6.3 Immunocytochemistry

Dishes with fixed cells (see PR preparation B.1.2.1) were washed three times in DPBS and incubated with blocking solution for one hour at RT. Next, primary antibody diluted in ICC primary antibody buffer (for dilutions see A.5) was applied and kept for overnight at 4°C. Then, dishes were washed 3 times for 5min with DPBS and the cells were incubated with secondary antibody diluted in ICC secondary antibody buffer (for

dilutions see A.5) for one hour at RT. Next, the cells were washed once with DPBS and Hoechst 33342 diluted in DPBS (1:5000) was applied for additional 8min. At the end, the cells were washed three times for 5min and were stored in DPBS at 4°C.

B.7 Protein biochemistry

B.7.1 Protein concentration measurements

B.7.1.1 Bradford assay

For evaluations of the protein concentration in cell lysates based on the Bradford assay, Bio-Rad Protein Assay Kit was used, following the manufacturer's instructions. Dye reagent concentrate was diluted 1:5 in ddH_2O. Cell samples (1-2µl) were pipetted to separate cuvettes followed by 1ml of diluted reagent. For standard curve, five cuvettes with BSA concentration raging from 0.5-6µg/µl were prepared. Absorption was measured at 595nm with an Ultraspec 3300 photometer and protein content was calculated based on the linear regression of the standard curve.

B.7.1.2 BCA assay

The bicinchoninic acid (BCA) assay was applied for samples containing high amounts of detergent (RIPA buffer), which interfere with the Bradford assay. Measurements were conducted using 96-well microtiter plates filled with 200µl final volume in each well. Eight points were measured in duplicates, to established standard curves – with final BSA concentrations rom 0.001 to 0.05µg/µl. Samples were measured in duplicates, applying 1-2µl per well. Absorption was measured at 562nm was determined with a Synergy HT plate reader. The initial protein concentration in samples was calculated using Excel 2010.

B.7.2 SDS-PAGE

One-dimensional SDS-polyacrylamide gel electrophoresis (SDS-PAGE) was conducted to separate mixtures of proteins in cell lysates. Gels were prepared using casting chambers for mini gels with 1 or 1.5 mm spacers (for gels see A.7.4). First, separating gel solutions (10% acrylamide) was poured into the casting chambers, followed by covering with isopropanol, to prevent drying of the gel while polymerization. Following polymerization of the resolving gel, the isopropanol was removed and the stacking gel was overlaid. Finally, 10-well combs were placed on the upper rim of the glass plates. After polymerization, gels were placed in a Mini Protean Tetra Cell electrophoresis chamber, filled with SDS electrophoresis buffer (for buffers see Materials A.7.4). In order to prepare protein samples for loading, they were denatured by incubation with 5x SDS sample buffer at 94°C for 4min. Afterwards samples (10-20µg of protein) or a pre-stained protein marker were loaded onto the gel and electrophoresis was started at 70V until the bromophenol blue reached the end of stacking gel. Then, the voltage was changed to

110V till the end of the electrophoresis. Electrophoresis was stopped when bromophenol blue reached the end of the separating gel.

B.7.3 Western blotting and immunodetection

Western blotting was performed using the wet blotting technique. Proteins from the samples separated with SDS-PAGE were blotted onto polyvinylidene fluorie (PVDF) membranes according to manufacturer's instructions. SDS gels with separated proteins were incubated in blotting buffer for 5min. Next PVDF membranes were activated in methanol for 15 seconds followed by hydration in blotting buffer. Subsequently, the proteins from the gel were transferred with electrotransfer, in a cold cabinet (4°C) with a constant voltage of 100V for 90 minutes. After the wet transfer, membranes were blocked with 5% milk in TBS-T for one hour on a roller at RT to prevent unspecific binding. Blocked membranes were incubated overnight at 4°C with primary antibodies (for dilutions see A.5) diluted in 5% milk in TBS-T. The next day, the membranes were washed three times with TBS-T, and incubated with horseradish peroxidase-coupled secondary antibodies diluted 1:11000 in 5% milk in TBS-T for one hour at RT. After washing the membranes three times in TBS-T, they were incubated with signal ECL+ enhanced chemiluminescence kit for 4min and transferred to a hypercassette. Chemiluminescence signal was detected using Hyperfilm ECL and an Agfa Curix 60 developer. The films were digitalized using an Epson perfection scanner. To verify equal protein loading, membranes were stripped in a buffer for 30min at 50°C and reprobed, as described before, with appropriate primary and secondary antibodies. Quantifications of the blots were done using the ImageJ freeware.

B.7.4 Mouse cytokine membrane array

Nitrocellulose Proteome Profiler^{TM} Mouse Angiogenesis Arrays were blocked for one hour on a rocking platform shaker with blocking buffer supplied by manufacturer. Next, supernatants and lysates from control and experimental mRMG were combined with a cocktail of biotinylated detection antibodies and incubated for an hour at RT. Following, prepared sample and antibody mixtures were put on the membranes and incubated overnight at 4°C on a rocking platform shaker. Next, the membranes were washed with the washing buffer supplied by the manufacturer and incubated for 30min with horseradish peroxidase labelled streptavidin (streptavidin-HRP) on a rocking platform shaker at RT. Afterwards the membranes were washed with washing buffer and incubated with chemiluminescent detection reagents (Chemi Reagent Mix, supplied by the manufacturer) for one minute. Next, the membranes were placed in an autoradiography film cassette, exposed to X-ray film and developed with the Agfa Curix 60 developer. The Proteome arrays contain antibodies that are spotted in duplicates for each protein. Intensity of the signal at each antibody spot relates to the amount of captured protein. Array image scans were analysed using Image J (NIH Image) as indicated by manufacturer.

B.7.5 Mass spectrometry based proteomics

B.7.5.1 Preparation of RMG cells secretome

Porcine RMG cells were plated onto 10cm dishes and cultured until their confluence exceeded 75%. Then, the cells were washed and starved in DMEM without phenol red serum-free for 2h. Next the medium was exchanged for DMEM without phenol red serum-free medium supplemented with 0.5µg/ml Cyr61 (for treatment samples) or medium without supplementation (serving as controls). Cells were stimulated for 24h after which supernatants, containing RMG secretome proteins, were collected and centrifuged at 150 x g for 3min, to remove detached cells from the suspension.

B.7.5.2 Filter aided sample preparation (FASP) digestion of secretome proteins

Next, the secretome proteins from the medium were digested according to the filter aided sample preparation (FASP) protocol. 5µg of protein from supernatant was mixed with 100mM DTT in HPLC water and incubated with shaking for 30min at 60°C. After cooling down to RT, 100µl of UA buffer followed by 10µl of 300mM IAA in HPLC water were added and the samples were incubated in the dark for 30min at RT. Next, samples were transferred to a 30kDa cut-off ultrafiltration filter (pre-washed with 50mM ABC) and centrifuged at 14000 x g for 15min at RT. Afterwards, the flow-through was discarded and the column was washed three times with 200µl of UA buffer (each time the flow through was discarded) followed by two times washing with 100µl of 50mM ABC (the flow through was discarded after each centrifugation). Next, the columns were transferred to fresh Protein LoBind tubes. and 40µl of 50mM ABC supplemented with 1µg of endoproteinase Lys-C was applied on the filters and incubated for 2h in RT. Then, 2µg of trypsin in 10µl of 50mM ABC was added onto each filter and tubes were closed with parafilm. Samples were digested overnight at 37°C. The next day, to elute the peptides from the filter, tubes were centrifuged at 16000 x g for 5min. In a second elution step, 20µl of 50mM ABC containing 2% acetonitrile (ACN) were added to the filters and the tubes were additionally centrifuged at 16000 x g for 15min at RT. Before loading onto the liquid chromatography – tandem mass spectrometry (LC-MS/MS) system, samples were acidified with trifluoroacetic acid (TFA) to yield pH 2.

B.7.5.3 LC-MS/MS analysis of FASP digests and label-free quantification

For each experiment four control and four treatment replicates (stimulated with 0.5µg/ml Cyr61 for 24h) were prepared. The samples were analysed in cooperation with the Helmholtz Core Facility Proteomics and Alexander Schäfer. Proteins were identified and quantified by LC-MS/MS. Peptides from FASP tryptic digests were loaded onto an LC-MS/MS system composed of a nano-HPLC coupled online to an Orbitrap XL mass spectrometer. Peptides were separated by reverse-phase chromatogry on C18 analytical columns using a water/acetonitrile gradient of 170min length. Simultaneously, peptides were detected by the OrbitrapXL mass spectrometer. Full scan MS1 data for intact

peptides was acquired to determine mass and charge of peptides for identification and to enable label-free quantification later. During each cycle the ten most intense multiply charged ions were selected for collision induced dissociation (CID) based fragment spectrum (MS/MS) generation.

Resulting raw files were imported into Progenesis LC-MS Version 3.1 for label free quantification. MS/MS spectra were exported and used for identification of proteins using Mascot Version 2.3.0.2. Mascot results were processed with Percolator to yield peptide false discovery rates of 1%, before they were reimported into Progenesis LC-MS. Proteins were quantified by the sum of their peptide MS1 intensities. Statistical evaluation was performed using a two-tailed Student's t-test.

B.8 Quantitative real-time PCR

B.8.1 Isolation of mRNA

Primary porcine RMG cells were prepared as described in the section B.1.2.2. Isolated cells were cultured on 6cm dishes till confluence exceeded 75%. Before the stimulation, cells were washed and starved in serum-free medium for 2h followed by medium exchange onto new serum-free medium supplemented with 0.5µg Cyr61 (for treatment samples) or without supplementation (for control samples). Cells were stimulated for 24h or 48h, after which RNA was isolated as described before (Chomczynski 1993). During RNA isolation, gloves, pipettes and work place were wiped with RNase decontamination solution. The RMG supernatant was discarded, cells were washed with DPBS and harvested in 750µl of TRIzol®. Next, 150µl of chloroform were added and the whole sample was vortexed for 15sec followed by 3min incubation at RT. Subsequently, the samples were centrifuged at 16000 x g for 15min at 4°C. The aqueous phase containing RNA was collected to new eppendorf tubes containing 375µl of isopropanol and incubated for 10min at RT. Next, samples were centrifuged at 16000 x g for 15min at 4°C. After removing the supernatant, the pellet was washed with 750µl of 75% ethanol and resuspended in 50µl of HPLC water. The concentration and purity of RNA was measured using a NanoDrop spectrophotometer.

B.8.2 Synthesis of cDNA

B.8.2.1 First strand cDNA synthesis

Complementary DNA (cDNA) was synthetized form messenger RNA (mRNA) with reverse transcriptase- polymerase chain reaction (RT-PCR), using the RevertAid First Strand cDNA Synthesis Kit, according to the manufacturer's instructions. First, one µg of total RNA from each sample (obtained from RMG, see B.8.1) was mixed with one µl of oligo (dT) 18 primer and filled up with HPLC water to 12µl. Second, 4µl of reaction buffer, 1µl of RiboLock RNase Inhibitor (20U/µl), 2µl of 10mM dNTP Mix and 1µl of RevertAid M-MuLV reverse transcriptase (200U/µl) were added, so the total volume of

reaction for each sample was equal to 20µl (see Table 1). The reaction mixtures were then incubated for 60min at 42°C. The reaction was terminated by 5min heating to 70°C. The samples were then evaluated for the amount of DNA with a NanoDrop spectrofluorometer. Samples were stored at -80°C.

Table 1. PCR reaction mix for the first strand cDNA amplification.

Reagents	Final concentration	Amount
cDNA (1:1000)	100ng	1µl
Taq buffer 10x	1x	2µl
$MgCl_2$ (25mM)	1.5mM	1.2µl
primer forward (10µM)	0.5µM	1µl
primer reverse (10µM)	0.5µM	1µl
dNTPs (10mM)	250µM	0.5µl
Taq (5U/µl)	25mU/µl	0.1µl
HPLC H_2O	Up to 20µl	13.6µl

B.8.3 Quantitative real-time PCR reaction

Quantitative changes in mRNA for selected proteins were performed applying the qPCR method. Reaction mixtures were prepared in the special 4titued® 96 well plates, according to the Table 2. Next, the plates were sealed with appropriate foil supplied by the manufacturer and spin at 1500 x g for 3min. Then, the plates were placed in the LightCycler© 480 and processed according to the program in Table 3. For loading control, reaction mixture of GAPDH for each analysed gene was placed on the same plate.

Table 2. qPCR reaction mix.

Reagents	Amount
cDNA (1:20)	2.5µl
KAPA SYBR© FAST QPCR MasterMix	5µl
Forward Primer* 10µM	0.2µl
Reverse Primer* 10µM	0.2µl
HPLC water	2.1µl
Total volume	**10µl**

*Primers were designed with NCBI Blast tool. For list of used primers see A.4 Oligonucleotides

Using LightCycler© 480 software after each qPCR reaction, analysis of melting curve for each well in 96-well plate was performed, to confirm correct PCR conditions. Obtained data from the PCR run was calculated into crossing point (C_p) values (with LightCycler© 480 software) and imported into Excel where all further analyses of relative changes in genes expression were performed. Each gene was quantified in four repetitions on the 96-well plate.

B.8.4 Quantitative analysis of relative changes in gene expression

The quantitative analysis were done using the delta-delta-CP' (ΔΔCP) method (Pfaffl 2001). The statistical quantifications were made using the Mann Whitney U test and GraphPad software. Levels of significance were included accordingly: *p < 0.05, **p < 0.01, ***p <0.001

Table 3. Program for qPCR.

Step	Temperature	Time	Number of Cycles
Initial denaturation	94°C	3 minutes	1
Denaturation	94°C	30 seconds	25
Annealing	*°C	30 seconds	
Extension	72°C	45 seconds	
Final extension	72°C	10 minutes	1

*The annealing temperature was set according to calculated Tm for primers used in the reaction (see A.4)

III. RESULTS

Retinitis pigmentosa is a group of retinal degenerations in which inherited mutations disturb the proper function of PR or RPE, leading to progressive visual loss. The affected genes are responsible for a variety of functions within the retina, which includes components of the visual transduction cascade, visual cycle and retinol metabolism as well as renewal and shedding of the rod outer segments (van Soest et al. 1999). Gene therapy of RP can prevent vision loss, but the high heterogeneity in gene mutations causing RP, restricts one gene therapy only to a subset of patients. In contrast, trophic factor delivery cannot be curative for RP, but protects PR irrespective of the underlying gene defect leading to significant delay in photoreceptors death and preserving residual vision for a longer time.

In a first set of experiments (Part one), primary mouse RMG (mRMG) cells were stimulated with the neuroprotective factor GDNF and a list of seven highly upregulated proteins was established. Subsequently, Cyr61 was chosen for validation as the molecule with the greatest potential for neuroprotective activity. *Ex vivo* experiments on short term and long term rd1 mouse retinal explants showed increased PR survival and proved Cyr61's neurotrophic activity.

In a second set of experiments (Part two), emphasis was put on describing the spectrum of action of Cyr61 within the retinal cells as well as induction of the molecular pathways leading to the observed neuroprotection. Stimulation of the whole retinal tissue revealed activation of mitogen-activated protein kinase (MAPK)/Erk and janus kinase (JAK)/Stat pathways, but not phosphoinositide 3-kinase (PI3K)/Akt. Stimulation of very pure PR preparations with Cyr61 showed no activation of any of mentioned pathways thus suggesting no direct prosurvival effect of Cyr61 on PR. Further analysis of primary porcine RMG cells showed an increase in phosphorylation of all investigated proteins: Erk1/2, Stat3 and Akt, revealing a positive feedback loop of Cyr61 action on RMG and implying its indirect neuroprotection through RMG. Treatment of primary porcine RPE cells with Cyr61 uncovered very strong activation of MAPK/Erk and PI3K/Akt but not JAK/Stat3, suggesting indirect protection of PR through RPE stimulation. Treatment of MIO-M1 and ARPE19 (human RMG and RPE cell lines, respectively) with Cyr61, led robust activation of MAPK/Erk and its nuclear translocation as well as weaker activation of PI3K/Akt. On the other hand, MIO-M1 cells did not show activation of the JAK/Stat pathway, indicating changes and limits of this cell line model in comparison to porcine primary cell cultures.

The indirect manner of the neuroprotective effect led to the question if an RMG secreted factor may be the link between RMG/RPE stimulation and neuroprotection. This question

was addressed in Part three, where the influence of Cyr61 on protein secretion in primary porcine RMG cells was analysed. Quantification of secretome changes using LC-MS/MS based quantitative proteomics for primary RMG cell cultures revealed an increase in the secretion of a few proteins involved in extracellular matrix organization. Additional qPCR quantifications for three of the proteins chose from the secretome data or literature, showed mRNA increase in collagen, type III alpha 1 (COL3A1) and family with sequence similarity 3, member C (FAM3C), but not in VEGF.

In the last section (Part four), preliminary data of an *in vivo* application of Cyr61 was investigated in a study on S334ter-3 rats. Cyr61, injected two times with two day intervals into the vitreous body of seven day old rats, caused high changes in vascularization of the retina and did not decrease the number of TUNEL positive cells in ONL. Furthermore, injections of Cyr61 significantly increased the percentage of TUNEL positive cells in INL, possibly due to vasculature disorganization. The obtained data implies a too high dosage of the applied Cyr61 in this first *in vivo* experiment, causing vasculature impairment, which might have diminished neuroprotective potential of Cyr61.

Taken together, these results introduce Cyr61 as a novel neuroprotective agent that prolongs PR survival in an indirect way through stimulation of RMG and RPE cells. Attempts to elucidate the mechanism through which RMG and RPE mediate neuroprotection of PR are ongoing. In parallel, the adaptation of the promising Cyr61 treatment of retinitis pigmentosa in the S334ter rat model will be investigated thoroughly in the future.

Part one: Cyr61 is secreted by RMG and prolongs PR survival in the rd1 mouse model of retinitis pigmentosa

1.1 GDNF induces changes in the secretome of primary mouse RMG

The following results are based on the experimental work of Patricia del Rio (Research Unit Protein Science, Helmholtz Zentrum München, Germany), who kindly provided the raw data for subsequent analyses.

Injection of GDNF into the subretinal space of rd1 mice delayed PR cell death (Frasson et al. 1999a). The fact that RMG cells, but not PR, posses GDNF receptors on their membrane (Harada et al. 2003, Hauck et al. 2006b) suggests that the prosurvival effect of GDNF on PR is indirect, mediated by RMG (Hauck et al. 2006b). However, it remained unclear which factors released by GDNF stimulated RMG, directly influenced PR and led to their prolonged survival.

In order to identify which factors are synthesized and secreted by RMG upon GDNF stimulation, protein expression profile changes were investigated in primary mRMG cells

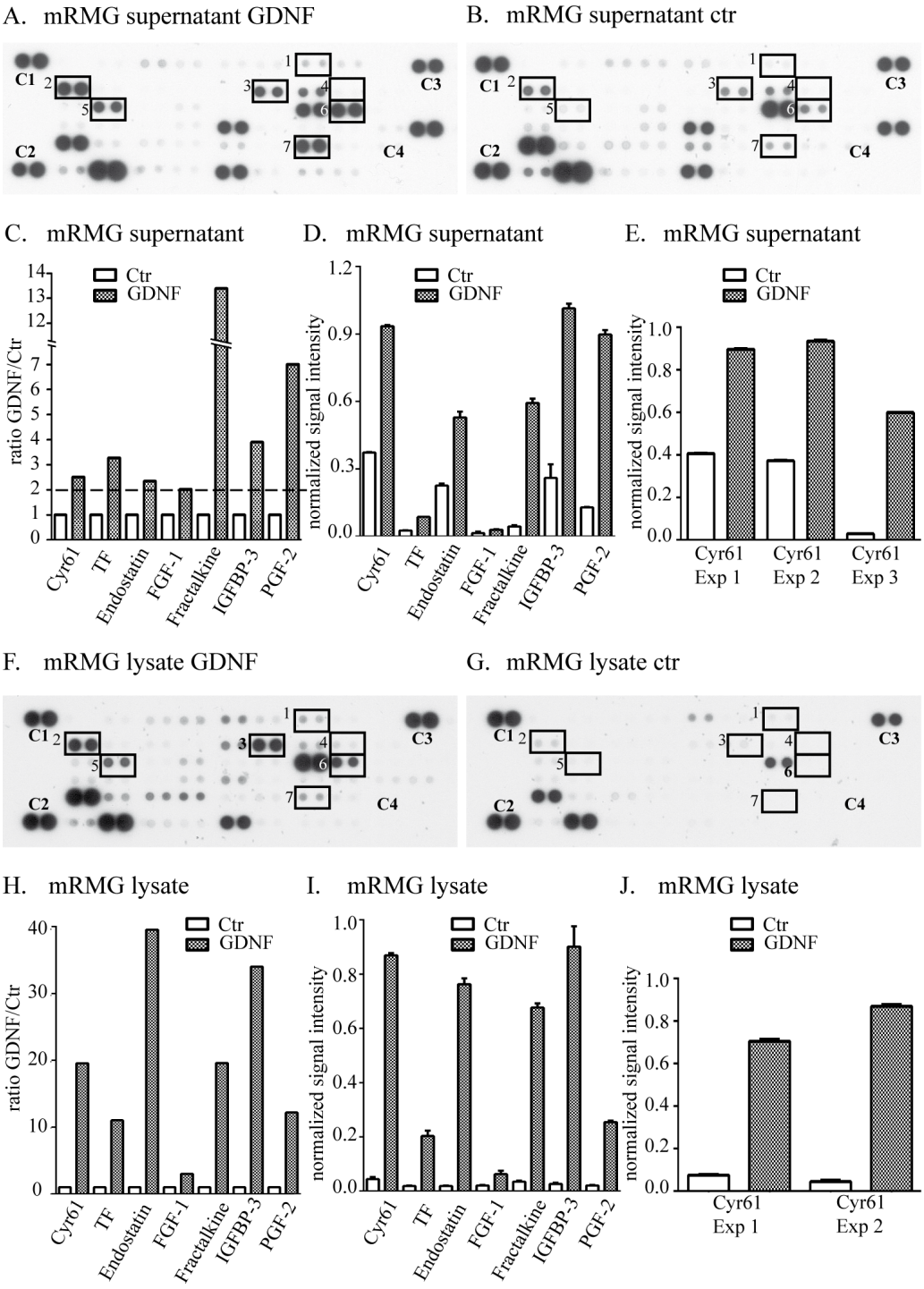

Figure 14. Cyr61 is secreted by GDNF stimulated Müller glial cells.
Mouse retinal Müller glial cells (RMG) cells were stimulated with 0,1µg/ml GDNF. The changes in secreted proteins between stimulated (A) and control (B) arrays were quantified and proteins with significantly increased abundance are presented showing fold changes (C) as well as normalized signal intensity (D). Normalized signal intensity for Cyr61 in all experiments are shown on panel E. Intracellular changes in protein content between stimulated mRMG (F) and control (G) membranes were quantified confirming increase in synthesis of all seven proteins selected based on supernatant data. Induction of each individual protein is shown as the ratio of stimulated cells to control (H) or as normalized signal intensity (I). Additionally, normalized signal intensity differences of Cyr61 for both experiments are shown on panel J. Error bars indicate standard error of measurements (SEM).

with antibody-based arrays (Fig. 14). Pure RMG cell preparations were prepared from the retinas of GFAP-eGFP/C57BL6 mice, which express eGFP under the control of the GFAP promoter. Consequently, their RMG and astrocyte cells are labelled with green fluorescence, making it possible to confirm RMG enrichment in the obtained cultures after isolation from the retinal tissue. The medium with secreted proteins (Fig. 14A) and whole cell lysates (Fig. 14F) of mRMG treated with 0,1µg/ml GDNF were compared to conditioned media and cells lysate of untreated controls (Fig. 14B, G). First, mRMG supernatants were analysed, as secretome changes were the most likely mechanism of GDNF mediated neuroprotection. When defining a threshold of at least two-fold expression change in all three repetitions of the experiment, seven proteins were found to be significantly induced: tissue factor (TF), Cyr61, endostatin, fibroblast growth factor 1 (FGF-1), fractalkine (CX3CL1), insulin-like growth factor-binding protein 3 (IGFBP-3) and placental growth factor 2 (PGF-2) (for details see Table 4 and Fig. 14C). Additionally, increases in abundance of these seven proteins were plotted as a comparison of normalized signal intensities for one representative experiment (Fig. 14D). Ratio changes for intracellular level of the proteins were calculated, using the same criteria of regulation through GDNF as for the supernatants. In the mRMG total cell lysates, twenty-two proteins displayed a greater than two-fold change in abundance relative to controls in response to GDNF treatment (see Table 4).

Finally, differential protein expression in lysates and supernatants were compared. All seven proteins induced in the supernatant were also highly increased on the intracellular level, confirming the validity of the identified secretome changes (Table 4 and Fig. 14H). Changes in quantity for these seven proteins are additionally presented as normalized signal intensities for one representative experiment (Fig. 14I). From the pool of secreted proteins significantly increased after GDNF treatment, Cyr61 appeared to be the most promising candidate to be a neuroprotective factor. This extracellular matrix protein is well known for its prosurvival effect in oral squamous cell carcinoma (Kok *et al.* 2010), breast cancer cells (Menendez et al. 2005), osteosarcoma (Sabile et al. 2012) and many other malignant tumour cells (Babic *et al.* 1998, Tang *et al.* 2011). Additionally, downregulation of Cyr61 expression has been reported in infantile Batten disease where one of the first symptoms is lost of vision leading to blindness (Haltia 2006, Qiao et al. 2007).

Based on these studies pointing to a potential pro-survival activity of neuronal cells and due to the robust induction of Cyr61 in mRMG supernatants (Table 4 and Fig. 14C - E) as well as in cell lysates (Table 4 and Fig. 14H – J), this protein was selected for further functional studies.

Table 4. Changes in mouse retinal Müller glial cells secretome and cell lysates after stimulation with 0,1µg/ml GDNF.

Index[1)]	Name of the protein[2)]	Abbreviation	Supernatant[3)]			Lysate[4)]	
			Exp 1	Exp 2	Exp 3	Exp 1	Exp 2
1	tissue factor, coagulation factor III	TF	3.3	5.5	2.3	4.4	11.0
2	cystein rich protein 61	Cyr61, CCN1	2.5	2.2	20.4	9.4	19.6
3	endostatin, colagen XVIII		2.3	2.2	3.8	14.0	39.6
4	fibroblast growth factor 1	FGF-1	2.0	7.3	4.1	6.2	3.0
5	fractalkine	CX3CL1	13.4	2.0	13.3	12.4	19.6
6	insuline-like growth factor binding protein 3	IGFBP-3	3.9	14.9	10.8	39.4	34.0
7	placenta growth factor 2	PGF-2	7.0	5.3	82.2	16.1	12.2
8	amphiregulin	AR	3.0	1.8	1.4	3.3	3.3
9	angiogenin	ANG	1.9	1.4	0.6	7.8	6.1
10	endoglin	CD105	8.1	1.0	1.4	11.4	7.6
11	endothelin-1	ET-1	4.3	9.9	1.4	10.2	7.3
12	heparin-binding EGF-like growth factor	HB-EGF	1.9	2.0	0.5	13.5	4.8
13	insulin-like growth factor binding protein 1	IGFBP-1	3.8	3.1	0.6	2.7	3.2
14	insulin-like growth factor binding protein 2	IGFBP-2	1.0	1.1	0.9	2.1	2.1
15	chemokine (C-X-C motif) ligand 10	IP-10, CXCL10, CRG-2	1.4	6.8	0.8	2.5	2.8
16	leptin	OB	1.9	2.2	0.3	2.5	2.7
17	chemokine (C-C motif) receptor 2	MCP-1, CCL2/JE	2.1	22.0	1.2	21.4	12.1
18	matrix metallopeptidase 3	MMP-3	6.1	4.4	1.9	2.5	3.4
19	matrix metallopeptidase 8	MMP-8	6.7	1.0	2.0	4.2	6.2
20	platelet-derived growth factor alpha polypeptide	PDGF-AA	1.3	2.3	0.4	6.7	4.2
21	platelet-derived growth factor beta polypeptide	PDGF-AB	2.0	3.1	0.4	63.5	12.7

[1] *Index of the protein on the membrane array (Fig. 14)*
[2] *Name of proteins according to the mouse cytokine membrane array protocol*
[3] *Ratio treated/untreated for supernatant for three independent experiments*
[4] *Ratio treated/untreated for lysate from two independent experiments*

1.2 Cyr61 reduces cell death in Pde6b^{rd1} retinal explant cultures

The observed upregulation of Cyr61 synthesis and secretion by GDNF stimulated mRMG implied its participation in the prolonged survival of PR, observed in the eyes of rd1 mice injected with GDNF (Frasson et al. 1999a). In order to validate this hypothesis, the effect

of Cyr61 application on PR survival rates was examined in explanted retinal cultures (for details see Materials and Methods B.3). The main advantage of this organotypic system is the possibility of study in *in vivo*-like complex behaviour of a tissue under simple in vitro settings (Oh *et al.* 2013). On the other hand, the retinal explanted tissue is studied without the other parts of the eye like vitreous body or the choroid layer, which may also contribute to an overall answer to the factor.

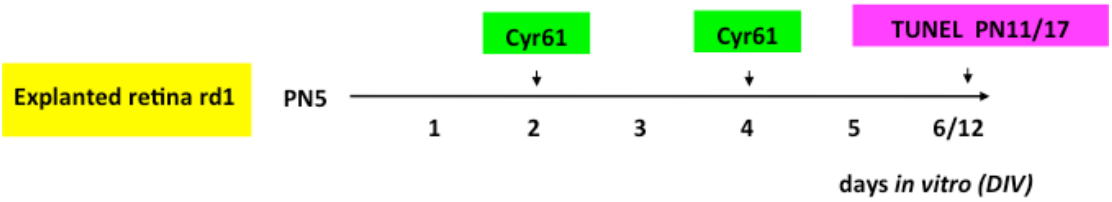

Figure 15. Experimental setup of Cyr61 stimulation of retinal explants.
Retinal explants were prepared from postnatal day (PN)5 rd1 mice. The applied treatment regimen consisted of medium changes every second day. Cyr61 was added to the fresh medium at a final concentration of 0.5 or 1µg/ml (for short- or long-term retinal explants, respectively) for treatment samples (green) but omitted for control sample retinas. PR survival was analysed using a TUNEL assay at either PN11 or PN17 (violet).

Short-term and long-term retinal cultures were prepared by Patricia del Rio (Research Unit Protein Science, Helmholtz Zentrum München, Germany) and Blanca Arango-Gonzalez (Institute of Ophthalmic Research, at University of Tübingen, Germany), respectively. They kindly provided the data on which following paragraph is based on. Retinal explant cultures were prepared from rd1 mice, which possess a mutation in the gene coding for the PDE6β-subunit, what causes a rapid PR degeneration starting at PN8 and leading to complete loss of rods within the central retina within the next three weeks (PN36) (Bowes et al. 1990, Pennesi et al. 2012). As a result, their retinas are an expedient system to study neuroprotective effects, as they exhibit a basal level of PR apoptosis in *ex vivo* culture.

To prepare an organotypic culture, PN5 rd1 mice were scarified, eyes were enucleated and retinas were explanted on polycarbonate membranes, which separate explants from the medium (Fig. 13). The tissue was cultured in R-16 supplemented medium (see Materials and Methods A.7.1) that was exchanged every second day for control as well as for experimental samples. As Cyr61 was added to the fresh medium for all treatment samples, the first Cyr61 application took place at the second day of retinal explant culturing. All retinal explants were cultured for six days (short term retinal explants) with R-16 supplemented medium (control samples) or with R-16 supplemented medium with addition of 0.5 µg/ml Cyr61 (four days of Cyr61 treatment) (Fig. 15). After six days of culture all retinas were fixed and TUNEL analysis was performed (Fig. 16). Cyr61 did indeed reduce the number of apoptotic cells in short term explants, based on the TUNEL analysis. Specifically, photoreceptor death rates in explants treated with Cyr61 (mean

2,3%; ±0,42 of TUNEL positive cells in the ONL; Fig. 16C) were reduced to almost half that of untreated controls (mean 5,1%; ±0,94 of TUNEL positive cells in the ONL; Fig. 16C). In order to further confirm this outcome, long term retinal explants were prepared in the same way as described above, but the tissue was cultured for 12 days (10 days of Cyr61 stimulation) and the medium of Cyr61 treated retinas was supplemented with 1µg/ml Cyr61 (Fig. 16A) as opposed to untreated explants (Fig. 16B). After long term Cyr61 treatment of the tissue, reduced rate of TUNEL positive cells was

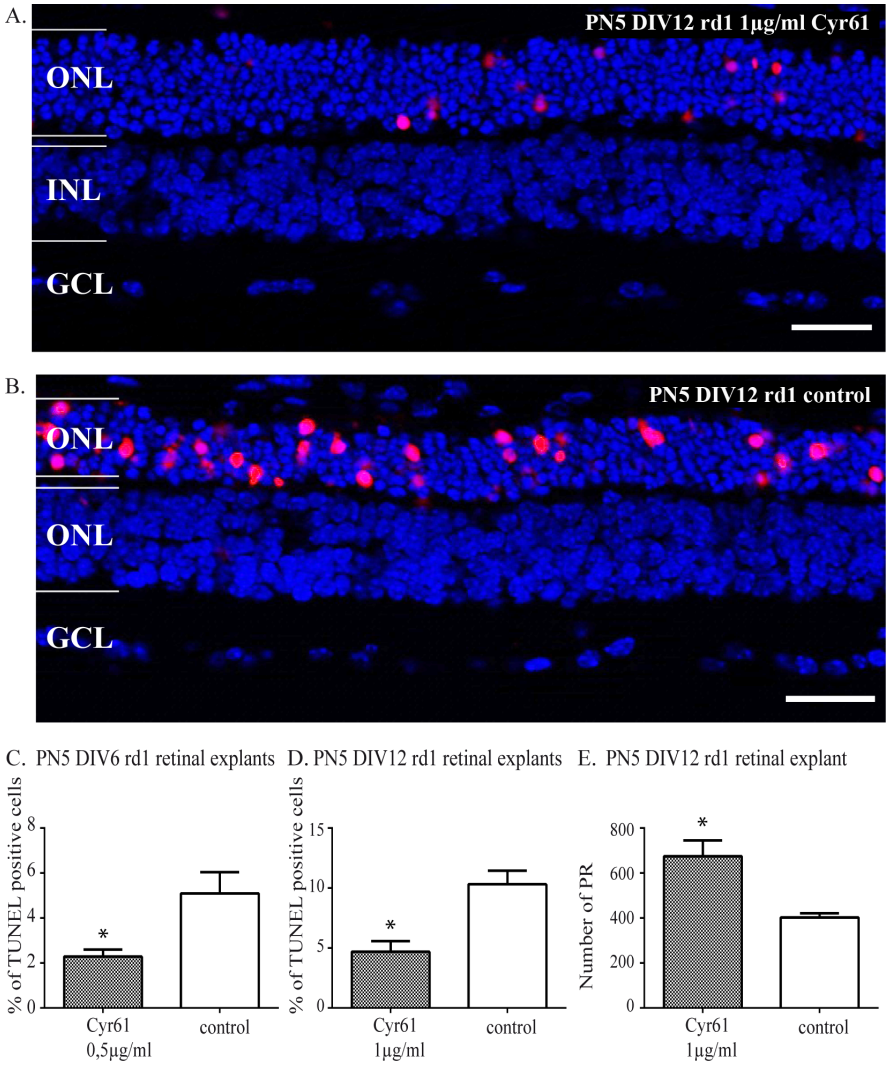

Figure 16. Cyr61 prolongs photoreceptor survival in rd1 mouse retinal explants.
Retinal tissue was explanted and cultured for a short period of time (postnatal (PN)5 days in vitro (DIV)6) with 0.5µg/ml Cyr61 or for a long period of time (PN5 DIV12) with 1µg/ml Cyr61. After the experiment, retinas were fixed and stained according to the TUNEL protocol (see Materials and Methods B.5). Quantifications of photoreceptor cell death were performed for short term (C) as well as for long-term (D) retinal explants. Moreover, in the long-term retinal explants the number of photoreceptors (PR) was quantified and compared to the control values (E). Graphs show data from at least three independent experiments. TUNEL positive cells (red), DAPI stained nuclei (blue). Error bars indicate standard error of measurements (SEM); levels of significance: *p < 0.05, Scale bars - 50µm.

still evident (mean 4,7%; ±0,9 of TUNEL positive cells in the ONL; Fig. 16D) in comparison to controls (mean 10,3%; ±1.14 of TUNEL positive cells in the ONL).

Moreover, in the long term retinal explants this decreased death rate translated into a significantly higher numbers of residual PR (mean 682; ±66) in comparison to control samples (403; ±19) (Fig. 16E).

In conclusion, Cyr61 is a molecule secreted by RMG and with neuroprotective activity on retinal PR cells.

Part two: Molecular pathway and mechanism of Cyr61 action within the retina

Screening the secretome of GDNF stimulated RMG cells led to a list of seven upregulated proteins, out of which only Cyr61 was chosen for validation of its neuroprotective potential. The *ex vivo* experiments shown in the previous section revealed its prosurvival action on PR of the retinitis pigmentosa rd1 mouse model. Nevertheless, these experiments could by their nature give no information about the responsiveness of particular cell types within the retina. However, a variety of different primary cell culture systems were used to determine which retinal cell types are primarily responsive to Cyr61 and which prosurvival signalling pathways are activated.

Given the fact that Cyr61 binds to integrins or heparan sulfate proteoglycans (HSPG) on the cell surface (Kular *et al.* 2011) thus influencing cell processes, four hypothesis were formulated:

1. Cyr61 protects PR directly through integrins (Brem *et al.* 1994) and/or HSPG expressed on PR (Tawara & Inomata 1987, Tawara et al. 1989, Landers *et al.* 1994).
2. Cyr61 protects PR indirectly through stimulation of RMG by binding to integrins and HSPG, whose presence on RMG plasma membranes has previously been published (Hering *et al.* 2000, Aricescu *et al.* 2002).
3. Cyr61 protects PR indirectly through stimulation of RPE cells by binding to integrins and HSPG, both of which are known to be present on RPE plasma membranes (Clegg *et al.* 2000, Geraldes *et al.* 2007).
4. Combinations of any of the previous hypotheses.

In order to test these hypotheses, we analysed three types of retinal cells separately: PR, RMG cells and RPE cells. Primary porcine cells of all three types were used along with two human cell lines – MIO-M1 and ARPE19. In these, three main signalling pathways related to survival were investigated: PI3K/Akt, MAPK/Erk and JAK/Stat, to determine the effect of Cyr61 on retinal cell function. The rationale for focussing on the PI3K/Akt and MAPK/Erk prosurvival pathways lies in their known activation by Cyr61 in different cancer cells (Menendez et al. 2005, Yoshida et al. 2007, Sabile et al. 2012, Zhang et al. 2012c). In contrast, there have been no reports showing Cyr61 activation of JAK/Stat signalling, but Cyr61 was shown to be activated via JAK/Stat pathway (Klein *et al.* 2012) and activation of this cascade has been found in many studies on retinal neuroprotection

(Adamus *et al.* 2003, Maier *et al.* 2004, Joly *et al.* 2008, Chollangi *et al.* 2009, Schallenberg et al. 2012).

2.1 Cyr61 activates the MAPK/Erk and JAK/Stat pathways in an *ex vivo* organotypic stimulation model

In a first step, the response of the selected signalling pathways to Cyr61 was investigated on whole retinal tissue. To this end, very short-term organotypic tissue cultures were established, which gave the opportunity to monitor molecular changes in the conditions very similar to the *in vivo* situation, without the necessity to perform an experiment on a living animal.

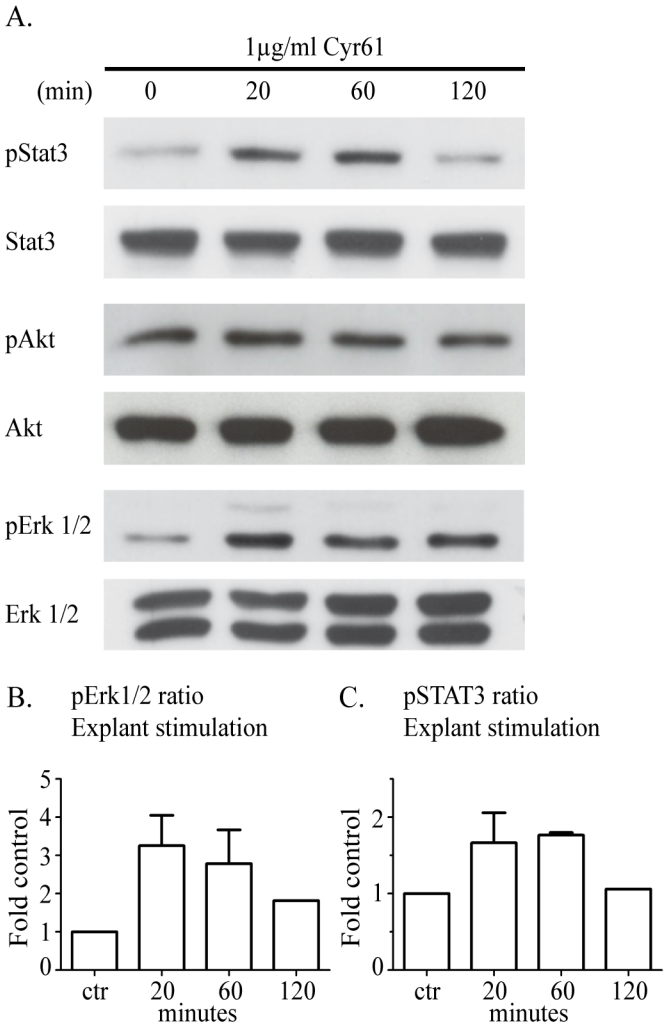

Figure 17. Cyr61 induce MAPK/Erk and JAK/Stat activity in rd1 mouse retinal explants.
Retinas of rd1 mice were explanted, mounted onto polycarbonate membranes and allowed to recover for six hours in serum free medium. Following this recovery and starvation period, retinas were treated with 1µg/ml Cyr61 for the indicated durations. Stimulated retinas were lysed, and phosphorylation of Stat3, Akt and Erk was assessed by western blot, using antibodies against the unmodified proteins as well as against Tyr705 of Stat3, Ser473 of Akt and Thr202/Tyr204 of Erk1/2 (A). pErk1/2 and pStat3 band intensities from two replicates were quantified and normalized to the band intensity of Erk1/2 and Stat3, B and C respectively. Error bars indicate standard error of measurements (SEM).

Retinas from rd1 mice were dissected and prepared as for the short term and long-term retinal explants, described above. After dissection, the polycarbonate membranes with retinas were placed in basal medium and retinas were kept in an incubator for six hours, to allow the stressed tissue to recover after the preparation procedure. Subsequently, mouse retinal explants were treated with 1µg/ml Cyr61, lysed and analysed using the western blot technique, detecting critical components of the JAK/Stat, PI3K/Akt and MAPK/Erk pathways (Fig. 17). Phosphorylation of Tyr705 in Stat3 is crucial for its activation, followed by its dimerization, nuclear translocation and binding to DNA (Ihle 1995, Bromberg *et al.* 1999). Phosphorylation of Akt at Ser473 is the critical step to fully activate Akt Ser/Thr kinase (Sarbassov *et al.* 2005). Activation of the MAPK/Erk pathway was followed by the observation of parallel Erk1 and Erk2 phosphorylation at Thr202 and Tyr204, respectively, which is essential for the enzyme activation (Roskoski 2012).

Cyr61 stimulation resulted in an increase of phosphorylated Erk1/2, indicative of increased MAPK activity, which peaked at 20 minutes (ratio 3.3), slowly declining to a ratio of 1.8 after two hours (Fig. 17A, B). Likewise, Cyr61 treatment induced phosphorylation of Stat3, one of the main transcriptional activator downstream of JAK, which was evident after 20 minutes (ratio 1.7) persisted until 60min (ratio 1.8) but had returned to baseline levels by 120 minutes. Contrary to activation of Erk1/2, induction of Stat3 decreased to control levels after two hours (Fig. 17A, C). In contrast, no difference in Akt phosphorylation though Cyr61 was found in stimulated explants (Fig. 18A).

Taken together, analysis of Cyr61's effect on the whole retinal tissue revealed significant phosphorylation of key signalling components of the JAK/Stat and MAPK/Erk but not PI3K/Akt pathways.

2.2 Cyr61 does not stimulate PR in primary cell culture

In order to test the hypothesis that Cyr61 stimulates PR survival through a direct mechanism, we prepared primary PR from porcine eyes. Porcine retina has two main advantages for the study: One is that this retina is very similar to the human one and can serve as a good substitute for human studies. The second one is that the bigger size of a pig eye in comparison to a mouse eye, allows obtaining ample numbers of cells translating to a much higher yield in terms of protein amounts in comparison to mouse eyes, thus facilitating subsequent western blot analyses considerably.

Primary PR, prepared from porcine eyes, were the next day serum starved for two hours the day after preparation and treated with 1µg/ml Cyr61 for 10, 20 or 120 minutes. The comparably short starvation time was chosen to conserve PR cell viability (24h starvation lead to PR death, data not shown) and has been used successfully for stimulation of other cells during this study.

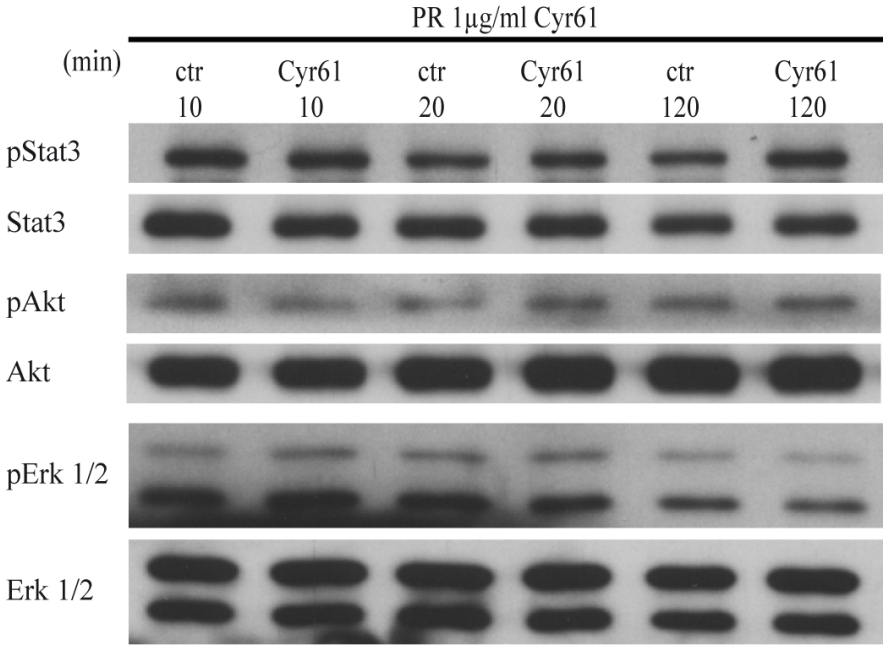

Figure 18. Cyr61 does not stimulate photoreceptors directly.
Cultured photoreceptors (PR) were stimulated with 1µg/ml Cyr61 for the indicated periods of time. Afterwards, the cells were lysed and analyzed by western blotting using antibodies against pStat3, pAkt and pErk1/2 as well as their unmodified form to control the loading.

PR cell lysates were analysed using western blot in the same way as whole retinal lysates (see 2.1). PR cells displayed basal levels of phosphorylated Akt, Erk and Stat3 at all analysed time points, but no significant changes in the phosphorylation state of either of those three proteins was observed following Cyr61 stimulation at any time point (Fig. 18).

In order to exclude the possibility that the failure of PR cells to respond to Cyr61 was caused by low cell viability, control dishes were stained with the dead cell marker propidium iodide (PI) or the live cell marker calcein (Fig 19). The majority of cells were still viable at the time of the experiment (Fig. 19A), while a certain portion of cells were dead, as shown by their failure to exclude PI (Fig. 19B). Based on these results the possibility that PR did not react to Cyr61 because of low vitality can be excluded.

In summary, the lack of Cyr61 mediated activation on the three neuroprotective signalling pathways in PR, led to the rejection of the hypothesis of a direct mechanism of neuroprotection through Cyr61.

2.3 Cyr61 activates the JAK/Stat, PI3K/Akt and MAPK/Erk pathways in primary RMG cells

Since PR did not answer directly to Cyr61 treatment, the second hypothesis, stating that Cyr61 prolongs PR survival indirectly through RMG stimulation, was pursued further.

To this end, primary RMG cells were isolated from porcine eyes and cultivated for up to 11 days (Fig. 20A) to achieve >75% confluence (for details see Materials and Methods

B.1.2.2). At the day of experiment cells were serum starved for two hours in followed by treatment with 1µg/ml Cyr61 for different periods of time. Stimulation of signal transduction pathways was monitored by western blot analogous to the previous experiments.

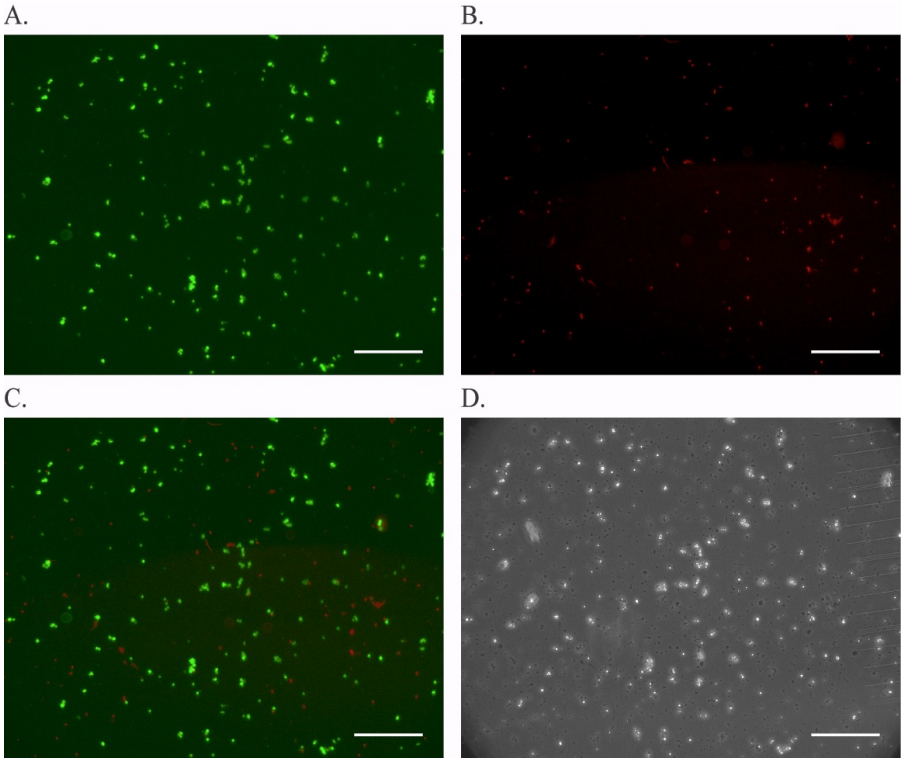

Figure 19. Porcine photoreceptor cells were prepared with sufficient viability.
At the day of experiment photoreceptor (PR) cells were fixed and their viability was assessed with two different fluorescent probes. Living cells were visualized with calcein, (green, A). Dead cells were stained with PI (red, B). Overlay of A and B is shown on panel C while phase contrast picture of PR is presented on panel D. Scale bars 200µm.

Cyr61 did indeed induce the phosphorylation of all three monitored proteins in RMG cells (Fig. 20). Interestingly, the activation of each of the three proteins showed a different kinetic. Activation of Stat3 was evident from the beginning of the experiment but relatively short lived, dropping to values lower than in control samples after 120 minutes stimulation. Increase in Stat3 phosphorylation (Fig. 20B) reached its peak after 10 minutes of Cyr61 stimulation, (ratio 4.4), after which the signal decreased to a ratio 2.2 after 20 minutes. After 60 minutes, phosphorylation of Stat3 dropped below control level to ratio 0.6 and did not recover even after 120 minutes (ratio 0.6).

Similarly, the peak in phosphorylation of Akt occurred at 10 minutes (ratio 2.6, Fig. 20C) although the stimulation was much weaker compared to Stat3 activation. After 20 minutes the effect on Akt was slowly diminishing (ratio 1.8) and, like for Stat3, decreased below control level after 60 minutes (ratio 0.4) and stayed low till the last observed time point - 120 minutes (ratio 0.5). In contrast, the activation pattern of Erk1/2 was characterised by a robust and sustained activation with ratios staying significantly

elevated till the end of the stimulation. Specifically, phosphorylation of Erk1/2 (Fig. 20D) was significantly increased after 30 minutes (ratio 2.1) and decreased very slowly, reaching a ratio of 1.9 and 1.8, after 60 and 120 minutes, respectively (Fig. 20D).

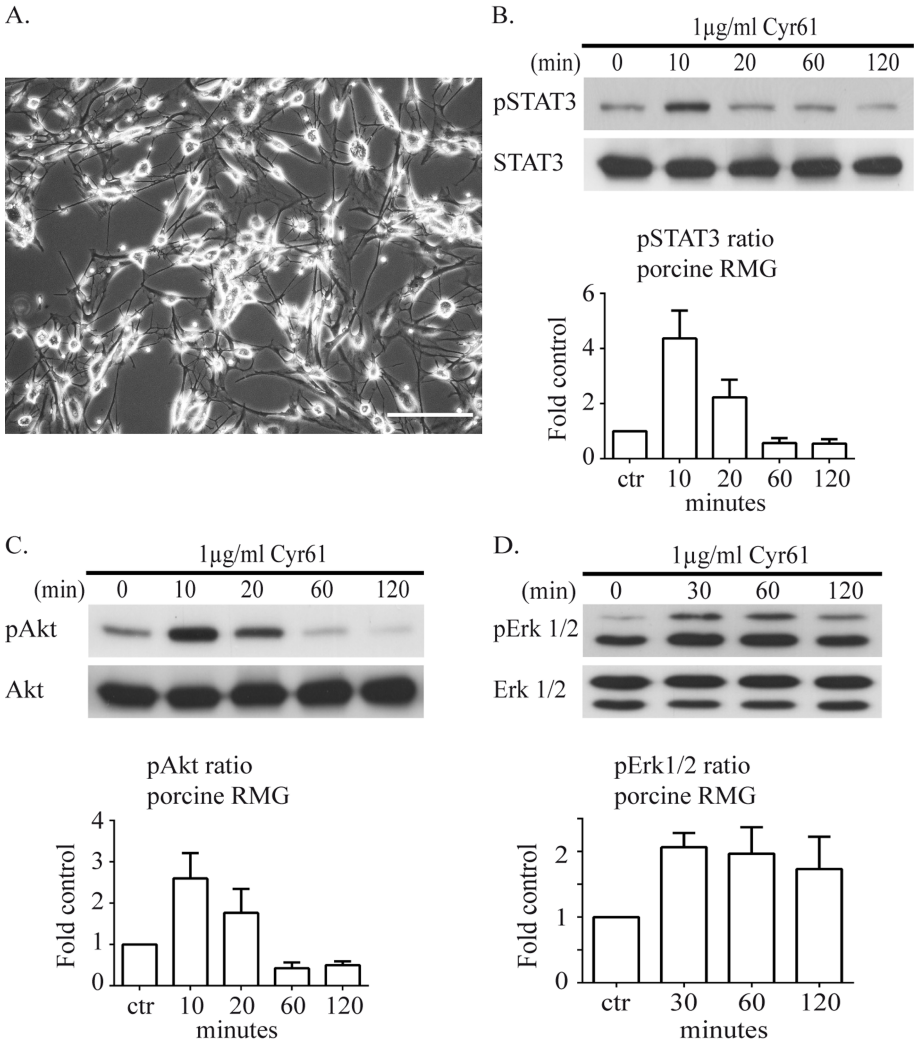

Figure 20. Cyr61 induces the JAK/Stat, PI3K/Akt and MAPK/Erk pathways in primary retinal Müller glial cells.

Primary porcine retinal Müller glial (RMG) cells (A) were stimulated with 1µg/ml Cyr61 for the indicated periods of time. Next, the cells were lysed and analysed by western blot. Membranes were probed with antibodies against phosphorylated Stat3 (B), Akt (C) and Erk1/2 (D). Graphs show data from three independent experiments. Error bars indicate standard error of measurements (SEM). Scale Bar - 200 µm.

Taken together, the responsiveness of primary RMGs to Cyr61 treatment is in line with the second hypothesis, postulating an indirect PR protection through RMG stimulation. Moreover, while PI3K/Akt and MAPK/Erk are often activated by the same receptor, here most notably by integrins, Stat3 is associated with a different set of receptors – cytokine receptors. It is therefore tempting to speculate that Cyr61 may bind to more than one cognate receptor on the RMG cell surface.

2.4 RMG cell contamination of PR cultures can be a dominant confounding factor for functional assays

In light of the findings that RMG but not PR are responsive to Cyr61, an important technical point concerning isolation of primary retinal cells is worth highlighting. Contamination of PR cultures with a small number of RMG can skew the results drastically and may even lead to incorrect conclusions. Initially, PR cell cultures were prepared according to the previously published protocol I, where a first fraction of PR is isolated form retinas and combined with a second fraction, prepared by repeated and more vigorous dissociation of the retina to increase the efficiency of isolation (for details see Materials and Methods B.1.2.1). Many experiments were performed according to the described protocol I, but results were not reproducible and misleading, showing stimulation of different proteins in some instances but not in others (Fig. 21).

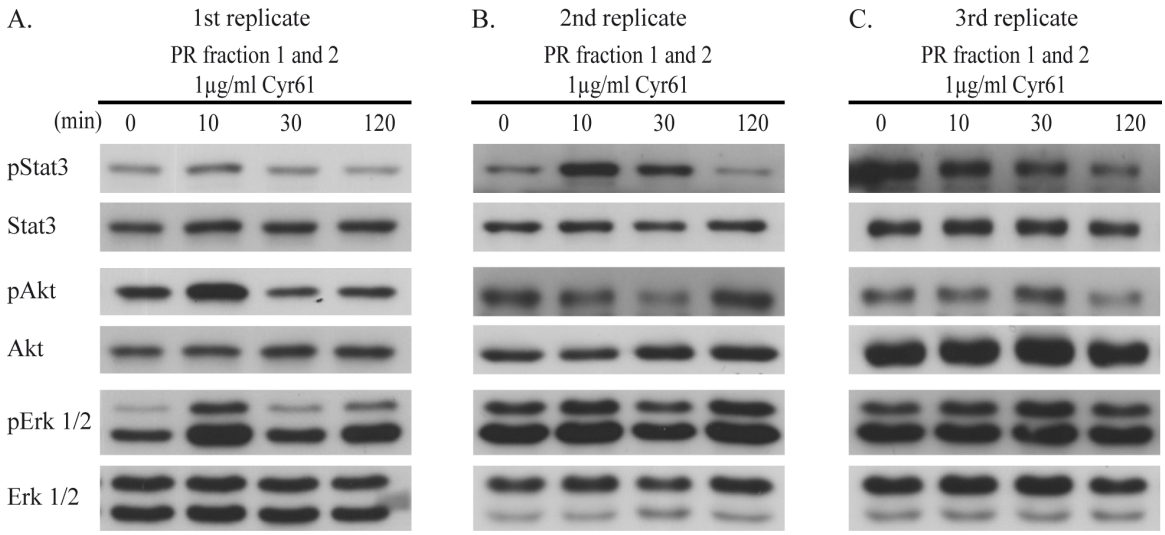

Figure 21. Contamination of photoreceptor cultures with retinal Müller glial cells is a major confounding factor in assessing the functional outcome of Cyr61 stimulation.
Both fractions of the photoreceptor (PR) isolation, contaminated with retinal Müller glial (RMG) cells, were mixed and plated onto culture dishes (see Materials and Methods B.1.2.1). Three repplicates, each showing different stimulation pattern are presented. Conflicting results indicated three different activation patterns with increases in pAkt and pErk1/2 but not pStat3 (A), increase in pStat3 but not pAkt and pErk1/2 (B) or no stimulation at all (C).

To find the reason for this inconsistency, the first and second fractions were collected separately and representative aliquots were stained for PR and RMG marker proteins to evaluate the purity of each fraction. The first fraction showed almost exclusively recoverin stained PR cells (Fig. 22A). Here, RMG cells were almost absent as shown by the extremely low number of GS positive cells (Fig. 22B). In contrast, the second fraction

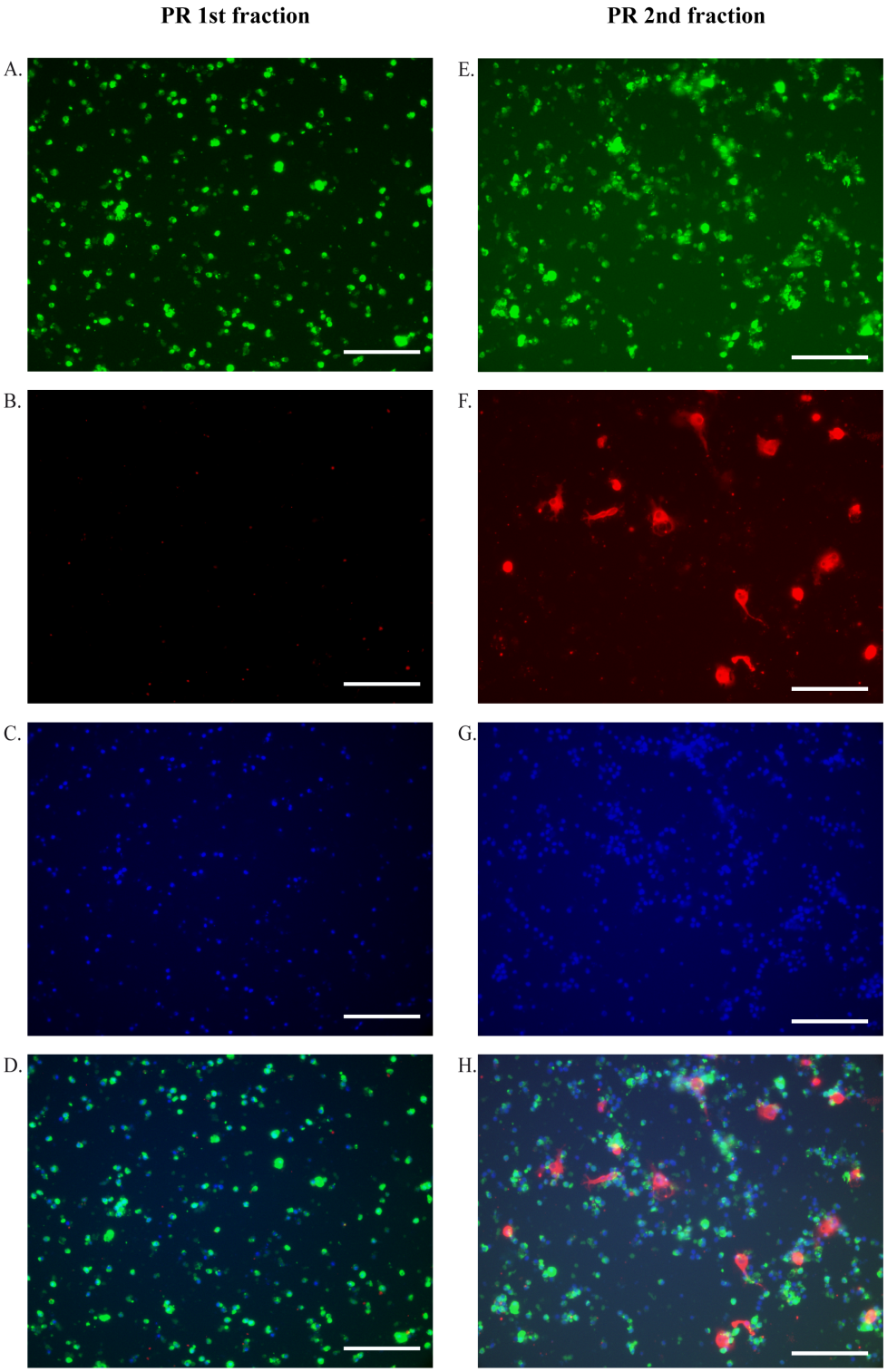

Figure 22. The first photoreceptor fraction has extremely high purity while the second PR fraction is contaminated with retinal Müller glial cells.
First and second photoreceptor (PR) fractions were isolated from porcine retina as described in Materials and Methods B.1.2.1. Aliquots of the fractions were plated separately onto 6cm dish for the following immunocytochemistry analysis. The next day the cells were fixed and stained with recoverin to visualise photoreceptors (green; A, E), glutamine synthetase to visualise retinal Müller glial (RMG) cells (red; B, F) and with Hoechst 33342 to visualise nuclei (blue; C, G). Panels D and H present merged channels for the first and second fractions respectively. Scale bar - 200μm.

contained many GS positive RMG cells (Fig.22F) interspersed with recoverin positive PR cells (Fig. 22E), as well as other not identified cells (for both fractions compare nuclei with PR and RGM staining, Fig. 22).

For this reason only the first fraction of the PR isolations, with highest purity, was used for testing the effect of Cyr61 on PR presented in section 2.2. To ensure highest purity, PR culture purity was monitored by two different methods: western blotting and ICC (for details see Materials and methods B.1.2.1). Given the outcome of Cyr61 stimulation on pure and viable PR cultures presented in 2.2 and on RMG cultures presented in 2.3, it appears very likely that varying degrees of RMG contamination account for the inconsistently observed stimulation of the different signalling pathways shown in Fig 21. Strikingly, even a minor contamination of PR culture with RMG (Fig. 22) can have a major impact on the outcome of biological assays, in this instance implying a false positive PR responsiveness to Cyr61.

2.5 Cyr61 activates the PI3K/Akt and MAPK/Erk pathway in MIO-M1 cell cultures

In addition to primary porcine RMG, the responsiveness of the human RMG cell line MIO-M1 to Cyr61 was investigated. MIO-M1 in culture preserve the same morphological features and express, except for GFAP, characteristic for primary RMG markers: cellular retinaldehyde binding protein (CRALBP), epidermal growth factor receptor (EGF-R), GS, and alpha smooth muscle actin (α-SMA) (Limb et al. 2002).

As descibred for primary cultures, cells were starved for two hours and treated for different time points with 1µg/ml Cyr61. Next, obtained lysates form the cells were analysed with regard to activation of the three signal transduction pathways by western blots. Similar to primary RMG cells increased phosphorylation of Akt after 10 minutes was found in MIO-M1 cells, but the induction was much weaker (ratio 1.6) and no stimulation of Akt was visible after 20 minutes and later time-point (Fig. 23A, B). Analysis of MAPK/Erk pathway activation revealed an increase in pErk1/2 already after 10 minutes (ratio 1.9), staying at the same level at 20 minutes (ratio 1.9) and 60 minutes (ratio 1.8) but dropping to a ratio of 1.3 after two hours of stimulation (Fig. 23A, C). Similar to primary RMG cells, Erk1/2 phosphorylation in MIO-M1 was strong and sustained, contrasting it to the activation of Akt. On the other hand, the observed cell line response with both proteins was always weaker and shorter than the answer of primary RMG.

Western blot analysis of activation of Stat3 did not reveal any activation of the protein, which is at odds with the results from primary porcine RMGs.

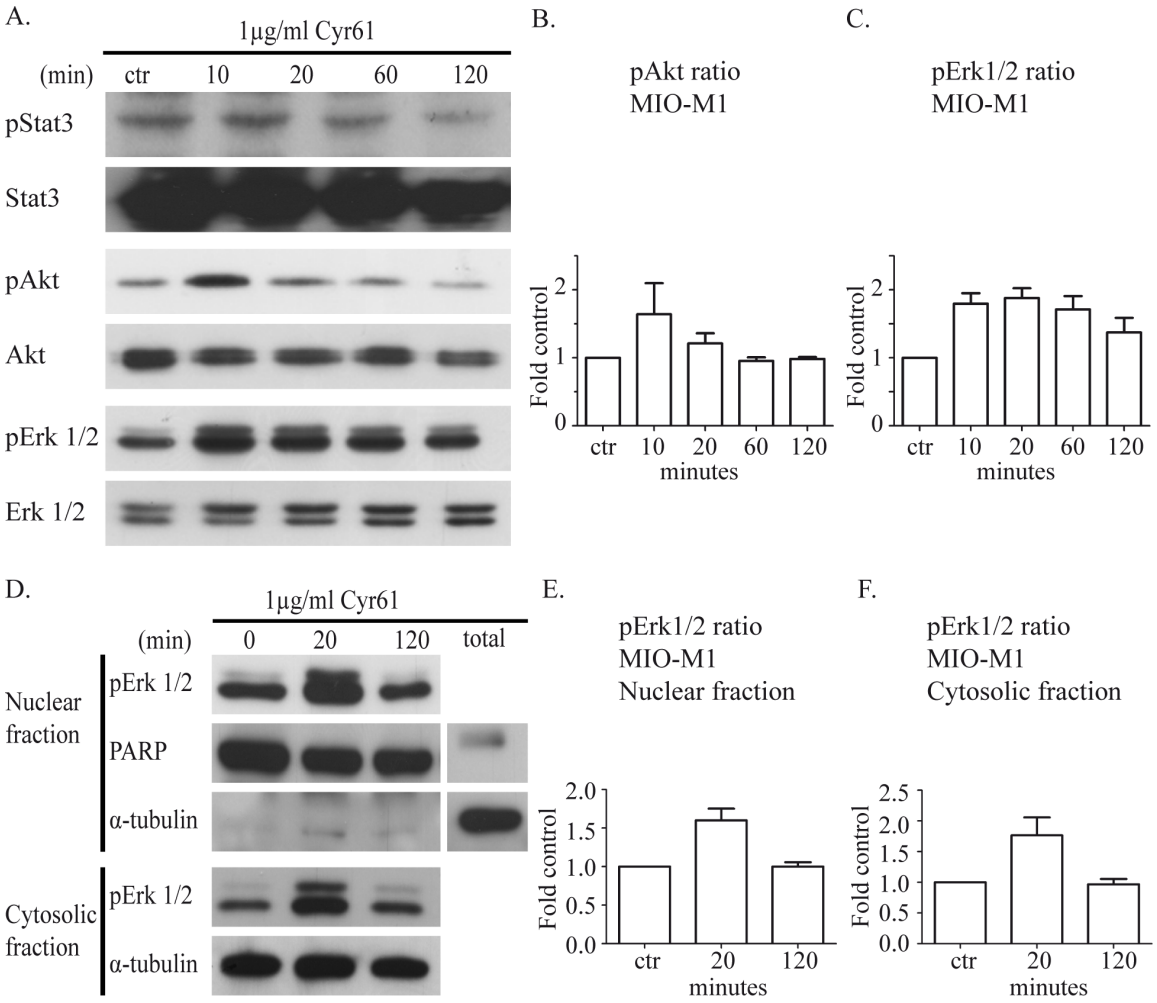

Figure 23. Cyr61 activates the PI3K/Akt and MAPK/Erk pathways in the human retinal Müller glial cell line MIO-M1.

MIO-M1 cells were stimulated with 1µg/ml Cyr61, and changes in phosphorylation of Akt (A, B), Erk1/2 (A, C) and Stat3 (A) were investigated using the western blotting technique. Additionally, analyses of nuclear and cytosolic fractions were conducted to show pErk1/2 nuclear translocation (D, E) and changes of pErk1/2 in cytosolic fractions (D, F). Nuclear fractions were additionally blotted with total cell fractions (total, D) and tested for PARP to show the efficiency of nuclear fraction isolation as well to with α-tubulin to control for cytoplasmic contaminations. Graphs show data from at least three independent experiments. Error bars indicate standard error of measurements (SEM).

Nuclear translocation of pErk1/2 in astrocytes increases genes transcription and secretion of prosurvival factors (Dhandapani *et al.* 2007). To investigate nuclear movement of pErk1/2 in MIO-M1, cells were stimulated with Cyr61 as described above but then separated intonuclear and cytoplasmic fractions and analysed using western blotting. To control purity of nuclear fractions, additional detection of α-tubulin was performed (Fig. 23D). In Cyr61 stimulated MIO-M1 cells, phosphorylated Erk1/2 was abundant in nuclear fractions already after 20 minutes of Cyr61 stimulation (ratio 1.7; Fig. 23D, E) which corresponded to the presence of activated Erk1/2 in the cytosolic fractions (ratio 1.8; Fig. 23D, F). Nevertheless, after two hours the effect of stimulation was diminished in both fractions (Fig. 23D, E, F).

Taken together, these results show that the human RMG cell line can also be used to study Cyr61's action within the retina, but with some limitations. MIO-M1 cells answer to Cyr61 treatment similarly to primary RMG cells with activation of Akt and Erk1/2. On the other hand, MIO-M1 cells treated with Cyr61 do not respond with Stat3 activation, contrasting their response to that of primary RMG cells. In addition, nuclear movement of pErk1/2 upon Cyr61 treatment could be shown in MIO-M1 cells, suggesting changes in transcriptome and secretome of RMG cells through Cyr61 as a possible mechanism of its indirect neuroprotective effect on PR cells.

2.6 Cyr61 activates the PI3K/Akt and MAPK/Erk pathways in primary RPE cells

Eventually, the third hypothesis, stating that Cyr61 protects PR survival indirectly through RPE stimulation, was tested. To investigate the responsiveness of RPE to Cyr61, primary porcine RPE cell cultures were prepared (Fig. 24A) (for details see Materials and Methods B.1.2.3). RPE cells were cultured for up to eight days to achieve >95% confluence (Fig. 24A). Subsequently, primary RPE were stimulated in the same way as primary PR and RMG (see above).

Cyr61 stimulation increased phosphorylation of two of the studied signalling molecules: Akt and Erk1/2, but not Stat3 (Fig. 24). Activation of Akt was characterised by a strong and long answer, still clearly visible till the end of stimulation. Robust phosphorylation of Akt was visible already 10 minutes after Cyr61 activation (ratio 2.7) with a peak after 20 minutes (ratio 3.5) and decreasing to a ratio of 2.6 after two hours (Fig. 24B). Phosphorylation of Erk1/2 was distinctly visible at all time points (Fig. 24C) with a strong increase in pErk1/2 already after 10 minutes (ratio 4.5) reaching its maximum after 20 minutes (ratio 4.8) and then dropping to a ratio of 3.1 after 120 minutes (Fig. 24C).

In summary, Cyr61 stimulates primary porcine RPE cells leading to activation of the PI3K/Akt and MAPK/Erk signalling pathways. Thus, the hypothesis, that Cyr61 protects PR through stimulation of RPE cells cannot be excluded.

2.7 Cyr61 activates the PI3K/Akt and MAPK/Erk pathway in the ARPE19 cells

To analyse the response of a human RPE cell line to Cyr61 the commercially available ARPE19 cell line was used. ARPE19 is a spontaneously evolved human cell line which express markers specific for RPE cells: CRALBP and RPE65. Furthermore, when plated on laminin-coated Transwell-COL filters they exhibit morphological polarization and form tight-junctions (Dunn et al. 1996), indicating that they retain characteristics of RPE cells. ARPE19 cells were serum starved for two hours and analysed with the western blot technique (Fig. 25), as described for the MIO-M1 cell line.

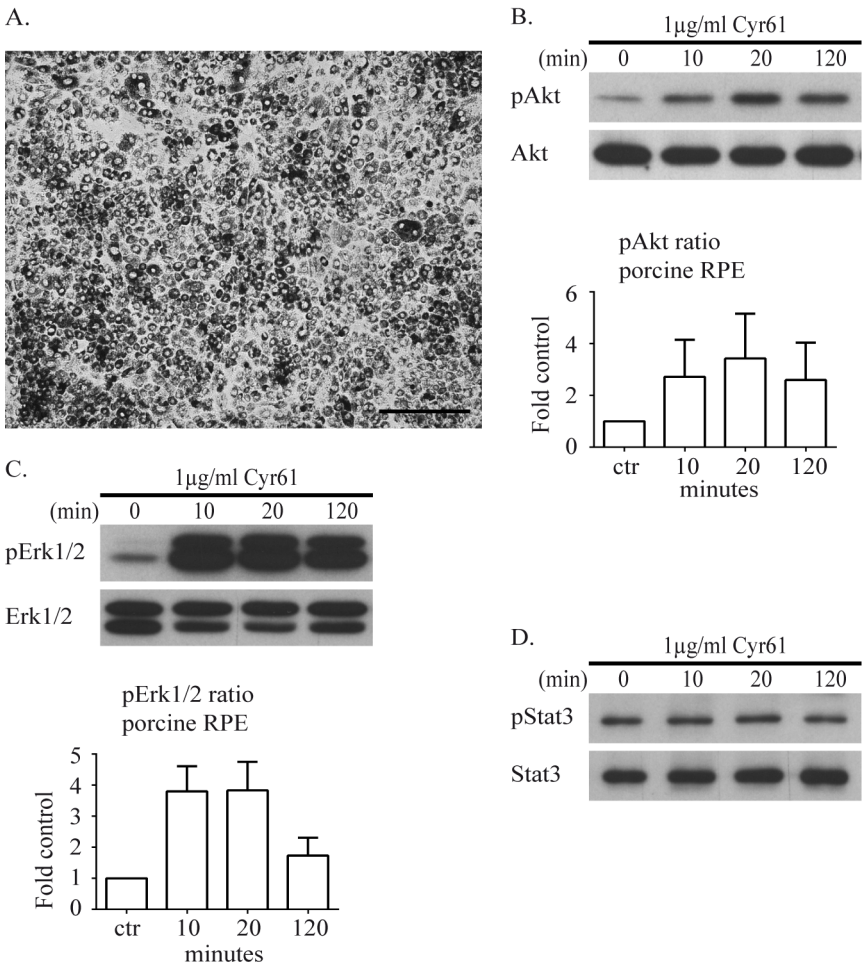

Figure 24. Cyr61 induces the PI3K/Akt and MAPK/Erk pathways in primary porcine retinal pigment epithelium cells.

Primary porcine retinal pigment epithelium (RPE) cells (A) were stimulated with 1µg/ml Cyr61 for indicated periods of time. Cells were lysed and analysed by western blotting. Membranes were incubated with antibodies against phosphorylated Akt (B), Erk1/2 (C) and Stat3 (D) signalling molecules to show changes in activation of the proteins. Graphs show data from three biologically independent experiments. Error bars indicate standard error of measurements (SEM). Scale Bar - 200µm.

Activation of Akt started from the beginning of the experiment (10 minutes, ratio 2.2) and stayed high until the end of the stimulation (Fig. 25A, B). Analysis of Erk1/2 phosphorylation revealed a kinetic similar to pAkt but with a higher peak of fold activation at 20 minutes (ratio 5), after which the stimulation declined to a ratio of 2.45 at 60 minutes, but rebounded to a ratio of 3.6 at 120 minutes (Fig. 25A, C).

Similarly to primary porcine RPE cells, analysis of the whole cell lysate towards phosphorylation of Stat3 showed no influence of Cyr61 on JAK/Stat3 pathway activation.

To investigate whether activation of Erk1/2 may lead to changes on the transcriptional level, analysis of the nuclear movement of pErk1/2 was conducted in the same way as for MIO-M1 cells (see above). Purity of the nuclear fraction was controlled with additional α-tubulin staining (Fig. 25D). Similarly as observed for MIO-M1 cells, after 20 minutes phosphorylated Erk1/2 was significantly enriched in the nuclear fraction (ratio 2.7; Fig.

25D, E) and even to a higher extend in the cytosolic fraction (ratio 3.6; Fig. 25D, F). Two hours after Cy61 treatment, the level of Erk1/2 phosphorylation started to decrease slowly, but in contrast to MIO-M1 cells, stayed high until the end of the experiment (ratios 2.5 and 2.3, for nuclear and cytoplasmic factions, respectively) (compare Fig. 23D, E, F and 25D, E, F).

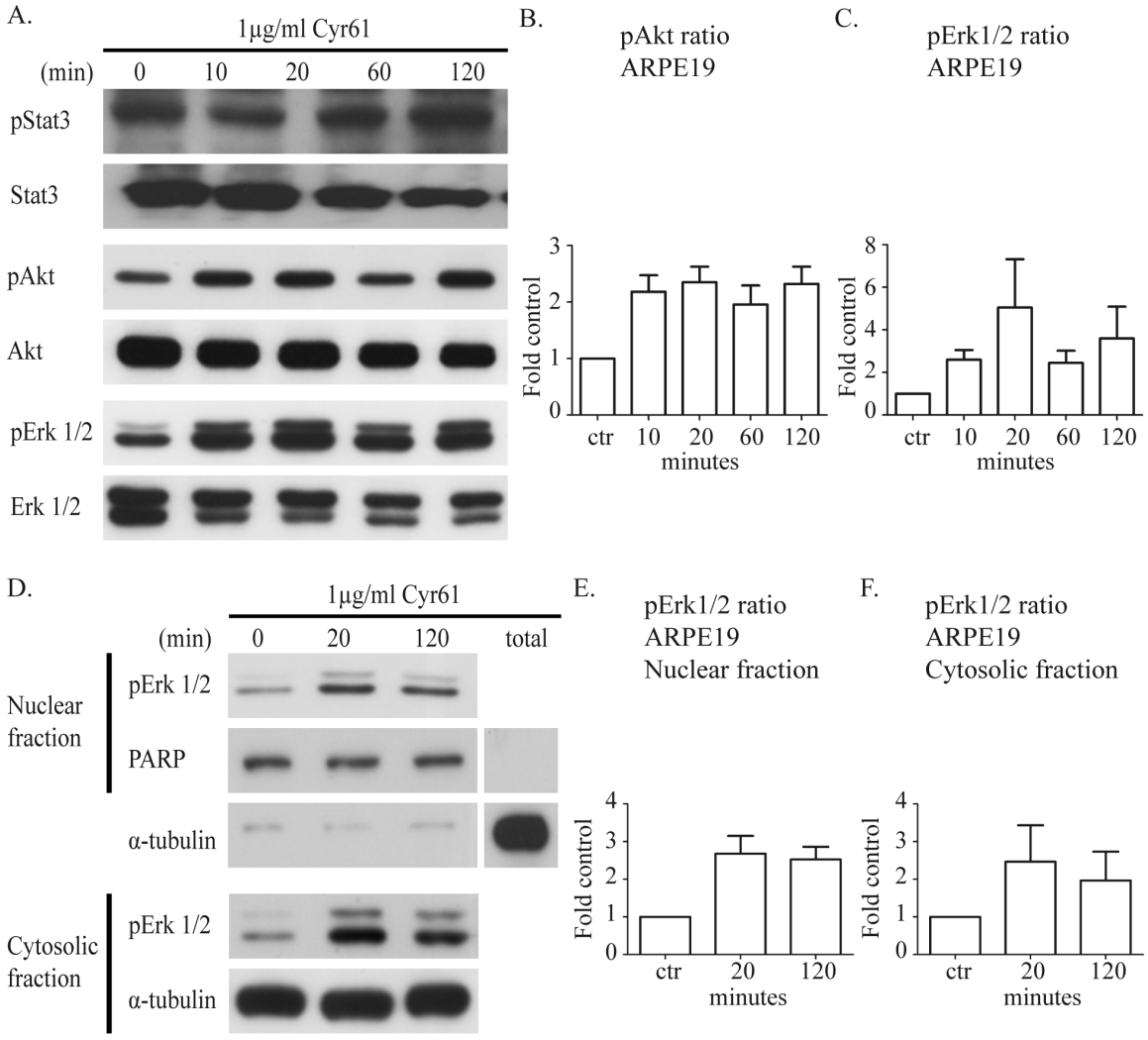

Figure 25. Cyr61 activates the PI3K/Akt and MAPK/Erk pathways in the human retinal pigment epithelium cell line ARPE19.
Cells were incubated with 1µg/ml Cyr61 and the changes in activation of the observed pathways were determined applying the western blotting method. Membranes with separated proteins from the lysates were incubated with antibodies against phosphorylated Akt (A, B), Erk1/2 (A, C) and Stat3 (A). Moreover, cell lysate was separated into two fractions and analysed for changes in pErk1/2 in nuclear (D, E) as well as cytosolic fraction (D, F). To confirm the purity of isolation, nuclear fractions were blotted with total cell fraction (total, D) and controlled for α-tubulin content. Additionally, staining with PARP presents the efficiency of nuclear fraction isolation. Graphs show data from at least three independent experiments. Error bars indicate standard error of measurements (SEM).

The presented data shows that ARPE19 cells are a good substitute for primary porcine RPE cells in regard to Cyr61. Cyr61 activated the same two signalling pathways in APRE19 as in primary RPE cells, with comparable kinetic and magnitude. Additionally,

the nuclear translocation of pErk1/2 in Cyr61 stimulated ARPE19 cells could be shown, implying its influence on transcriptome and secretome changes.

Part three: Investigation of the influence of Cyr61 on the RMG secretome

Results pertaining to Cyr61's influence on intracellular signalling pathways activity provided new insights into its influence on retinal cells. However, the experiments up to this point did not give any information concerning putative protein expression and secretome changes following Cyr61 stimulation.

Two methods were applied, quantitative proteomics and quantitative PCR (qPCR) to investigate Cyr61's influence on transcriptome and secretome of primary porcine RMG cells. Due to time constraints of the presented thesis, the results are based on four (proteomics) or on two (qPCR data) replicates. These results provide first clues about the influence of Cyr61 on RMG transcriptome and secretome changes. Further improvement of the experimental design will be necessary to obtain comprehensive results and confirm these preliminary data.

3.1 Proteomic analysis of protein secretion after Cyr61 stimulation of primary RMG cells

The samples were analysed in cooperation with the Helmholtz Core Facility Proteomics and Alexander Schäfer.

To investigate secretome changes, RMG cells were starved for two hours in serum-free medium followed by 0.5µg/ml Cyr61 medium supplementation for 24 hours. The next day, medium enriched in proteins secreted by the cells was collected and the secretomes were compared using quantitative LC-MS/MS based proteomics. To this end, secreted proteins were digested with trypsin using the filter aided sample preparation (FASP) digestion protocol (for details see Materials and Methods B.9.4). The resulting tryptic peptides were analysed by LC-MS/MS (four biological replicates for both control and Cyr61 stimulation) on an Orbitrap XL LC-MS system.

Following data acquisition, proteins were identified using the Mascot search engine and quantified using a label-free approach implemented in the Progenesis LC-MS software (described in detail in Materials and Methods B.9.4). In this way, a list of 1754 quantified proteins was generated out of which only a few showed differences in abundance in Cyr61 treated samples. It should be noted however, that many of these proteins represent cytoplasmatic protein like actin, and are most likely contaminations originating from cells dying during the stimulation period of the experiment. This heavy contamination of conditioned medium with cytoplasmic proteins is a well-known problem of non-targeted proteomic analysis of secretomes (Dupont *et al.* 2004, Zwickl *et al.* 2005). As the current

working hypothesis stated that Cyr61 causes changes in proteins secreted by RMG to protect PR, only proteins with significantly altered abundance which are known to be secreted (soluble factors or extracellular matrix constituents) are reported in this thesis. In total, only seven proteins fulfilled these criteria (Table 5).

Table 5. List of secreted proteins significantly increased in supernatants of primary porcine retinal Müller glial cells after stimulation with 0,5µg/ml Cyr61.

Protein name	Human gene symbol	Peptide count	Peptide used for quantification	t-test (p)	Ratio Cyr61/ctr
collagen, type III, alpha 1	COL3A1	24	7	0,000	4,9
insulin-like growth factor binding protein 5	IGFBP-5	13	1	0,023	1,6
Cystatin E/M	CYTM	4	1	0,002	1,5
family with sequence similarity 3, member C	FAM3C	13	3	0,042	1,4
retinaldehyde binding protein 1	RLBP1	11	4	0,026	1,3
matrilin 4	MATN4	20	10	0,044	1,3
chondroadherin	CHAD	15	2	0,043	0,6

Collagen type III, alpha 1 showed the highest upregulation with a ratio of 4.9, while most other regulated proteins had much smaller increases: insulin-like growth factor binding protein 5 (IGFBP-5, ratio 1.6), cystatin E/M (CYTM; ratio 1.5), FAM3C (ratio 1.4), retinaldehyde binding protein 1 (RLBP1, ratio 1.3), matrilin 4 (MATN4, ratio 1.3), On the other hand, one extracellular matrix protein – chondroadherin (CHAD), was found to be downregulated after Cyr61 treatment, dropping to the ratio 0.6.

In summary, Cyr61 caused distinct changes in the secretion of several proteins by RMG cells.

3.2 Changes in mRNA of stimulated primary RMG after Cyr61 stimulation

In order to confirm changes in protein secretion after Cyr61 stimulation, three proteins were analysed with qPCR to show their induction at the transcriptional level. The extracellular matrix protein COL3A1 was chosen, taking into account its significant 4.9 fold increased secretion after Cyr61 stimulation of RMG (Table 5). Additionally, the secreted factor FAM3C was monitored, considering its increase in secretion by stimulation of RMG (Table 5). Transcriptional changes in VEGF expression were also investigated. Although VEGF showed no significant increase in the RMG secretome (data not shown), its potential regulation by Cyr61 is very important considering Cyr61's

possible proangiogenic activity (Zhou *et al.* 2005, Yu *et al.* 2008), which may give rise to detrimental side effects for its prospective use in treatment.

Transcriptional induction of COL3A1 and FAM3C, but not VEGF, after 48 hours of 0.5µg/ml Cyr61 medium supplementation was found, confirming results obtained by secretome analysis (Fig. 26A, B, C).

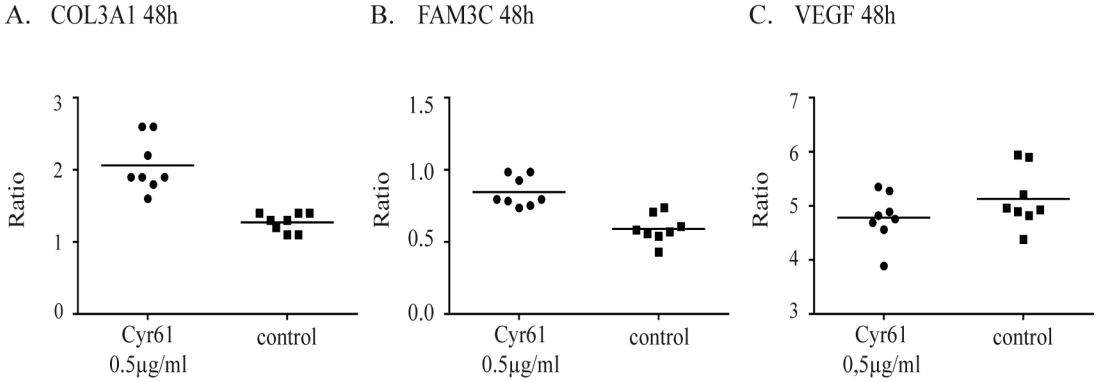

Figure 26. Cyr61 influences transcription of secreted proteins in porcine retinal Müller glial cells.
Primary retinal Müller glial (RMG) cells were stimulated with 0.5µg/ml Cyr61 and mRNA levels of collagen, type III, alpha 1 (COL3A1; A), family with sequence similarity 3, member C (FAM3C; B) and vascular endothelial growth factor (VEGF; C) were compared using qPCR. Relative expression levels were normalized to glyceraldehyde 3-phosphate dehydrogenase (GAPDH). Markers for each group correspond to two independent experiments with four technical replicates each. Bars indicate mean ratios for each group.

Taken together, the presented data show that Cyr61 causes changes in the secretion of a distinct group of proteins comprised of soluble factors and extracellular matrix proteins in RMG. It appears very likely that this influence of Cyr61 on the RMG secretome is mediated by modulation at the transcript as shown for two examples of both types of proteins: COL3A1 and FAM3C. The seven identified Cyr61 induced proteins are candidates for mediation of the indirect neuroprotective effect. However, the comparatively low grade induction (30-60% change in abundance for six of seven proteins) of most of these proteins warrants more detailed investigation of Cyr61's effect on the RMG secretome in future experiments. Particularly, Cyr61 treatment duration and dose will need to be optimized and the contamination with cytoplasmatic proteins reduced in order to obtain clearer results.

Part four: *In vivo* application of Cyr61 in the S334ter line 3 rat model of RP

Results up to this point showed that Cyr61 is a prosurvival factor for PR employing an indirect mechanism of neuroprotection through stimulation of surrounding retinal cells. One plausible model may be activation of RMG and probably RPE cells leading to changes in their gene expression followed by alterations in factor secretion and/or modification of the extracellular matrix. However, all described experiments were

performed *in vitro*, dissecting retina or retinal cells from the intact eye. They therefore do not give direct answers how application of Cyr61 will influence the development of RP in a living organism. In the last part of the thesis, preliminary data from the first *in vivo* application of Cyr61 to eyes of S334ter-3 rats is presented. The S334ter-3 rat is an RP rodent model, similar to rd1 mice. In both models rapid PR degeneration as well as increased activation of PARP combined with calpastatin down-regulation, increased oxidative DNA damage and accumulation of PAR polymers can be observed (Kaur et al. 2011). The rationale for switching models lies in the feasibility of intravitreal injection into PN7 rat eye in contrast to mouse eye. Following injection of Cyr61, the cell death ratio after Cyr61 was monitored in two retinal layers: ONL and INL. In addition, the number of ganglion cells in the ganglion cell layer was compared. Finally, changes in vasculature organization after Cyr61 injections were monitored using confocal scanning laser ophthalmoscopy.

4.1 Application of Cyr61 to S334ter-3 rat eye did not prolong PR survival *in vivo*.

The *in vivo* validation of Cyr61 was conducted in cooperation with Blanca Arango-Gonzalez (Institute of Ophthalmic Research, at University of Tübingen, Germany), who injected rat eyes as well as prepared cryostock from the eyes.

In order to test the neuroprotective activity of Cyr61 in intact eyes, ten S334ter-3 rats were injected with 0.25μg Cyr61 at PN7 and PN10 in their right eyes, while the left eyes were injected with PBS to serve as controls. At PN12, after five days of Cyr61 treatment, rats were sacrificed, the retinas were prepared and the level of PR cell death in two nuclear layers (ONL and INL) was evaluated using the TUNEL method (Fig. 27). Next, changes in the number of ganglion cells in GCL between control and Cyr61 treated eyes were evaluated. To get a more comprehensive picture, two areas of each retina were evaluated microscopically: one next to the optic nerve and the other from the peripheral retina.

The statistical analyses of the optic nerve region in the ONL showed no difference in the level of percentage of TUNEL positive cells between Cyr61 treated (18.6 ± 2.62) and control (19.44 ± 2.02) retinas (Fig. 28A). Similarly, no difference was found in the ONL in the peripheral retina (14.01 ± 2.00 versus 13.68 ± 1.30, for Cyr61 treated and control, respectively; Fig. 28B). On the other hand, quantification of changes in cell vitality in the INL revealed a statistically significant increase in cell death in the region of optical nerve area after Cyr61 treatment (3.08 ± 0.43) versus control (1.71 ± 0.11, Fig. 27 and 28C). Similarly, the average number of TUNEL positive cells in the INL of the peripheral retina was higher between Cyr61 stimulated (2.2 ± 0.47) and DPBS treated retinas (1.66 ± 0.17), although this difference was not significant (Fig. 28D). Analysis of the GC layer showed that there was no difference in the number of ganglion cells in the optic nerve area (22 ±1.55 versus 23.30 ± 2.57, for Cyr61 treated and control, respectively; Fig. 28E)

or the peripheral retina (31.88 ± 2.49 versus 29.70 ± 2.57, for Cyr61 treated and control, respectively; Fig. 28F).

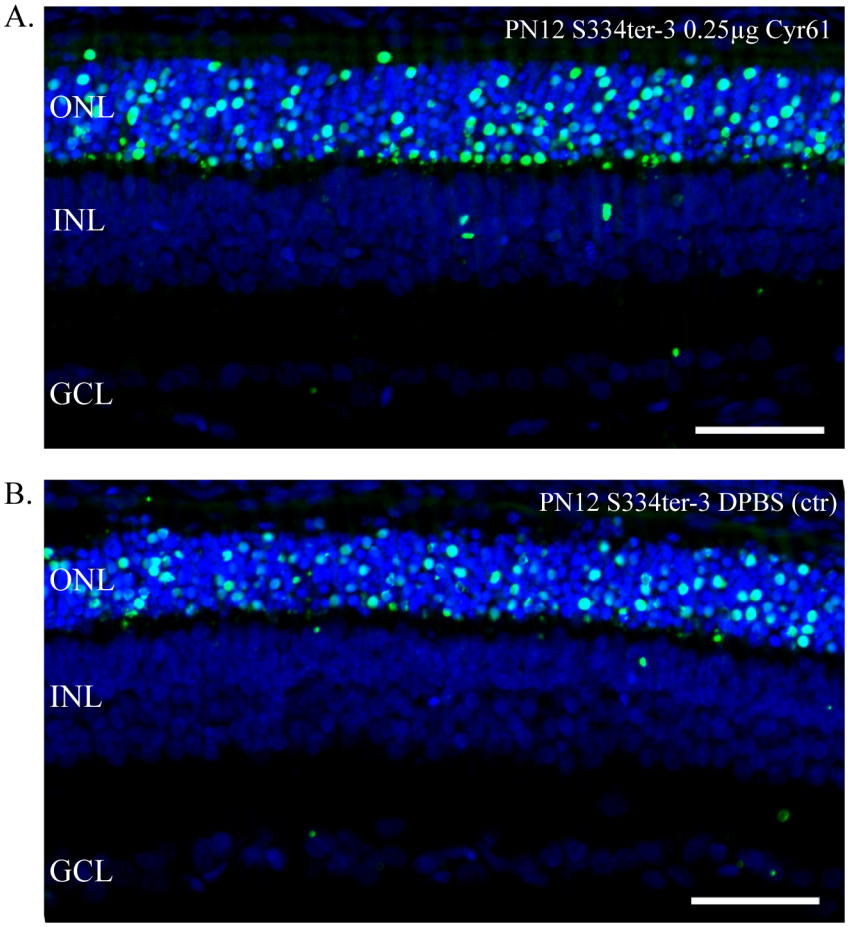

Figure 27. Cyr61 does not decrease cellular death within the outer nuclear layer in S334-ter-3 rats.
Representative TUNEL staining from the optic nerve region of retinas from eyes treated with Cyr61 or Dulbecco's phosphate-buffered saline (DPBS). S334ter-3 rat were injected twice with 0.25µg Cyr61 in the right eye (A) or with DPBS in the left eye (B). After four days the animals were sacrificed and retinas were analysed with the TUNEL method. TUNEL positive cells are marked by green fluorescence; nuclei were counterstained with Hoechst 33342 (blue). Outer nuclear layer (ONL), inner nuclear layer (INL), ganglion cell layer (GCL); Scale bar 50µm.

4.2 Cyr61 can cause pathological retinal vascularization in S334ter-3 rats

Retinal vasculature analyses were made in Tübingen by Vinícius Monteiro de Castro (University of São Paulo, São Paulo, Brazil) and Blanca Arango-Gonzalez (Institute of Ophthalmic Research, at University of Tübingen, Germany).

In light of Cyr61's potential angiogenic activity (Brigstock 2002, Harris et al. 2012) and the detrimental effect that initiation of angiogenesis can have in the retina (Lopez & Green 1992, McVicar *et al.* 2011), the effect of Cyr61 on the developing vasculature of

S334ter-3 rats was also evaluated in the present experiment. Evaluation of the vessels was performed with cSLO, a technique that allows observing vasculature within retinal tissue

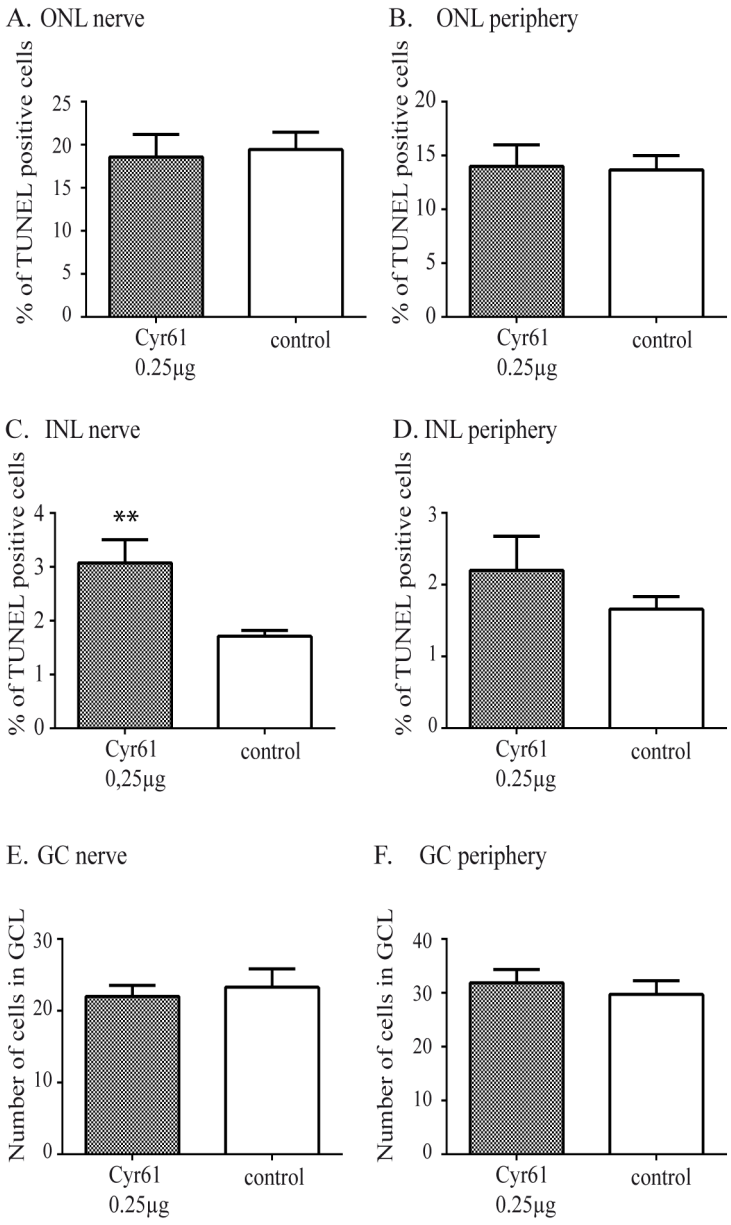

Figure 28. Cyr61 increases cell death in inner nuclear layer of S334ter-3 rats.
Quantification of the percentage of TUNEL positive cells between five days Cyr61 treated eyes and control eyes injected with Dulbecco's phosphate-buffered saline (DPBS). TUNEL stained retinas from 0.25µg Cyr61 treated S334ter-3 rats were analysed using the Defensis 2 software to determine the total cell number as well as the number of TUNEL positive nuclei for outer nuclear layer (ONL) and inner nuclear layer (INL) from eight Cyr61 and ten control eyes. The percentage of TUNEL positive cell was compared in the ONL near the optic nerve (A) and the peripheral retina (B) as well as in the INL near the optic nerve (C) and in the peripheral retina (D). Additionally, the number of ganglion cells (GC) in ganglion cell layer (GCL) was compared in the optic nerve region (E) and from the peripheral retina (F). Bars show mean values, error bars indicate standard error of measurements (SEM), levels of significance: **$p < 0.01$ (Mann Whitney U test).

(deep and superficial capillary plexus), but without detailed distinction between deep and superficial layers (Bartsch & Freeman 1994, Elsner et al. 1996). At the end of the

experiment (PN12), rats were scarified and their eyes were evaluated for vasculature changes using cSLO infrared reflectance imaging (excitation laser 815nm, Fig. 29) and red-free reflectance imaging (excitation laser 488nm) immediately afterwards. In the Cyr61 injected eyes, we could observe sprouting of smaller capillaries from the larger vessels of the retinal layers (Fig. 29, left panel) in comparison to control eyes (Fig. 29, right panel).

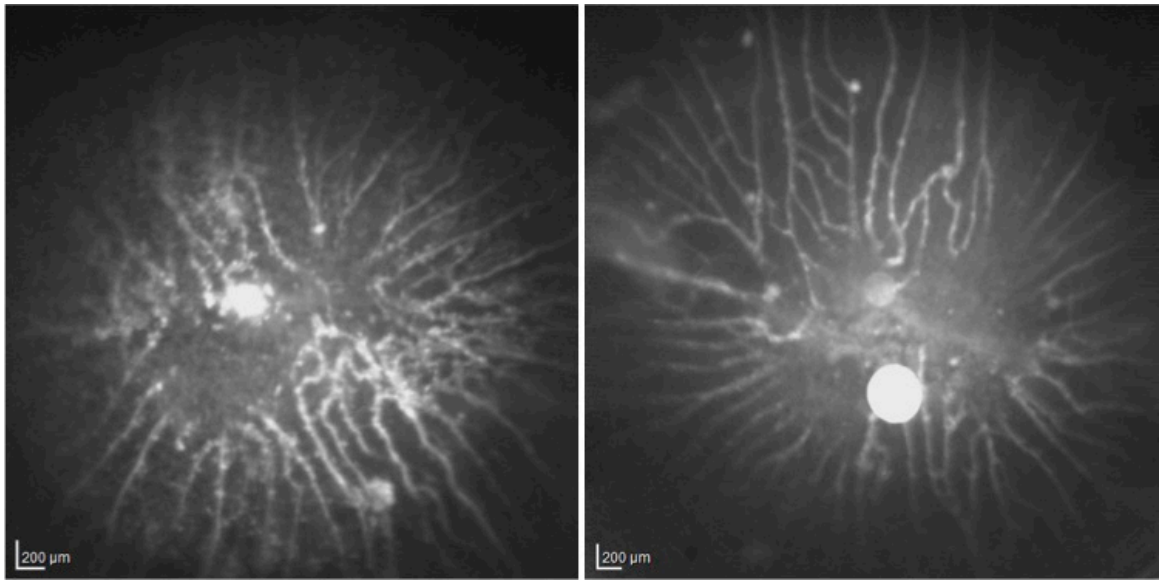

Figure 29. Cyr61 increases sprouting of new capillaries from existing vessels in the rat retina.
Retinas of Cyr61 treated (left panel) and control eyes treated with Dulbecco's phosphate-buffered saline (DPBS) (right panel) of S334ter-3 rats were analysed right after the animals were sacrificed on postnatal day (PN)12, using infrared reflectance imaging (excitation laser 815nm) confocal scanning laser ophthalmoscopy.

In summary, Cyr61 did not protect PR from degeneration in S334ter-3 rats in this first attempt at *in vivo* validation of neuroprotective potential. In fact, apoptosis rates in the INL appeared significantly higher in Cyr61 treated animals. Additionally, ophthalmoscopy scans of the superficial and deep vascular plexus of the retina showed a strong disturbance in the vasculature development of the Cyr61 treated eyes. Future test of Cyr61's neuroprotective capabilities in the intact eyes should explore the issue of finding the right dosage and duration of application of the factor as a first step. Nevertheless, caution concerning the proangiogenic properties of Cyr61 is warranted and changes within the vasculature of the eye, if confirmed in future studies, are likely to prohibit further *in vivo* applications.

IV. DISCUSSION

1. Neuroprotective potential of GDNF induces changes in RMG secretome

Our research was aimed at identifying a novel neuroprotective factor, which in the future could be applied as a therapy for patients with retinitis pigmentosa and possibly with other retinal degenerations. We focused on Müller cells, which are the main retinal glial cells guarding metabolic and ion homeostasis within the retinal tissue, responding to internal as well as external stimuli (Reichenbach & Bringmann 2013). In case of retinal disease, RMG react with cytoprotective activity, which involve a wide range of different mechanisms including synthesis and secretion of cytokines as well as neurotrophic and growth factors (Limb et al. 2002, Joly et al. 2008, Bringmann et al. 2009). It must be mentioned though, that if the pathologic condition is recurrent or chronic, RMG can answer with gliosis, leading to further degeneration of the retina (Reichenbach & Bringmann 2013). Since GDNF, one of the RMG secreted factors, has already well documented prosurvival activity for the retinal neurons (Frasson et al. 1999a), we started our study from a closer examination of its neuroprotective action. Although some publications claim the presence of GDNF receptors on PR membranes (Jomary et al. 2004, Rothermel et al. 2004) the neuroprotective effect of GDNF has rather been attributed to an indirect mechanism through RMG stimulation (Harada et al. 2003, Hauck et al. 2006b). Similarly, indirect prosurvival effects on PR through RMG stimulation were found for other growth factors, like CNTF, BDNF (Adamus et al. 2003, Wen *et al.* 2006, Wen *et al.* 2008, Saito *et al.* 2009) as well as for a member of IL-6 family - oncostatin M (Xia *et al.* 2011). Therefore, we focused on GDNF induced changes in the RMG secretome, which yielded a list of seven significantly upregulated candidate proteins. Out of this list, and based on the available literature, we selected the extracellular matrix protein - Cyr61 (mean upregulation through GDNF 8.4) for further analysis. This protein already has well documented prosurvival effects in the context of cancer (Dunn et al. 1996, Kok et al. 2010, Tang et al. 2011, Sabile et al. 2012), but has not been studied yet in a context of neuroprotective action within retinal tissue. We refrained from investigating the remaining six proteins from the list, for various reasons discussed in detail below. Some of these factors have therapeutic potential, similar to Cyr61, while others are unlikely to be useful for this purpose.

Considering the mean value out of the three conducted experiments the highest increase in secretion was found for PGF-2 (mean ratio 31.5). PGF-2 is an angiogenic factor (Park *et al.* 1994, Luttun *et al.* 2002), whose biology as well as action within retinal tissue has already been broadly investigated. It is a member of the VEGF family and secreted, among others, by endothelial (Zhao *et al.* 2004, Yao *et al.* 2005) and RPE cells (Hollborn *et al.* 2006). It stimulates cells via binding to VEGF receptor 1 (VEGF-R1) (Park et al.

1994) or HSPG (Hauser & Weich 1993). Since VEGF-R1 is present on pericytes and endothelial cells, while only VEGF-R2 has been found on PR and GC (Cao *et al.* 2010), it is likely that PGF-2 does not have direct neurotrophic action on retinal neurons. PGF-2 expression can be stimulated by VEGF (Zhao et al. 2004, Yao et al. 2005) and amplify VEGF action on endothelial cells (Yao et al. 2005). PGF-2 is expressed during neonatal retinal development, but its neutralization caused only a marked persistence of the hyaloid vessels without affecting development of retinal vasculature (Feeney *et al.* 2003). In the adult retina, PGF-2 is absent and its expression is associated with pathologic neovascularization in proliferative retinopathy (Khaliq *et al.* 1998), but it does not disrupt permeability of the retinal-endothelial cell barrier (Deissler *et al.* 2013). PGF-2 expression is increased in GC under hyperoxic conditions, but not under hypoxic conditions (Simpson *et al.* 1999). Furthermore, in a mouse model of retinopathy of prematurity, therapeutic intravitreal injections of PGF-2 remarkably decreased hyperoxia-induced vaso-obliteration without stimulation of vascular proliferation or neovascularization (Shih *et al.* 2003). In summary, PGF-2 has well documented angiogenic activity within the retinal tissue but there is currently no evidence for a potent neuroprotective action.

The second upregulated protein, with mean ratio of 9.9, was IGFBP-3. Increase in expression of this protein by RPE cells can be induced by stimulation with IGF-1 (Slomiany & Rosenzweig 2004) or in neovascular tufts by hypoxic conditions (Lofqvist *et al.* 2009). Functionally, IGFBP-3 forms heterotrimeric complexes with approximately 75% of serum IGF-1 and IGF-2 (Chang *et al.* 2007). IGFBP-3 is increased in hypoxic conditions and can enhance neovascularization (Chang et al. 2007). Moreover, it induces CD34+ endothelial precursor cell differentiation into endothelial cells, increases their migration and capillary tube formation (Chang et al. 2007), but it has no mitogenic/proliferative effect on porcine RMG (King & Guidry 2012). IGFBP-3 has already been widely studied in the context of retinal degenerations. Elevated protein levels of IGFBP-3 were found in the vitreous bodies in proliferative diabetic retinopathy as well as in diabetic ischemic eyes (Pfeiffer *et al.* 1997). Similarly, IGFBP-3 mRNA was increased in retinas of a mouse model of oxygen induced retinopathy (Ishikawa *et al.* 2010). These upregulation appear to be compensatory mechanisms rather than noxious influences, as intravitreal injections of IGFBP-3 prevent VEGF caused loss of junction integrity by retinal endothelial cells forming blood retinal barrier (Jarajapu *et al.* 2012). The IGFBP-3 injections could also reduce vascular leakage in VEGF-induced retinal vascular permeability in mice (Kielczewski *et al.* 2011b). Therefore, IGFBP-3 has been suggested as a novel protective therapy in ocular diseases like diabetic retinopathy (Jarajapu et al. 2012). Additionally, IGFBP-3 was successfully validated as a protective factor under hypoxic conditions. Overexpression of IGFBP-3 by endothelial cells in mouse pups that underwent oxygen-induced retinopathy resulted in decreased apoptosis of neurons of INL as well as pericyte and increased pericyte ensheathment and microglia

apoptosis (Kielczewski *et al.* 2011a). Moreover, administration of IGFBP3 to eyes of a mouse model of oxygen-induced retinopathy resulted in protection from hyperoxia-induced vasculature regression (Chang et al. 2007). In diabetic retina, pharmacological elevation of IGFBP-3 prevented retinal endothelial cell apoptosis under hyperglycemic conditions (Zhang *et al.* 2012b, Zhang *et al.* 2013). Furthermore, IGFBP-3 may have a role in regulating inflammation in diabetic retinopathy (Zhang et al. 2013a). IGFBP-3 knockout mice showed decreased b-wave as well as oscillatory potential amplitudes in ERG, which was accompanied by increased apoptosis in the GCL (Zhang et al. 2013a). These ERG alterations point to a loss of electric activity and by extension excitability in the retina. By the same token, repression of IGFBP-3 expression through 21 days propranolol treatment of rats resulted in a decrease of the b-wave amplitude (Jiang & Steinle 2010). On the other hand, in studies on cancer cells, IGFBP-3 was successfully applied as a therapeutic, activating apoptosis, and was successfully applied as an anti-cancer therapeutic for prostate cancer cells, where it increased activation of caspase-3 and -7 (Liu *et al.* 2005). Similarly, through activation of caspase-7 and -8, IGFBP-3 induced apoptotic death in MCF-7 breast cancer cells (Kim *et al.* 2004). In summary, IGFBP-3 is a molecule regulating retinal vasculature development as well as neuronal cells function, but without indication for prosurvival action within retinal tissue.

The third upregulated protein, fractalkine (mean ratio 9.6), is a proangiogenic chemokine highly expressed in developing healthy as well as rd1 mouse retina (Zeng et al. 2005), although it is not required in the first postnatal week for normal vascular and neuronal development of this tissue (Zhao *et al.* 2009). Within the eye, fractalkine is expressed by endothelial, RMG, GC and RPE cells as well as by the choroid (Silverman *et al.* 2003). Many investigations addressing fractalkine's activity within the retina have already been conducted. In the light-injury rat model of retinal degeneration, fractalkine expression increased mainly in PR cells, enhancing their survival but also inducing microglia migration and release of inflammatory cytokines like IL-1β or TNF-α (Zhang *et al.* 2012a). Since fractalkine modulates microglia migration in response to tissue injury (Liang *et al.* 2009), it has also been suggested to play an important role in regulating leukocyte efflux in inflammatory eye diseases, like anterior uveitis, retinochoroiditis (Silverman et al. 2003), endotoxin-induced uveitis (Chu *et al.* 2009) or in oxidative and ischemia reperfusion conditions (Juel *et al.* 2012). Fractalkine knockout led to uncontrolled retinal inflammation and increased retinal degeneration as well as increased PR death, underscoring its important function in modulating microglia function (Juel et al. 2012). In contrast, in age-related retinal degeneration, fractalkine deficiency in mice impaired microglial and macrophage trafficking, but did not influence loss of PR (Luhmann *et al.* 2013). Similarly, in experiments on oxygen-induced retinopathy, mice lacking fractalkine did not show any difference in INL neuronal cells survival as well as in retinal vascular repair or neovascularization following ischemia (Zhao et al. 2009). To

sum up, fractalkine activity within retina has already been broadly investigated and its influence on the cells depends on the pathologic conditions the tissue is challenged with.

The fourth factor, FGF-1 with a mean ratio 4.5, has already been shown to play a prosurvival role for PR (Bugra & Hicks 1997). FGF-1 is present in GCL, within INL, in photoreceptor ROS and in the RPE cells (Mascarelli *et al.* 1989, Guillonneau *et al.* 1998). Its expression in the rat retina increases during development achieves the highest level in adults (Bugra & Hicks 1997). Receptors for FGF-1 are present in OPL, photoreceptor IS and RPE, but not in INL or on GC, and its transcription increases in light-induced retinal degeneration (Mascarelli et al. 1989). FGF-1 was partially protective in retinal degeneration induced by N-methyl-N-nitrosourea in rats by induction of the antiapoptotic protein Bcl-2 and repression of the proapoptotic protein Bax (Xu *et al.* 2008). Furthermore, in $NaIO_3$ induced retinal degeneration in rats, intravitreal application of FGF-1 not only improved ERG amplitudes of a- and b-waves but also preserved the structure of photoreceptor OS and increased the integrity of the RPE monolayer. Additionally, the thickness of the FGF-1 treated retinal tissue was similar to the normal eyes, showing FGF-1 prosurvival effect on PR (Chen *et al.* 2009). On the other hand, neither the levels of FGF-1 transcript in whole retinal tissue (Bugra & Hicks 1997) nor the protein expression in RPE cells (Malecaze *et al.* 1993) was altered in the RCS rat model of retinitis pigmentosa. In summary, FGF-1 is an established prosurvival factor confirming the validity of our approach.

Tissue factor, the fifth factor with a mean 3.7 fold induction through GDNF, is a cell surface protein, initiating mammalian blood coagulation and is expressed constitutively by vascular subendothelial cells (Drake *et al.* 1989). Considering retinal tissue, TF is expressed in IPL, OPL and the nerve fiber layers (Cho *et al.* 2011). It can promote inflammation (Chu 2005) and angiogenesis (Belting *et al.* 2004). TF is highly upregulated on the transcript as well as protein level in human age-related macula degeneration (AMD) maculae as well as in retinal lesions, neuroretinal tissue and cultured RPE cells of the DKO mouse model of age-related macular degeneration (Cho et al. 2011). Processes that accompany AMD - inflammation and oxidative stress - increase TF expression. Moreover, increasing TF mRNA level as a function of age suggests that TF expression may play a role in the pathogenesis of AMD (Cho et al. 2011). Given TF's association with angiogenesis, inflammation and AMD it did not appear to be a promising candidate for neuroprotection.

The last GDNF induced factor, endostatin, with a mean induction of 2.8 fold, is a 20-kDa proteolytic product of collagen XVIII that is crucial for proper eye vasculature development. A loss of function mutation in endostatin, present in Knobloch syndrome, causes vitreoretinal degeneration, retinal detachment and myopia (Fukai *et al.* 2002). In fact, lack of endostatin leads to RPE and PR abnormalities as well as increased GFAP expression in the retina, which causes a progressive age-dependent visual loss (Marneros

et al. 2004). Additionally, endostatin can inhibit angiogenesis (O'Reilly *et al.* 1997, Bhutto *et al.* 2008) as well as decrease endothelial cell migration and proliferation (O'Reilly et al. 1997) and its level is increased in patients with neovascular AMD (Muether et al. 2013). In studies on a mouse model of retinopathy of prematurity, AAV vector mediated delivery of endostatin to mice eyes inhibited ischemia-induced neovascularization (Auricchio *et al.* 2002). Moreover, after photodynamic therapy in neurovascular AMD, an increase in endostatin levels, rather than a decrease in VEGF, was suggested to reduce neovascularization (Tatar *et al.* 2007, Tatar *et al.* 2008). Considering its inhibitory effect on choroidal neurovascular growth and vascular leakage, endostatin was already proposed as a new therapeutic for treatment of neurovascular AMD (Balaggan *et al.* 2006, Tatar *et al.* 2006, Marneros *et al.* 2007) and proliferative diabetic retinopathy (Orosz *et al.* 2004).

2. Cyr61's neuroprotective effect in the context of the rd1 mouse model of retinitis pigmentosa

To validate Cyr61's neuroprotective activity on degenerating PR, we prepared retinal explants from rd1 mouse model of retinitis pigmentosa. The timing chosen for our short-term explants, PN7 and PN11, coincides with a critical phase for PR survival in rd1 mice. At PN8 swollen mitochondria – one of the first visible sights of molecular disturbances, can be observed in the inner segments of the cells (Farber & Lolley 1974). This is accompanied by increased uptake of oxygen, higher glucose utilization and production of lactic acid (Bowes et al. 1990). Moreover, at PN10, nuclei become pyknotic (Carter-Dawson et al. 1978) and despite cellular integrity and thickness of ONL in mutant retina compared to healthy tissue, OS of PR already show signs of disruption (Carter-Dawson et al. 1978). According to the experimental schedule, the explanted tissue was collected at PN11, when the level of rod death rapidly increases, but the general number of PR is still equal to wild type retina (Portera-Cailliau et al. 1994). In our investigations, Cyr61 applied to medium of rd1 retinal explants for only four days resulted in a decreased percentage of PR death. This encouraged us to challenge Cyr61's neuroprotective potential and study its effect after the peak of PR degeneration, which falls between PN12 and PN14 in rd1 mice (Sanyal & Bal 1973, Carter-Dawson et al. 1978). In this experiment with long term retinal explants, the tissue was stimulated with the factor between PN7 and PN18, covering the first symptoms and cases of rods death as well as the peak of degeneration and even a few of the following days. In this type of experiment we could show the sustained neurotrophic activity of Cyr61 on PR, resulting in significantly higher numbers of preserved PR in ONL versus control explants. This positive result motivated us to follow Cyr61 neuroprotective action and describe its mechanism.

3. Elucidation of the neuroprotective pathways, stimulated by Cyr61 within the retinal tissue

Studies on prolonged PR survival indicate the PI3K/Akt (Kayama *et al.* 2011) and MAPK/Erk (German *et al.* 2006) pathways to be one of the most important for PR survival in retinal degenerations. We decided to monitor changes in activation of these pathways, considering the prosurvival effect of Cyr61 on different cancer cells through phosphorylation of Akt and Erk1/2 (Menendez et al. 2005, Yoshida et al. 2007, Sabile et al. 2012, Zhang et al. 2012c). Furthermore, we decided to monitor the JAK/Stat pathway, which has already been linked with PR survival in different models of retinal degeneration (Adamus et al. 2003, Maier et al. 2004, Joly et al. 2008, Chollangi et al. 2009, Schallenberg et al. 2012) and implicated in the regulation of Cyr61 expression (Klein et al. 2012), although it has not yet been shown to be induced after Cyr61 stimulation.

The first step to find the molecular mechanism of Cyr61's prosurvival action was stimulation of the whole explanted retinal tissue. For this experiment, retina at the age of PN6 was chosen, before any visible signs of PR degeneration. We found phosphorylation of Stat3 and Erk1/2, but not Akt. Activation of Stat3 was already found to be protective for PR in light induced retinal degeneration after treatment with LIF (Burgi *et al.* 2009) as well as in the RCS rat model of inherited retinal degeneration treated with GM-CSF (Schallenberg et al. 2012). Moreover, in experimental antibody-induced retinal degeneration, injections of AAV-CNTF viruses into Lewis rats resulted in an increase in pStat3 in the whole retinal tissue (Adamus et al. 2003). Furthermore, therapies leading to protection of PR from light-induced degeneration, like 24h to 48h of subtoxic levels of continuous illumination or administration of agonists for α2-adrenergic receptors, increased pStat3 in the whole retinal tissue (Peterson *et al.* 2000). On the other hand, docosahexaenoic acid protected PR survival during development and upon oxidative stress via stimulation of the MAPK/Erk signalling pathway (German et al. 2006). Furthermore, preconditioning of the rat retina with bright light, before applying light of the intensity necessary to induce degeneration, resulted in increased survival of PR, accompanied by Erk1/2 activation (Liu *et al.* 1998). Similarly, induced upregulation of GDNF and BDNF after optic nerve injury and activation of Erk1/2 increased GC survival (Nakatani *et al.* 2011). Moreover, CNTF intravitreal injections into rat eyes from a multiple sclerosis model protected GC through activation of Erk1/2 and Stat3 (Maier et al. 2004). Additionally, in experiments on axotomized GC, treatment with IL2 or FGF-2 resulted in increased neuronal survival mediated by activation of the MAPK/Erk together with the JAK/Stat3 pathway or only the MAPK/Erk pathway, respectively (Rios-Munoz *et al.* 2005, Marra *et al.* 2011). Interestingly, the PI3K/Akt pathway was not activated in these studies.

Thus, a variety of neuroprotective factors activate MAPK/Erk and JAK/Stat, but not necessarily PI3K/Akt, showing these two signalling pathways to be the main mediators of neuronal survival in retinal degenerations.

4. Dissection of retinal cell type responsiveness to Cyr61 prosurvival action

4.1 Photoreceptors

Cyr61 can stimulate cells through integrins and via binding to HSPG (Kular et al. 2011, Lau 2011). To reveal the mechanism of Cyr61 neurotrophic activity within rd1 retinal tissue, we first tested whether Cyr61 may stimulate PR directly via binding to integrins present at PR (Brem et al. 1994) and/or through HSPG (Tawara & Inomata 1987, Tawara et al. 1989, Landers et al. 1994). Pig retina was shown to be similar to human retina, which made it an attractive model to use in our study (Chandler *et al.* 1999, Hendrickson & Hicks 2002, Hendrickson *et al.* 2008). We prepared primary porcine PR cells of very high cell-type purity and vitality, and monitored changes in phosphorylation of Stat3, Akt and Erk1/2 upon Cyr61 stimulation. Although PRs showed basic level of phosphorylation of all three signalling molecules, we could not observe any influence of Cyr61 on them at any of the investigated time points. This result implies that direct stimulation of PR by Cyr61 is very likely not the mechanism behind prolonged PR survival. Although there are integrins present on PR (α_2, α_4, α_5, and β_2) none of these integrins have been shown to bind Cyr61 (except for α_2 but only when coupled to β_1 (Lin *et al.* 2007)). This led us to investigate other PR supporting cells, potentially responding to Cyr61. It should be noted though, that Cyr61 might stimulate PR cells by activating other prosurvival pathways not investigated in this study.

4.2 Retinal Müller glial cells

RMG cells secrete a variety of neurotrophic factors to protect PR from external injury (Bringmann et al. 2009). In order to test an indirect neuroprotective action of Cyr61 through binding to integrins (Guidry *et al.* 2003) and/or HSPG (Aricescu et al. 2002) on RMG cell membranes, we used primary porcine RMG cell cultures as well as cultures of MIO-M1 – a human RMG cell line. After Cyr61 stimulation of primary porcine RMG, we could observe activation of all three investigated pathways – JAK/Stat, PI3K/Akt and MAPK/Erk. In contrast, Cyr61 stimulation of MIO-M1 increased phosphorylation of Akt as well as Erk1/2, but not Stat3. The fact that Cyr61 treatment of MIO-M1 did not stimulate the JAK/Stat pathway may rather suggest changes in cellular membrane receptor content, although differences between species cannot be excluded.

Increase in phosphorylation of Stat3, Akt and Erk1/2 suggests a marked induction of RMG intracellular signalling pathways leading to complex transcriptome and secretome changes. It has already been described that activation of Stat3 in RMG cells, but not in PR, in S334ter-3 rats by intravitreal injection of oncostatin M, a member of IL-6 family of cytokines, promoted regeneration of cone OS in an indirect way in the early stages of

their degeneration (Xia et al. 2011). By the same token, CNTF was shown to protect PR survival indirectly through RMG and this effect was dependent on Stat3 activation (LaVail et al. 1998, Rhee *et al.* 2013). Similarly, phosphorylation of Stat3 is also increased in RMG in developing retina and stimulation of progenitor cells with CNTF enhances genesis of RMG through pStat3 (Goureau *et al.* 2004). In fact, increase in Stat3 activity is required for maximal RMG proliferation during regeneration of the light-damaged zebrafish retina (Kassen *et al.* 2009, Nelson *et al.* 2012). All these examples support the hypothesis that Cyr61 stimulated RMG can protect PR from preliminary death via activation of the JAK/Stat signalling pathway.

In our studies, Cyr61 treatment of RMG resulted also in a strong and persistent phosphorylation of Erk1/2. As has already been documented, RMG cells answer to endotoxin-induced uveitis (Takeda *et al.* 2002) or to mechanical stress (Lindqvist *et al.* 2010) with increased phosphorylation of Erk1/2, most probably to protect the retina from ensuing damage. Moreover, we could show nuclear movement of pErk1/2 in MIO-M1 cells. Considering that activated Erk1/2 was shown to phosphorylate c-Fos (Chen *et al.* 1996), Elk-1 (Gille *et al.* 1995) or Sap-1 (Janknecht *et al.* 1995) influencing transcriptome and proteome changes (Roberts & Der 2007) this observation strongly suggests that Cyr61 protects PR survival indirectly, through modulation of RMG and/or RPE protein expression or secretion patterns. It has already been shown, in experiment on rats, that preconditioning of the retina with bright light increased pErk1/2 in RMG, which was accompanied by increased expression of FGF-2 and CNTF in the whole retinal tissue (Liu et al. 1998). Furthermore, GNDF induced activation of the MAPK/Erk signalling pathway in RMG led to increased secretion of neuroprotective FGF-2 (Hauck et al. 2006b). Additionally, in zebrafish light-damaged retina, CNTF indirectly protected PR through increase pErk1/2 but not the pStat3 or pAkt signalling molecules in RMG (Kassen et al. 2009). In accordance with these results, inhibition of Erk1/2 activation in RMG resulted in increased death of GC in a rat model of ischemia and reperfusion (Akiyama *et al.* 2002).

Activation of PI3K/Akt has been observed in RMG cells in response to GDNF (Hauck et al. 2006b), but no available data imply this pathway to be crucial in upregulated secretion of neuroprotective factors. Nevertheless, Akt activation was shown to be a prosurvival mechanism of RMG rather than PR (Kuser-Abali *et al.* 2013) and can be protective for RMG from a cytotoxic environment within the retina, caused by massively degenerating PR.

Activation of three different signalling pathways suggests activation of two different receptors on RMG cell membrane, as MAPK/Erk and PI3K/Akt are often activated by the same receptors, e.g. receptor tyrosine kinases (McCubrey *et al.* 2012), while Stat is activated by cytokine receptors (Stepkowski *et al.* 2008). Integrins like α_1, α_2, α_3, and β_1 are expressed on the RMG cell membrane (Guidry et al. 2003). In cardiac myocytes cells,

Cyr61 increased phosphorylation of Akt as well as Erk1/2 through interaction with integrin β_1, but the observed antiapoptotic effect was mainly due to the PI3K/Akt induced signalling cascade (Gille et al. 1995). In this study we show for the first time that Cyr61 stimulates Stat3 phosphorylation. While the most likely suspect would be a cytokine receptor, it is interesting to note that binding of fibronectin to β_1 integrin on breast cancer cells was also shown to induced the JAK/Stat signalling pathway (Balanis *et al.* 2013).

To sum up, our data shows that Cyr61 secreted by RMG in turn activates an autocrine-signalling loop involving at least three different cellular signalling pathways, which may mediate a sustained prosurvival action within the retinal tissue (Fig. 30).

4.3 Retinal pigment epithelium cells

Similar to RMG, retinal RPE cells support PR through releasing a variety of neurotrophic factors (Li et al. 2011) and participating in the PR visual cycle (Wright et al. 2010). Unlike the former they are also responsible for phagocytosis of PR outer segments (Kandel et al. 2000). After excluding the possibility that Cyr61 directly prolonged survival of PR and confirming its autocrine stimulation of RMG, we additionally focused on Cyr61's influence on RPE cells.

After Cyr61 stimulation of primary porcine RPE cells we observed increases in the activation of the MAPK/Erk and PI3K/Akt, but not the JAK/Stat signalling pathways. Furthermore, experiments conducted on the human ARPE19 cell line confirmed this result and showed that nuclear translocation of Erk1/2 happened analogous to MIO-M1 cells. Activation of the two pathways in RPE cells may lead to the secretion of prosurvival factors similar to RMG, but it is also conceivable in the context of the rd1 model that it is part of a defence mechanism against oxidative stress.

Severe mitochondrial oxidative stress is noticeable already after one week of rd1 mouse life (Farber & Lolley 1974, Vlachantoni et al. 2011), which may be caused by calcium overload, shown in neuronal cells to results in mitochondrial depolarization and subsequent reactive oxygen species production (Lipton & Nicotera 1998). This led to the conclusion that mitochondrial oxidative stress can be one of the reasons leading to the massive RPE atrophy following PR degeneration that is observed in some patients with RP (Mitamura et al. 2012) as well as in rodent models of this disease - rd1 (Pennesi et al. 2012) and the rd10 mice (Pennesi et al. 2012, Samardzija et al. 2012). Along these lines, activation of Akt and Erk1/2, observed in RPE, may protect the cells from harmful substances released by degenerating PR, allowing for their sustained supporting activity. Phosphorylation of Erk1/2 after PEDF treatment was shown to protect ARPE19 cells from oxidative stress (Tsao *et al.* 2006). By the same token, stimulation of the PI3K/Akt signalling pathway with NDP1 as well as with clusterin increased RPE survival during oxidative-stress induced apoptosis (Faghiri & Bazan 2010, Halapin & Bazan 2010, Kim *et al.* 2010). Similarly, an autocrine loop involving VEGF secretion and stimulation exists

in ARPE19 cells, which enhances their survival under induction of oxidative stress via the PI3K/Akt signalling pathway (Byeon *et al.* 2010). Additionally, activation of Akt was involved in protection of ARPE19 from H_2O_2 through the carotenoid Astaxanthin, which reduced apoptosis and intracellular reactive oxygen species production (Li *et al.* 2013).

Cyr61 stimulation of PI3K/Akt and MAPK/Erk signalling pathways suggests it's binding to integrins on the RPE cell membrane, like $\alpha_v\beta_5$ integrins (Nandrot *et al.* 2004) or $\alpha_v\beta_3$ (Finnemann & Rodriguez-Boulan 1999). There are examples for activation of MAPK/Erk and PI3K/Akt through binding of Cyr61 to these specific integrin heterodimers in diverse cell types. In synoviocytes, Cyr61 could activate Akt by binding to $\alpha_v\beta_5$ integrins (Lin *et al.* 2012) and Erk1/2 in osteosarcoma cells through binding to $\alpha_v\beta_3$ integrins (Tan et al. 2009). Similarly, the induction of VEGF in decidual natural killer cells through Cyr61 was mediated through $\alpha_v\beta_3$ integrin and Akt, but not Erk1/2 (Zhang et al. 2012c). In this regard, it is also noteworthy that thrombospondin 1 employs the same receptors as Cyr61, $\alpha_5\beta_1$ and $\alpha_v\beta_5$ integrins, to dramatically induce secretion of FGF-2 and VEGF from RPE cells (Mousa *et al.* 1999).

To sum up, RMG secreted Cyr61 increases PR survival through stimulation of RMG in an autocrine way and RPE cells in a paracrine way, probably by binding to their integrin receptors (Fig. 30). Stimulation of RPE cells may induce secretion of prosurvival factors from RPE but it may also improve their adaptation to oxidative stress.

5. Cyr61 induces transcriptome and secretome changes in RMG cells

In order to test the hypothesis that Cyr61 triggers transcriptome and secretome changes in RMG, we performed quantitative proteomic analysis of Cyr61 stimulated RMG secretomes. In this way, we found six proteins, whose abundance in RMG supernatants increases significantly after Cyr61 treatment and one, whose amount decreased. The available information on these proteins in the context of the eye and retinal degeneration is discussed below.

The highest increase was found for COL3A1. The upregulation of this protein was also confirmed at the mRNA level. Upregulation of COL3A1 mRNA expression after Cyr61 was already shown in a fibroblast cell line stimulated with TGF-β. Selective blockage of this effect *in vivo* decreased choroidal neovascular lesion size and fibrosis (Caballero *et al.* 2011). COL3A1 belongs to the fibrillar collagen family and is a late marker of fibrosis (Zou *et al.* 2012). It can be upregulated by low levels of mechanical stress (Chen *et al.* 2013) and downregulated by oxidative stress (Luna *et al.* 2009). COL3A1 increase extracellular matrix stability (Chen et al. 2013), decrease cell motility (Yun *et al.* 2014) and takes part in scar formation in wound healing (Moura *et al.* 2014). It is essential for proper fibrillogenesis of all organs in the body. Consequently, heterogeneous mutations in the COL3A1 gene cause Ehlers-Danlos syndrome, where reduction of collagen synthesis

results in general fragility of tissue organs and in some cases can also lead to retinal detachment (Omori *et al.* 2011, Beridze & Frishman 2012).

The second highest Cyr61 induced protein was IGFBP-5. During eye development IGFBP-5 is expressed in neuroepithelium, INL, GCL and it probably influences cell differentiation into neuron and glial cells (de la Rosa *et al.* 1994). It can bind with high-affinity to neuroprotective insulin-like growth factors (IGF-1, IGF-2), which were already shown to promote PR survival (Savchenko et al. 2001, Englund-Johansson *et al.* 2010), or to other extracellular matrix proteins like osteopontin or thrombospondin-1 which are known to enhance cellular prosurvival responses to IGF-1 (Jones *et al.* 1993, Nam *et al.* 2000). IGFBP-5 induces human breast cancer cell adhesion and increases cell survival but inhibits cell migration (Sureshbabu *et al.* 2012) and angiogenesis (Hung *et al.* 2008). IGFBP-5 was also shown to mediate RPE endocytosis (Ainscough *et al.* 2009), which may support RPE cells during retinal degeneration in RP.

Cystatin E/M is a secreted glycoprotein belonging to the human family 2 cystatins and a protease inhibitor (Ni *et al.* 1997), and its expression is developmentally regulated (Hong *et al.* 2002). Differentiation of hippocampal neuronal cells induced by FGF-2 treatment is accompanied by increased expression of cystatin E/M, its glycosylation and secretion into the medium (Hong et al. 2002). Although cystatin E/M is a classically secreted protein, its activity is not restricted to the extracellular matrix. It can localize to the nuclei of cells and regulate the intra- and extracellular activity of other proteins (Smith *et al.* 2012). Cystatin E/M has mainly been investigated in the context of cancer. It was found upregulated in human squamous cell carcinomas (Haider *et al.* 2006), but downregulated in cervical cancer cells (Veena *et al.* 2008), malignant glioma cancer cells (Qiu *et al.* 2008), prostate tumor tissues (Pulukuri *et al.* 2009) melanoma cells (Briggs *et al.* 2010), and breast cancer cells (Jin *et al.* 2012). Cystatin E/M medium supplementation for either of these cells inhibited growth, motility, proliferation or invasion.

The next candidate protein is FAM3C, which was also confirmed to be upregulated on the transcriptional level. FAM3C is a secreted protein expressed in retina, brain and many other tissues (Zhu *et al.* 2002, Katahira *et al.* 2010). FAM3C is probably involved in regulation of energy metabolism (Yang & Guan 2013) as well as retinal laminar formation and a loss of function mutations of FAM3C has been reported to cause PR dislocation (Katahira et al. 2010). Moreover, the FAM3C protein level is increased in aqueous humor in patients suffering from Fuchs endothelial corneal dystrophy, where corneal endothelial decompensation leads to corneal edema, and vision impairment (Richardson *et al.* 2010). Interestingly, FAM3C is among a group of proteins containing a GG domain, which has been implicated in human muscle-eye-brain disease and non-syndromic hearing loss (Guo *et al.* 2006).

RLBP1, the fifth protein selected from our proteomics data, is a member of the family of retinoid-binding proteins found in RPE and RMG cells (Anderson *et al.* 1986) as well as in oligodendrocytes in the optic nerve (Saari *et al.* 1997). Its known ligands are 11-cis-retinaldehyde as well as 9- and 11-cis-retinol (Saari *et al.* 1982, Helbling *et al.* 2013). RLBP1 is involved in visual pigment regeneration, retinol metabolism (Saari *et al.* 2001) and contributes to trafficking and apical localization of retinoids within RPE cells (Nawrot *et al.* 2004). Some data implies, that there are more functions of RLBP1, which till now remain undiscovered (Saari et al. 1997). Alterations in molecular structure of the RLBP1 protein lead to serious retinal pathologies. Mutations disrupting the retinol binding activity of RLBP1 have been identified in autosomal recessive RP (Maw *et al.* 1997) and autosomal recessive RP of Bothnia type (Burstedt *et al.* 2001, Burstedt *et al.* 2008). Furthermore, a mutation in the RLBP1 gene was found in a patient with retinitis punctata albescens, a retinal degeneration characterised by delayed rod desensitization, white deposits and retinal pigmentary abnormalities (Morimura *et al.* 1999, Katsanis *et al.* 2001, Fishman *et al.* 2004). RLBP1 increases after prolonged light exposure of the retina (Zhang *et al.* 2010) but it does not change in neovascular age-related macular degeneration (Frank *et al.* 1999). Moreover, observed increase of RLBP1 in induced proliferative vitreoretinopathy (McGillem & Dacheux 1999) can be a defence mechanism, since laser injury of the RPE layer in rat retina resulted in decreased RLBP1 in these cells followed by their intense proliferation and subretinal neovascularization (Zhang *et al.* 1993). These findings are also supported by a study where induction of ARPE19 proliferation inhibited RLBP1 gene expression (Steindl-Kuscher *et al.* 2011). Although found in both RPE and RMG, RLBP1's transcriptional regulation is probably different in both cell types (Kennedy *et al.* 2003). Patients with a group of inherited macular dystrophies, fundus flavimaculatus, present with RPE cells filled with lipofuscin and with reduced RLBP1 expression, changes not observed in RMG (Birnbach *et al.* 1994). On the other hand, RLBP1 expression decreases in RMG cells together with progression of PR degeneration and retinal dystrophy in RCS rats and rd1 mouse (Sheedlo *et al.* 1995) as well as after experimental retinal detachment (Lewis *et al.* 1989). Furthermore, histopathological examination of RPE from RP patients revealed no immunoreactivity for RLBP1 nor for lipofuscin (Li *et al.* 1995).

The next Cyr61 upregulated protein in RMG, matrilin-4, belongs to the matrilin family of extracellular matrix proteins (Wagener *et al.* 1998). It is expressed in nervous, skeletal, epithelial, muscle and connective tissue as well as on the joint surface during their development (Klatt *et al.* 2002). In the eye, matrilin-4 is present in the stroma and epithelial basement membrane of the cornea. Its abundance is increased in granular and lattice type I dystrophies, which suggests its involvement in reorganization and regeneration of the corneal matrix (Szalai *et al.* 2012).

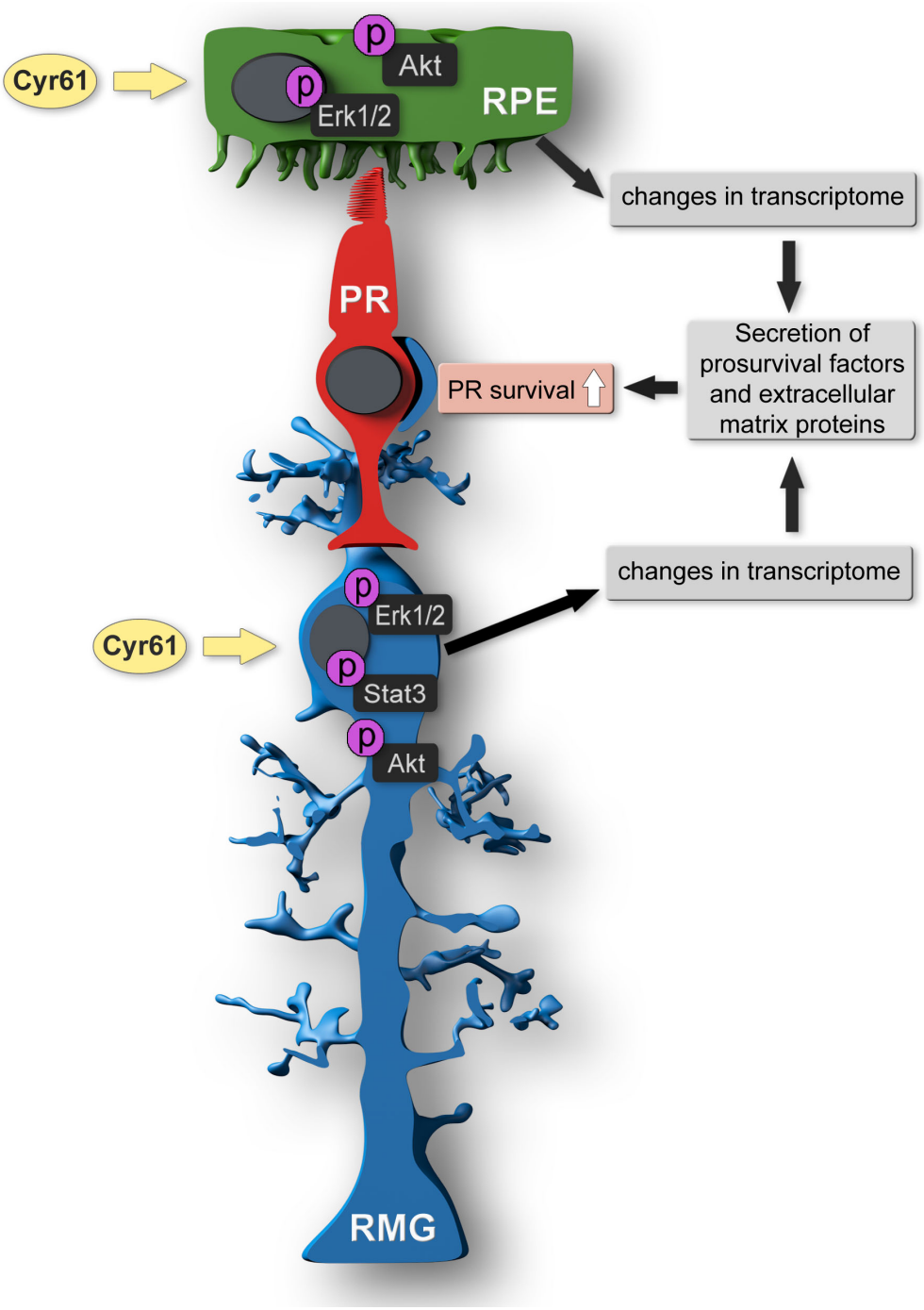

Figure 30. Model of Cyr61's neuroprotective action on photoreceptors within retinal tissue. Cyr61 stimulates retinal Müller glial cells (RMG) as well as retinal pigment epithelium cells (RPE), which leads to phosphorylation of the Stat3, Akt and Erk1/2 signalling molecules. The activated cascades lead to transcriptional and secretome changes of prosurvival factors and extracellular matrix proteins, which in the end leads to prolonged photoreceptor (PR) survival.

Chondroadherin is the only protein we found suppressed in RMG cell supernatants after Cyr61 stimulation. At this point, information about the function of chondroadherin in an eye is sparse. It is expressed in the cornea, lens and retina (Tasheva *et al.* 2004). Decreased mRNA levels of chondroadherin have been found during *Candida albicans* infection of the cornea, which has been suggested to contribute to the acute inflammatory

response to the fungus (Yuan *et al.* 2010). The best-researched functions of chondroadherin pertain to its role in cartilage. It binds to collagen, mediating adhesion of osteoblasts and chondrocytes (Mizuno *et al.* 1996, Mansson *et al.* 2001). In light of the importance of integrins for Cyr61, it is interesting to note that binding of chondroadherin to $\alpha_2\beta_1$ integrins or HSPG on chondrocytes increased intracellular signalling (Haglund *et al.* 2011, Haglund *et al.* 2013). Moreover, chondroadherin inhibits osteoclast and bone resorption through integrin binding (Capulli *et al.* 2014).

Taken together, Cyr61 induced RMG transcriptome changes, which led to alterations in a pattern of the RMG secretome. Considering that the proteins found to be upregulated are extracellular matrix proteins as well as secreted factors, the results suggest that neuroprotective action through RMG may include extracellular matrix remodelling as well as secretion of a factor directly influencing PR survival (Fig. 30).

6. Cyr61 *in vivo* application in the S334ter-3 rat retina

After showing the neuroprotective efficiency of Cyr61 in retinal mouse explants and dissecting the response of prosurvival pathways of three different retinal cell types, we conducted a first *in vivo* examination of Cyr61 prosurvival potential in the S334ter-3 rat model of retinal degeneration.

Delivery of the neurotrophic factor was achieved by local injection into the eye, since most of factors are either too big to cross the blood-retinal barrier (Kastin *et al.* 2003) or can elicit unacceptable systemic side effects. Therefore, local administration directly into the eye is regarded as the only practical way of factor delivery. For long term experiments, when injection of the factor would have to be applied repetitively, several delivery methods have been developed, including transduction of retinal cells using adeno associated viruses to secrete neuroprotection factors (McGee Sanftner et al. 2001) or cell based delivery of factors (MacDonald *et al.* 2007). Nevertheless, as a proof of concept experiment we decided to use two simple injections of recombinant human Cyr61. In some studies neurotrophic factors were tested by injection into the subretinal space (Frasson et al. 1999a) despite the accompanying retinal detachment and gliosis. We chose intravitreal injections over this method, since it causes less retinal trauma and pathologic gliosis (Dalkara et al. 2011).

In this first experiment, Cyr61 failed to reduce the number of TUNEL positive cell in the ONL and even led to an increase of apoptosis in the INL. There are several possible explanations for the failure of this experiment. The dose of Cyr61 may have been too high and will need to be titrated carefully in future projects. The amount of applied Cyr61 was 0.25µg in 1µl, which is 500 and 250 times more than used during short term and long term retinal explants, respectively. Alternatively, human Cyr61 may not work for the treatment of the S334ter-3 rat, although it was effective for rd1 mice. In this regard, other models of retinal degeneration may be explored, but it is impractical to perform

intravitreal injections on a mouse eye. However, the S334ter-3 rat model of retinitis pigmentosa may be substituted for a different model with a less rapidly proceeding PR degeneration. Although S334ter-3 rats were used in many studies on retinal degeneration, their PR never reach normal morphology and their rapid degeneration introduce changes in the retina, including fewer horizontal processes and bipolar cells dendrites than, for example, in the S334ter-5 rat (Martinez-Navarrete et al. 2011).

The influence of Cyr61 on the retinal vasculature also seems to have been a major confounding factor. In S334-ter-3 rats, degeneration of photoreceptors negatively influences development of the deep capillary plexus. By PN15, only 6-7% of the number observed in the wild type retinas is left and the capillary plexus vasculature atrophies (Pennesi et al. 2008). With the method we applied to visualise retinal vasculature we cannot distinguish deep capillary plexus from superficial capillary plexus. This could be achieved via injections of sodium fluorescein (Paques *et al.* 2006). Nevertheless, given that the experiment was conducted with the timeframe of the development of the deep capillary plexus and that Cyr61 is responsible for proper retinal vasculature development (Hasan et al. 2011), we would expect that Cyr61 would most prominently affect the development of the deep capillary plexus. In line with this hypothesis are our observations: Cyr61 increased cell death within INL, the layer penetrated by the deep capillary plexus. Moreover, Cyr61 did not influence the number of GC within the ganglion cell layer, which is supplied by the superficial capillary plexus. Therefore, the observed lack of neuroprotective action within PR cells could have been caused by severe changes in the inner plexiform vasculature leading to an increasing cell death rate within the INL. In this way the neurotrophic potential of Cyr61 may have been masked by its angiogenic property.

In the context of neovascularization, Cyr61 has already been associated with vascular alterations in diabetic retinopathy (You et al. 2009, You et al. 2012). On the other hand, it was also successfully validated as a therapeutic strategy in an animal model of retinopathy of prematurity (Hasan et al. 2011). Furthermore, Cyr61 was positively tested as a potential therapeutic factor in models of peripheral ischemic diseases (Fataccioli et al. 2002, Rayssac et al. 2009).

Two solutions for future *in vivo* experiments can be considered. First would be to titrate the dosage of Cyr61 to find the proper concentration that would promote PR survival, without introducing vascular disturbances. The second option would be to use a mutant of Cyr61 that does not bind to the endothelial αvβ3 receptor leading to their increased migration, adhesion, mitogenesis and tube formation (Leu et al. 2002). However, this mutant Cyr61 would have to be tested for neuroprotective activity first.

In summary, our first *in vivo* experiment failed to show Cyr61 neuroprotective action on PR in S334ter-3 rat model of retinitis pigmentosa. However, refinement of the

experimental approach and addressing the issue of Cyr61's angiogenic properties may yet lead to success in the future. The presented research up to this point demonstrates that Cyr61 is a potent neuroprotective factor within the retina and encourages further investigation of Cyr61's action with the goal of harnessing the therapeutic potential of this protein.

V. REFERENCES

Acland, G. M., Aguirre, G. D., Bennett, J. et al. (2005) Long-term restoration of rod and cone vision by single dose rAAV-mediated gene transfer to the retina in a canine model of childhood blindness. *Molecular therapy : the journal of the American Society of Gene Therapy,* 12, 1072-1082.

Acosta, M. L., Fletcher, E. L., Azizoglu, S., Foster, L. E., Farber, D. B. and Kalloniatis, M. (2005) Early markers of retinal degeneration in rd/rd mice. *Molecular vision,* 11, 717-728.

Adamus, G., Sugden, B., Shiraga, S., Timmers, A. M. and Hauswirth, W. W. (2003) Anti-apoptotic effects of CNTF gene transfer on photoreceptor degeneration in experimental antibody-induced retinopathy. *Journal of autoimmunity,* 21, 121-129.

Agca, C., Gubler, A., Traber, G., Beck, C., Imsand, C., Ail, D., Caprara, C. and Grimm, C. (2013) p38 MAPK signaling acts upstream of LIF-dependent neuroprotection during photoreceptor degeneration. *Cell death & disease,* 4, e785.

Ahuja, P., Caffe, A. R., Holmqvist, I., Soderpalm, A. K., Singh, D. P., Shinohara, T. and van Veen, T. (2001) Lens epithelium-derived growth factor (LEDGF) delays photoreceptor degeneration in explants of rd/rd mouse retina. *Neuroreport,* 12, 2951-2955.

Ainscough, S. L., Feigl, B., Malda, J. and Harkin, D. G. (2009) Discovery and characterization of IGFBP-mediated endocytosis in the human retinal pigment epithelial cell line ARPE-19. *Experimental eye research,* 89, 629-637.

Akiyama, H., Nakazawa, T., Shimura, M., Tomita, H. and Tamai, M. (2002) Presence of mitogen-activated protein kinase in retinal Muller cells and its neuroprotective effect ischemia-reperfusion injury. *Neuroreport,* 13, 2103-2107.

An, G. J., Asayama, N., Humayun, M. S., Weiland, J., Cao, J., Kim, S. Y., Grebe, R., de Juan, E., Jr. and Sadda, S. (2002) Ganglion cell responses to retinal light stimulation in the absence of photoreceptor outer segments from retinal degenerate rodents. *Current eye research,* 24, 26-32.

Anand-Apte, B. and Hollyfield, J. G. (2010) Developmental Anatomy of the Retinal and Choroidal Vasculature. In: *Encyclopedia of the Eye*, (D. A. Dartt ed.), pp. 9-15. Elsevier Ltd.

Anderson, D. H., Neitz, J., Saari, J. C., Kaska, D. D., Fenwick, J., Jacobs, G. H. and Fisher, S. K. (1986) Retinoid-binding proteins in cone-dominant retinas. *Investigative ophthalmology & visual science,* 27, 1015-1026.

Andreasson, S. O., Sandberg, M. A. and Berson, E. L. (1988) Narrow-band filtering for monitoring low-amplitude cone electroretinograms in retinitis pigmentosa. *American journal of ophthalmology,* 105, 500-503.

Arango-Gonzalez, B., Cellerino, A. and Kohler, K. (2009) Exogenous brain-derived neurotrophic factor (BDNF) reverts phenotypic changes in the retinas of transgenic mice lacking the BDNF gene. *Investigative ophthalmology & visual science,* 50, 1416-1422.

Arataki, S., Tomizawa, K., Moriwaki, A. et al. (2005) Calpain inhibitors prevent neuronal cell death and ameliorate motor disturbances after compression-induced spinal cord injury in rats. *Journal of neurotrauma,* 22, 398-406.

Aricescu, A. R., McKinnell, I. W., Halfter, W. and Stoker, A. W. (2002) Heparan sulfate proteoglycans are ligands for receptor protein tyrosine phosphatase sigma. *Molecular and cellular biology,* 22, 1881-1892.

Athanasopoulos, A. N., Schneider, D., Keiper, T. et al. (2007) Vascular endothelial growth factor (VEGF)-induced up-regulation of CCN1 in osteoblasts mediates proangiogenic activities in endothelial cells and promotes fracture healing. *The Journal of biological chemistry,* 282, 26746-26753.

Auricchio, A., Behling, K. C., Maguire, A. M., O'Connor, E. M., Bennett, J., Wilson, J. M. and Tolentino, M. J. (2002) Inhibition of retinal neovascularization by intraocular viral-mediated delivery of anti-angiogenic agents. *Molecular therapy : the journal of the American Society of Gene Therapy,* 6, 490-494.

Babic, A. M., Kireeva, M. L., Kolesnikova, T. V. and Lau, L. F. (1998) CYR61, a product of a growth factor-inducible immediate early gene, promotes angiogenesis and tumor growth. *Proceedings of the National Academy of Sciences of the United States of America,* 95, 6355-6360.

Baid, R., Upadhyay, A. K., Shinohara, T. and Kompella, U. B. (2013) Biosynthesis, characterization, and efficacy in retinal degenerative diseases of lens epithelium-derived growth factor fragment (LEDGF1-326), a novel therapeutic protein. *The Journal of biological chemistry,* 288, 17372-17383.

Balaggan, K. S., Binley, K., Esapa, M. et al. (2006) EIAV vector-mediated delivery of endostatin or angiostatin inhibits angiogenesis and vascular hyperpermeability in experimental CNV. *Gene therapy,* 13, 1153-1165.

Balanis, N., Wendt, M. K., Schiemann, B. J., Wang, Z., Schiemann, W. P. and Carlin, C. R. (2013) Epithelial to mesenchymal transition promotes breast cancer progression via a fibronectin-dependent STAT3 signaling pathway. *The Journal of biological chemistry,* 288, 17954-17967.

Bartsch, D. U. and Freeman, W. R. (1994) Axial intensity distribution analysis of the human retina with a confocal scanning laser tomograph. *Experimental eye research,* 58, 161-173.

Belting, M., Dorrell, M. I., Sandgren, S. et al. (2004) Regulation of angiogenesis by tissue factor cytoplasmic domain signaling. *Nature medicine,* 10, 502-509.

Beridze, N. and Frishman, W. H. (2012) Vascular Ehlers-Danlos syndrome: pathophysiology, diagnosis, and prevention and treatment of its complications. *Cardiology in review,* 20, 4-7.

Bharti, K., Rao, M., Hull, S. C., Stroncek, D., Brooks, B. P., Feigal, E., van Meurs, J. C., Huang, C. A. and Miller, S. S. (2014) Developing cellular therapies for retinal degenerative diseases. *Investigative ophthalmology & visual science,* 55, 1191-1202.

Bhutto, I. A., Uno, K., Merges, C., Zhang, L., McLeod, D. S. and Lutty, G. A. (2008) Reduction of endogenous angiogenesis inhibitors in Bruch's membrane of the submacular region in eyes with age-related macular degeneration. *Archives of ophthalmology,* 126, 670-678.

Bi, A., Cui, J., Ma, Y. P., Olshevskaya, E., Pu, M., Dizhoor, A. M. and Pan, Z. H. (2006) Ectopic expression of a microbial-type rhodopsin restores visual responses in mice with photoreceptor degeneration. *Neuron,* 50, 23-33.

Birch, D. G., Anderson, J. L. and Fish, G. E. (1999) Yearly rates of rod and cone functional loss in retinitis pigmentosa and cone-rod dystrophy. *Ophthalmology,* 106, 258-268.

Birnbach, C. D., Jarvelainen, M., Possin, D. E. and Milam, A. H. (1994) Histopathology and immunocytochemistry of the neurosensory retina in fundus flavimaculatus. *Ophthalmology,* 101, 1211-1219.

Borooah, S., Phillips, M. J., Bilican, B., Wright, A. F., Wilmut, I., Chandran, S., Gamm, D. and Dhillon, B. (2013) Using human induced pluripotent stem cells to treat retinal disease. *Progress in retinal and eye research,* 37, 163-181.

Bowes, C., Li, T., Danciger, M., Baxter, L. C., Applebury, M. L. and Farber, D. B. (1990) Retinal degeneration in the rd mouse is caused by a defect in the beta subunit of rod cGMP-phosphodiesterase. *Nature,* 347, 677-680.

Brelen, M. E., Duret, F., Gerard, B., Delbeke, J. and Veraart, C. (2005) Creating a meaningful visual perception in blind volunteers by optic nerve stimulation. *Journal of neural engineering,* 2, S22-28.

Brem, R. B., Robbins, S. G., Wilson, D. J., O'Rourke, L. M., Mixon, R. N., Robertson, J. E., Planck, S. R. and Rosenbaum, J. T. (1994) Immunolocalization of integrins in the human retina. *Investigative ophthalmology & visual science,* 35, 3466-3474.

Briggs, J. J., Haugen, M. H., Johansen, H. T., Riker, A. I., Abrahamson, M., Fodstad, O., Maelandsmo, G. M. and Solberg, R. (2010) Cystatin E/M suppresses legumain activity and invasion of human melanoma. *BMC cancer,* 10, 17.

Brigstock, D. R. (2002) Regulation of angiogenesis and endothelial cell function by connective tissue growth factor (CTGF) and cysteine-rich 61 (CYR61). *Angiogenesis,* 5, 153-165.

Bringmann, A., Iandiev, I., Pannicke, T., Wurm, A., Hollborn, M., Wiedemann, P., Osborne, N. N. and Reichenbach, A. (2009) Cellular signaling and factors involved in Muller cell gliosis: neuroprotective and detrimental effects. *Progress in retinal and eye research,* 28, 423-451.

Bringmann, A., Pannicke, T., Grosche, J., Francke, M., Wiedemann, P., Skatchkov, S. N., Osborne, N. N. and Reichenbach, A. (2006) Muller cells in the healthy and diseased retina. *Progress in retinal and eye research,* 25, 397-424.

Bringmann, A. and Reichenbach, A. (2001) Role of Muller cells in retinal degenerations. *Frontiers in bioscience : a journal and virtual library,* 6, E72-92.

Bromberg, J. F., Wrzeszczynska, M. H., Devgan, G., Zhao, Y., Pestell, R. G., Albanese, C. and Darnell, J. E., Jr. (1999) Stat3 as an oncogene. *Cell,* 98, 295-303.

Brunner, A., Chinn, J., Neubauer, M. and Purchio, A. F. (1991) Identification of a gene family regulated by transforming growth factor-beta. *DNA and cell biology,* 10, 293-300.

Buch, P. K., MacLaren, R. E., Duran, Y., Balaggan, K. S., MacNeil, A., Schlichtenbrede, F. C., Smith, A. J. and Ali, R. R. (2006) In contrast to AAV-mediated Cntf expression, AAV-mediated Gdnf expression enhances gene replacement therapy in rodent models of retinal degeneration. *Molecular therapy : the journal of the American Society of Gene Therapy,* 14, 700-709.

Bugra, K. and Hicks, D. (1997) Acidic and basic fibroblast growth factor messenger RNA and protein show increased expression in adult compared to developing normal and dystrophic rat retina. *Journal of molecular neuroscience : MN,* 9, 13-25.

Burgi, S., Samardzija, M. and Grimm, C. (2009) Endogenous leukemia inhibitory factor protects photoreceptor cells against light-induced degeneration. *Molecular vision,* 15, 1631-1637.

Burstedt, M. S., Forsman-Semb, K., Golovleva, I., Janunger, T., Wachtmeister, L. and Sandgren, O. (2001) Ocular phenotype of bothnia dystrophy, an autosomal recessive retinitis pigmentosa associated with an R234W mutation in the RLBP1 gene. *Archives of ophthalmology,* 119, 260-267.

Burstedt, M. S., Sandgren, O., Golovleva, I. and Wachtmeister, L. (2008) Effects of prolonged dark adaptation in patients with retinitis pigmentosa of Bothnia type: an electrophysiological study. *Documenta ophthalmologica. Advances in ophthalmology,* 116, 193-205.

Byeon, S. H., Lee, S. C., Choi, S. H., Lee, H. K., Lee, J. H., Chu, Y. K. and Kwon, O. W. (2010) Vascular endothelial growth factor as an autocrine survival factor for retinal pigment epithelial cells under oxidative stress via the VEGF-R2/PI3K/Akt. *Investigative ophthalmology & visual science,* 51, 1190-1197.

Caballero, S., Yang, R., Grant, M. B. and Chaqour, B. (2011) Selective blockade of cytoskeletal actin remodeling reduces experimental choroidal neovascularization. *Investigative ophthalmology & visual science,* 52, 2490-2496.

Caffe, A. R., Ahuja, P., Holmqvist, B., Azadi, S., Forsell, J., Holmqvist, I., Soderpalm, A. K. and van Veen, T. (2001) Mouse retina explants after long-term culture in serum free medium. *Journal of chemical neuroanatomy,* 22, 263-273.

Cairns, J. E. (1959) Normal development of the hyaloid and retinal vessels in the rat. *The British journal of ophthalmology,* 43, 385-393.

Caley, D. W., Johnson, C. and Liebelt, R. A. (1972) The postnatal development of the retina in the normal and rodless CBA mouse: a light and electron microscopic study. *The American journal of anatomy,* 133, 179-212.

Campochiaro, P. A., Hackett, S. F., Vinores, S. A. et al. (1994) Platelet-derived growth factor is an autocrine growth stimulator in retinal pigmented epithelial cells. *Journal of cell science,* 107 (Pt 9), 2459-2469.

Cao, R., Xue, Y., Hedlund, E. M. et al. (2010) VEGFR1-mediated pericyte ablation links VEGF and PlGF to cancer-associated retinopathy. *Proceedings of the National Academy of Sciences of the United States of America,* 107, 856-861.

Capulli, M., Olstad, O. K., Onnerfjord, P., Tillgren, V., Muraca, M., Gautvik, K. M., Heinegard, D., Rucci, N. and Teti, A. (2014) The C-Terminal Domain of Chondroadherin: A New Regulator of Osteoclast Motility Counteracting Bone Loss. *Journal of bone and mineral research : the official journal of the American Society for Bone and Mineral Research*.

Carter-Dawson, L. D., LaVail, M. M. and Sidman, R. L. (1978) Differential effect of the rd mutation on rods and cones in the mouse retina. *Investigative ophthalmology & visual science,* 17, 489-498.

Cayouette, M., Smith, S. B., Becerra, S. P. and Gravel, C. (1999) Pigment epithelium-derived factor delays the death of photoreceptors in mouse models of inherited retinal degenerations. *Neurobiology of disease,* 6, 523-532.

Chandler, M. J., Smith, P. J., Samuelson, D. A. and MacKay, E. O. (1999) Photoreceptor density of the domestic pig retina. *Veterinary ophthalmology,* 2, 179-184.

Chang, K. H., Chan-Ling, T., McFarland, E. L. et al. (2007) IGF binding protein-3 regulates hematopoietic stem cell and endothelial precursor cell function during vascular development. *Proceedings of the National Academy of Sciences of the United States of America,* 104, 10595-10600.

Chaqour, B. and Goppelt-Struebe, M. (2006) Mechanical regulation of the Cyr61/CCN1 and CTGF/CCN2 proteins. *The FEBS journal,* 273, 3639-3649.

Chen, R. H., Juo, P. C., Curran, T. and Blenis, J. (1996) Phosphorylation of c-Fos at the C-terminus enhances its transforming activity. *Oncogene,* 12, 1493-1502.

Chen, W., Yu, M., Wang, Y., Peng, Y., Li, X., Lam, D. M., Chen, X. and Liu, X. (2009) Non-mitogenic human acidic fibroblast growth factor reduces retinal degeneration induced by sodium iodate. *Journal of ocular pharmacology and therapeutics : the*

official journal of the Association for Ocular Pharmacology and Therapeutics, 25, 315-320.

Chen, Y. J., Jeng, J. H., Chang, H. H., Huang, M. Y., Tsai, F. F. and Yao, C. C. (2013) Differential regulation of collagen, lysyl oxidase and MMP-2 in human periodontal ligament cells by low- and high-level mechanical stretching. *Journal of periodontal research,* 48, 466-474.

Cho, Y., Cao, X., Shen, D., Tuo, J., Parver, L. M., Rickles, F. R. and Chan, C. C. (2011) Evidence for enhanced tissue factor expression in age-related macular degeneration. *Laboratory investigation; a journal of technical methods and pathology,* 91, 519-526.

Chollangi, S., Wang, J., Martin, A., Quinn, J. and Ash, J. D. (2009) Preconditioning-induced protection from oxidative injury is mediated by leukemia inhibitory factor receptor (LIFR) and its ligands in the retina. *Neurobiology of disease,* 34, 535-544.

Chomczynski, P. (1993) A reagent for the single-step simultaneous isolation of RNA, DNA and proteins from cell and tissue samples. *BioTechniques,* 15, 532-534, 536-537.

Chow, A. Y., Chow, V. Y., Packo, K. H., Pollack, J. S., Peyman, G. A. and Schuchard, R. (2004) The artificial silicon retina microchip for the treatment of vision loss from retinitis pigmentosa. *Archives of ophthalmology,* 122, 460-469.

Chu, A. J. (2005) Tissue factor mediates inflammation. *Archives of biochemistry and biophysics,* 440, 123-132.

Chu, L., Li, X., Yu, W., Qian, T., Qi, H., Huang, L. and Xu, Y. (2009) Expression of fractalkine (CX3CL1) and its receptor in endotoxin-induced uveitis. *Ophthalmic research,* 42, 160-166.

Chung, K. C. and Ahn, Y. S. (1998) Expression of immediate early gene cyr61 during the differentiation of immortalized embryonic hippocampal neuronal cells. *Neuroscience letters,* 255, 155-158.

Clegg, D. O., Mullick, L. H., Wingerd, K. L., Lin, H., Atienza, J. W., Bradshaw, A. D., Gervin, D. B. and Cann, G. M. (2000) Adhesive events in retinal development and function: the role of integrin receptors. *Results and problems in cell differentiation,* 31, 141-156.

Concepcion, F., Mendez, A. and Chen, J. (2002) The carboxyl-terminal domain is essential for rhodopsin transport in rod photoreceptors. *Vision research,* 42, 417-426.

Csoregh, L., Andersson, E. and Fried, G. (2009) Transcriptional analysis of estrogen effects in human embryonic neurons and glial cells. *Neuroendocrinology,* 89, 171-186.

Curcio, C. A., Sloan, K. R., Kalina, R. E. and Hendrickson, A. E. (1990) Human photoreceptor topography. *The Journal of comparative neurology,* 292, 497-523.

Dalkara, D., Kolstad, K. D., Guerin, K. I., Hoffmann, N. V., Visel, M., Klimczak, R. R., Schaffer, D. V. and Flannery, J. G. (2011) AAV mediated GDNF secretion from retinal glia slows down retinal degeneration in a rat model of retinitis pigmentosa. *Molecular therapy : the journal of the American Society of Gene Therapy,* 19, 1602-1608.

de la Rosa, E. J., Bondy, C. A., Hernandez-Sanchez, C., Wu, X., Zhou, J., Lopez-Carranza, A., Scavo, L. M. and de Pablo, F. (1994) Insulin and insulin-like growth factor system components gene expression in the chicken retina from early neurogenesis until late development and their effect on neuroepithelial cells. *The European journal of neuroscience,* 6, 1801-1810.

Deissler, H. L., Deissler, H., Lang, G. K. and Lang, G. E. (2013) VEGF but not PlGF disturbs the barrier of retinal endothelial cells. *Experimental eye research,* 115, 162-171.

Del Rio, P., Irmler, M., Arango-Gonzalez, B. et al. (2011) GDNF-induced osteopontin from Muller glial cells promotes photoreceptor survival in the Pde6brd1 mouse model of retinal degeneration. *Glia,* 59, 821-832.

Dhandapani, K. M., Khan, M. M., Wade, F. M., Wakade, C., Mahesh, V. B. and Brann, D. W. (2007) Induction of transforming growth factor-beta1 by basic fibroblast growth factor in rat C6 glioma cells and astrocytes is mediated by MEK/ERK signaling and AP-1 activation. *Journal of neuroscience research,* 85, 1033-1045.

Di Polo, A., Aigner, L. J., Dunn, R. J., Bray, G. M. and Aguayo, A. J. (1998) Prolonged delivery of brain-derived neurotrophic factor by adenovirus-infected Muller cells temporarily rescues injured retinal ganglion cells. *Proceedings of the National Academy of Sciences of the United States of America,* 95, 3978-3983.

Doonan, F., Donovan, M. and Cotter, T. G. (2003) Caspase-independent photoreceptor apoptosis in mouse models of retinal degeneration. *The Journal of neuroscience : the official journal of the Society for Neuroscience,* 23, 5723-5731.

Doonan, F., Donovan, M. and Cotter, T. G. (2005) Activation of multiple pathways during photoreceptor apoptosis in the rd mouse. *Investigative ophthalmology & visual science,* 46, 3530-3538.

Drake, T. A., Morrissey, J. H. and Edgington, T. S. (1989) Selective cellular expression of tissue factor in human tissues. Implications for disorders of hemostasis and thrombosis. *The American journal of pathology,* 134, 1087-1097.

Dunn, K. C., Aotaki-Keen, A. E., Putkey, F. R. and Hjelmeland, L. M. (1996) ARPE-19, a human retinal pigment epithelial cell line with differentiated properties. *Experimental eye research,* 62, 155-169.

Dupont, A., Tokarski, C., Dekeyzer, O., Guihot, A. L., Amouyel, P., Rolando, C. and Pinet, F. (2004) Two-dimensional maps and databases of the human macrophage proteome and secretome. *Proteomics,* 4, 1761-1778.

Edinger, A. L. and Thompson, C. B. (2004) Death by design: apoptosis, necrosis and autophagy. *Current opinion in cell biology,* 16, 663-669.

Eichler, W., Kuhrt, H., Hoffmann, S., Wiedemann, P. and Reichenbach, A. (2000) VEGF release by retinal glia depends on both oxygen and glucose supply. *Neuroreport,* 11, 3533-3537.

Eichler, W., Yafai, Y., Keller, T., Wiedemann, P. and Reichenbach, A. (2004) PEDF derived from glial Muller cells: a possible regulator of retinal angiogenesis. *Experimental cell research,* 299, 68-78.

Elsner, A. E., Burns, S. A., Weiter, J. J. and Delori, F. C. (1996) Infrared imaging of sub-retinal structures in the human ocular fundus. *Vision research,* 36, 191-205.

Engerman, R. L. and Meyer, R. K. (1965) Development of retinal vasculature in rats. *American journal of ophthalmology,* 60, 628-641.

Englund-Johansson, U., Mohlin, C., Liljekvist-Soltic, I., Ekstrom, P. and Johansson, K. (2010) Human neural progenitor cells promote photoreceptor survival in retinal explants. *Experimental eye research,* 90, 292-299.

Faghiri, Z. and Bazan, N. G. (2010) PI3K/Akt and mTOR/p70S6K pathways mediate neuroprotectin D1-induced retinal pigment epithelial cell survival during oxidative stress-induced apoptosis. *Experimental eye research,* 90, 718-725.

Faktorovich, E. G., Steinberg, R. H., Yasumura, D., Matthes, M. T. and LaVail, M. M. (1990) Photoreceptor degeneration in inherited retinal dystrophy delayed by basic fibroblast growth factor. *Nature,* 347, 83-86.

Farber, D. B. and Lolley, R. N. (1974) Cyclic guanosine monophosphate: elevation in degenerating photoreceptor cells of the C3H mouse retina. *Science,* 186, 449-451.
Fataccioli, V., Abergel, V., Wingertsmann, L., Neuville, P., Spitz, E., Adnot, S., Calenda, V. and Teiger, E. (2002) Stimulation of angiogenesis by Cyr61 gene: a new therapeutic candidate. *Human gene therapy,* 13, 1461-1470.
Feeney, S. A., Simpson, D. A., Gardiner, T. A., Boyle, C., Jamison, P. and Stitt, A. W. (2003) Role of vascular endothelial growth factor and placental growth factors during retinal vascular development and hyaloid regression. *Investigative ophthalmology & visual science,* 44, 839-847.
Finnemann, S. C. and Rodriguez-Boulan, E. (1999) Macrophage and retinal pigment epithelium phagocytosis: apoptotic cells and photoreceptors compete for alphavbeta3 and alphavbeta5 integrins, and protein kinase C regulates alphavbeta5 binding and cytoskeletal linkage. *The Journal of experimental medicine,* 190, 861-874.
Fishman, G. A., Anderson, R. J. and Lourenco, P. (1985) Prevalence of posterior subcapsular lens opacities in patients with retinitis pigmentosa. *The British journal of ophthalmology,* 69, 263-266.
Fishman, G. A., Farber, M. D. and Derlacki, D. J. (1988) X-linked retinitis pigmentosa. Profile of clinical findings. *Archives of ophthalmology,* 106, 369-375.
Fishman, G. A., Roberts, M. F., Derlacki, D. J., Grimsby, J. L., Yamamoto, H., Sharon, D., Nishiguchi, K. M. and Dryja, T. P. (2004) Novel mutations in the cellular retinaldehyde-binding protein gene (RLBP1) associated with retinitis punctata albescens: evidence of interfamilial genetic heterogeneity and fundus changes in heterozygotes. *Archives of ophthalmology,* 122, 70-75.
Fox, D. A., Poblenz, A. T. and He, L. (1999) Calcium overload triggers rod photoreceptor apoptotic cell death in chemical-induced and inherited retinal degenerations. *Annals of the New York Academy of Sciences,* 893, 282-285.
Fox, D. A., Poblenz, A. T., He, L., Harris, J. B. and Medrano, C. J. (2003) Pharmacological strategies to block rod photoreceptor apoptosis caused by calcium overload: a mechanistic target-site approach to neuroprotection. *European journal of ophthalmology,* 13 Suppl 3, S44-56.
Frank, R. N., Amin, R. H. and Puklin, J. E. (1999) Antioxidant enzymes in the macular retinal pigment epithelium of eyes with neovascular age-related macular degeneration. *American journal of ophthalmology,* 127, 694-709.
Franze, K., Grosche, J., Skatchkov, S. N. et al. (2007) Muller cells are living optical fibers in the vertebrate retina. *Proceedings of the National Academy of Sciences of the United States of America,* 104, 8287-8292.
Frasson, M., Picaud, S., Leveillard, T., Simonutti, M., Mohand-Said, S., Dreyfus, H., Hicks, D. and Sabel, J. (1999a) Glial cell line-derived neurotrophic factor induces histologic and functional protection of rod photoreceptors in the rd/rd mouse. *Investigative ophthalmology & visual science,* 40, 2724-2734.
Frasson, M., Sahel, J. A., Fabre, M., Simonutti, M., Dreyfus, H. and Picaud, S. (1999b) Retinitis pigmentosa: rod photoreceptor rescue by a calcium-channel blocker in the rd mouse. *Nature medicine,* 5, 1183-1187.
Fu, Y. (2010) Phototransduction in Rods and Cones. In: *Webvision: The Organization of the Retina and Visual System* (H. Kolb, R. Nelson and E. Fernandez eds.). Salt Lake City (UT): University of Utah Health Sciences Center; 1995-.
Fukai, N., Eklund, L., Marneros, A. G. et al. (2002) Lack of collagen XVIII/endostatin results in eye abnormalities. *The EMBO journal,* 21, 1535-1544.

Gardner, T. W., Lieth, E., Khin, S. A., Barber, A. J., Bonsall, D. J., Lesher, T., Rice, K. and Brennan, W. A., Jr. (1997) Astrocytes increase barrier properties and ZO-1 expression in retinal vascular endothelial cells. *Investigative ophthalmology & visual science,* 38, 2423-2427.

Gashaw, I., Stiller, S., Boing, C., Kimmig, R. and Winterhager, E. (2008) Premenstrual regulation of the pro-angiogenic factor CYR61 in human endometrium. *Endocrinology,* 149, 2261-2269.

Geller, A. M. and Sieving, P. A. (1993) Assessment of foveal cone photoreceptors in Stargardt's macular dystrophy using a small dot detection task. *Vision research,* 33, 1509-1524.

Geller, S. F., Lewis, G. P. and Fisher, S. K. (2001) FGFR1, signaling, and AP-1 expression after retinal detachment: reactive Muller and RPE cells. *Investigative ophthalmology & visual science,* 42, 1363-1369.

Geraldes, P., Yamagata, M., Rook, S. L. et al. (2007) Glypican 4, a membrane binding protein for bactericidal/permeability-increasing protein signaling pathways in retinal pigment epithelial cells. *Investigative ophthalmology & visual science,* 48, 5750-5755.

German, O. L., Insua, M. F., Gentili, C., Rotstein, N. P. and Politi, L. E. (2006) Docosahexaenoic acid prevents apoptosis of retina photoreceptors by activating the ERK/MAPK pathway. *Journal of neurochemistry,* 98, 1507-1520.

Ghosh, F. and Arner, K. (2010) Cell type differentiation dynamics in the developing porcine retina. *Developmental neuroscience,* 32, 47-58.

Gille, H., Kortenjann, M., Thomae, O., Moomaw, C., Slaughter, C., Cobb, M. H. and Shaw, P. E. (1995) ERK phosphorylation potentiates Elk-1-mediated ternary complex formation and transactivation. *The EMBO journal,* 14, 951-962.

Goureau, O., Rhee, K. D. and Yang, X. J. (2004) Ciliary neurotrophic factor promotes muller glia differentiation from the postnatal retinal progenitor pool. *Developmental neuroscience,* 26, 359-370.

Gregory-Evans, K., Chang, F., Hodges, M. D. and Gregory-Evans, C. Y. (2009) Ex vivo gene therapy using intravitreal injection of GDNF-secreting mouse embryonic stem cells in a rat model of retinal degeneration. *Molecular vision,* 15, 962-973.

Grosche, J., Hartig, W. and Reichenbach, A. (1995) Expression of glial fibrillary acidic protein (GFAP), glutamine synthetase (GS), and Bcl-2 protooncogene protein by Muller (glial) cells in retinal light damage of rats. *Neuroscience letters,* 185, 119-122.

Guduric-Fuchs, J., Ringland, L. J., Gu, P., Dellett, M., Archer, D. B. and Cogliati, T. (2009) Immunohistochemical study of pig retinal development. *Molecular vision,* 15, 1915-1928.

Guidry, C., Bradley, K. M. and King, J. L. (2003) Tractional force generation by human muller cells: growth factor responsiveness and integrin receptor involvement. *Investigative ophthalmology & visual science,* 44, 1355-1363.

Guillonneau, X., Regnier-Ricard, F., Laplace, O., Jonet, L., Bryckaert, M., Courtois, Y. and Mascarelli, F. (1998) Fibroblast growth factor (FGF) soluble receptor 1 acts as a natural inhibitor of FGF2 neurotrophic activity during retinal degeneration. *Molecular biology of the cell,* 9, 2785-2802.

Guo, J., Cheng, H., Zhao, S. and Yu, L. (2006) GG: a domain involved in phage LTF apparatus and implicated in human MEB and non-syndromic hearing loss diseases. *FEBS letters,* 580, 581-584.

Haglund, L., Tillgren, V., Addis, L., Wenglen, C., Recklies, A. and Heinegard, D. (2011) Identification and characterization of the integrin alpha2beta1 binding motif in

chondroadherin mediating cell attachment. *The Journal of biological chemistry,* 286, 3925-3934.
Haglund, L., Tillgren, V., Onnerfjord, P. and Heinegard, D. (2013) The C-terminal peptide of chondroadherin modulates cellular activity by selectively binding to heparan sulfate chains. *The Journal of biological chemistry,* 288, 995-1008.
Haider, A. S., Peters, S. B., Kaporis, H. et al. (2006) Genomic analysis defines a cancer-specific gene expression signature for human squamous cell carcinoma and distinguishes malignant hyperproliferation from benign hyperplasia. *The Journal of investigative dermatology,* 126, 869-881.
Halapin, N. A. and Bazan, N. G. (2010) NPD1 induction of retinal pigment epithelial cell survival involves PI3K/Akt phosphorylation signaling. *Neurochemical research,* 35, 1944-1947.
Haltia, M. (2006) The neuronal ceroid-lipofuscinoses: from past to present. *Biochimica et biophysica acta,* 1762, 850-856.
Hamilton, R. D. and Leach, L. (2011) Isolation and properties of an in vitro human outer blood-retinal barrier model. *Methods in molecular biology,* 686, 401-416.
Harada, C., Harada, T., Quah, H. M., Maekawa, F., Yoshida, K., Ohno, S., Wada, K., Parada, L. F. and Tanaka, K. (2003) Potential role of glial cell line-derived neurotrophic factor receptors in Muller glial cells during light-induced retinal degeneration. *Neuroscience,* 122, 229-235.
Harris, L. G., Pannell, L. K., Singh, S., Samant, R. S. and Shevde, L. A. (2012) Increased vascularity and spontaneous metastasis of breast cancer by hedgehog signaling mediated upregulation of cyr61. *Oncogene,* 31, 3370-3380.
Hartong, D. T., Berson, E. L. and Dryja, T. P. (2006) Retinitis pigmentosa. *Lancet,* 368, 1795-1809.
Hasan, A., Pokeza, N., Shaw, L., Lee, H. S., Lazzaro, D., Chintala, H., Rosenbaum, D., Grant, M. B. and Chaqour, B. (2011) The matricellular protein cysteine-rich protein 61 (CCN1/Cyr61) enhances physiological adaptation of retinal vessels and reduces pathological neovascularization associated with ischemic retinopathy. *The Journal of biological chemistry,* 286, 9542-9554.
Hauck, S. M., Ekstrom, P. A., Ahuja-Jensen, P., Suppmann, S., Paquet-Durand, F., van Veen, T. and Ueffing, M. (2006a) Differential modification of phosducin protein in degenerating rd1 retina is associated with constitutively active Ca2+/calmodulin kinase II in rod outer segments. *Molecular & cellular proteomics : MCP,* 5, 324-336.
Hauck, S. M., Gloeckner, C. J., Harley, M. E., Schoeffmann, S., Boldt, K., Ekstrom, P. A. and Ueffing, M. (2008) Identification of paracrine neuroprotective candidate proteins by a functional assay-driven proteomics approach. *Molecular & cellular proteomics : MCP,* 7, 1349-1361.
Hauck, S. M., Kinkl, N., Deeg, C. A., Swiatek-de Lange, M., Schoffmann, S. and Ueffing, M. (2006b) GDNF family ligands trigger indirect neuroprotective signaling in retinal glial cells. *Molecular and cellular biology,* 26, 2746-2757.
Hauck, S. M., Suppmann, S. and Ueffing, M. (2003) Proteomic profiling of primary retinal Muller glia cells reveals a shift in expression patterns upon adaptation to in vitro conditions. *Glia,* 44, 251-263.
Hauser, S. and Weich, H. A. (1993) A heparin-binding form of placenta growth factor (PlGF-2) is expressed in human umbilical vein endothelial cells and in placenta. *Growth factors,* 9, 259-268.

Haynes, L. W. (1992) Block of the cyclic GMP-gated channel of vertebrate rod and cone photoreceptors by l-cis-diltiazem. *The Journal of general physiology,* 100, 783-801.
Heckenlively, J. (1982) The frequency of posterior subcapsular cataract in the hereditary retinal degenerations. *American journal of ophthalmology,* 93, 733-738.
Helbling, R. E., Bolze, C. S., Golczak, M., Palczewski, K., Stocker, A. and Cascella, M. (2013) Cellular retinaldehyde binding protein-different binding modes and micro-solvation patterns for high-affinity 9-cis- and 11-cis-retinal substrates. *The journal of physical chemistry. B,* 117, 10719-10729.
Hellmich, H. L., Kos, L., Cho, E. S., Mahon, K. A. and Zimmer, A. (1996) Embryonic expression of glial cell-line derived neurotrophic factor (GDNF) suggests multiple developmental roles in neural differentiation and epithelial-mesenchymal interactions. *Mechanisms of development,* 54, 95-105.
Hendrickson, A., Bumsted-O'Brien, K., Natoli, R., Ramamurthy, V., Possin, D. and Provis, J. (2008) Rod photoreceptor differentiation in fetal and infant human retina. *Experimental eye research,* 87, 415-426.
Hendrickson, A. and Hicks, D. (2002) Distribution and density of medium- and short-wavelength selective cones in the domestic pig retina. *Experimental eye research,* 74, 435-444.
Hering, H., Koulen, P. and Kroger, S. (2000) Distribution of the integrin beta 1 subunit on radial cells in the embryonic and adult avian retina. *The Journal of comparative neurology,* 424, 153-164.
Holcik, M. and Korneluk, R. G. (2001) XIAP, the guardian angel. *Nature reviews. Molecular cell biology,* 2, 550-556.
Hollborn, M., Tenckhoff, S., Seifert, M., Kohler, S., Wiedemann, P., Bringmann, A. and Kohen, L. (2006) Human retinal epithelium produces and responds to placenta growth factor. *Graefe's archive for clinical and experimental ophthalmology = Albrecht von Graefes Archiv fur klinische und experimentelle Ophthalmologie,* 244, 732-741.
Homma, S., Oppenheim, R. W., Yaginuma, H. and Kimura, S. (2000) Expression pattern of GDNF, c-ret, and GFRalphas suggests novel roles for GDNF ligands during early organogenesis in the chick embryo. *Developmental biology,* 217, 121-137.
Hong, J., Yoshida, K. and Rosner, M. R. (2002) Characterization of a cysteine proteinase inhibitor induced during neuronal cell differentiation. *Journal of neurochemistry,* 81, 922-934.
Hung, P. S., Kao, S. Y., Shih, Y. H., Chiou, S. H., Liu, C. J., Chang, K. W. and Lin, S. C. (2008) Insulin-like growth factor binding protein-5 (IGFBP-5) suppresses the tumourigenesis of head and neck squamous cell carcinoma. *The Journal of pathology,* 214, 368-376.
Ihle, J. N. (1995) Cytokine receptor signalling. *Nature,* 377, 591-594.
Ikeda, T., Homma, Y., Nisida, K., Hirase, K., Sotozono, C., Kinoshita, S. and Puro, D. G. (1998) Expression of transforming growth factor-beta s and their receptors by human retinal glial cells. *Current eye research,* 17, 546-550.
Ishikawa, K., Yoshida, S., Kadota, K., Nakamura, T., Niiro, H., Arakawa, S., Yoshida, A., Akashi, K. and Ishibashi, T. (2010) Gene expression profile of hyperoxic and hypoxic retinas in a mouse model of oxygen-induced retinopathy. *Investigative ophthalmology & visual science,* 51, 4307-4319.
Jacobson, S. G., Cideciyan, A. V., Iannaccone, A. et al. (2000) Disease expression of RP1 mutations causing autosomal dominant retinitis pigmentosa. *Investigative ophthalmology & visual science,* 41, 1898-1908.

Jacobson, S. G., Kemp, C. M., Cideciyan, A. V., Macke, J. P., Sung, C. H. and Nathans, J. (1994) Phenotypes of stop codon and splice site rhodopsin mutations causing retinitis pigmentosa. *Investigative ophthalmology & visual science,* 35, 2521-2534.

Janknecht, R., Ernst, W. H. and Nordheim, A. (1995) SAP1a is a nuclear target of signaling cascades involving ERKs. *Oncogene,* 10, 1209-1216.

Jarajapu, Y. P., Cai, J., Yan, Y. et al. (2012) Protection of blood retinal barrier and systemic vasculature by insulin-like growth factor binding protein-3. *PloS one,* 7, e39398.

Ji, Y., Zhu, C. L., Grzywacz, N. M. and Lee, E. J. (2012) Rearrangement of the cone mosaic in the retina of the rat model of retinitis pigmentosa. *The Journal of comparative neurology,* 520, 874-888.

Jiang, Y. and Steinle, J. J. (2010) Systemic propranolol reduces b-wave amplitude in the ERG and increases IGF-1 receptor phosphorylation in rat retina. *Investigative ophthalmology & visual science,* 51, 2730-2735.

Jin, L., Zhang, Y., Li, H., Yao, L., Fu, D., Yao, X., Xu, L. X., Hu, X. and Hu, G. (2012) Differential secretome analysis reveals CST6 as a suppressor of breast cancer bone metastasis. *Cell research,* 22, 1356-1373.

Jing, S., Wen, D., Yu, Y. et al. (1996) GDNF-induced activation of the ret protein tyrosine kinase is mediated by GDNFR-alpha, a novel receptor for GDNF. *Cell,* 85, 1113-1124.

Johansson, U. E., Eftekhari, S. and Warfvinge, K. (2010) A battery of cell- and structure-specific markers for the adult porcine retina. *The journal of histochemistry and cytochemistry : official journal of the Histochemistry Society,* 58, 377-389.

Joly, S., Lange, C., Thiersch, M., Samardzija, M. and Grimm, C. (2008) Leukemia inhibitory factor extends the lifespan of injured photoreceptors in vivo. *The Journal of neuroscience : the official journal of the Society for Neuroscience,* 28, 13765-13774.

Jomary, C., Darrow, R. M., Wong, P., Organisciak, D. T. and Jones, S. E. (2004) Expression of neurturin, glial cell line-derived neurotrophic factor, and their receptor components in light-induced retinal degeneration. *Investigative ophthalmology & visual science,* 45, 1240-1246.

Jones, J. I., Gockerman, A., Busby, W. H., Jr., Camacho-Hubner, C. and Clemmons, D. R. (1993) Extracellular matrix contains insulin-like growth factor binding protein-5: potentiation of the effects of IGF-I. *The Journal of cell biology,* 121, 679-687.

Juel, H. B., Faber, C., Udsen, M. S., Folkersen, L. and Nissen, M. H. (2012) Chemokine expression in retinal pigment epithelial ARPE-19 cells in response to coculture with activated T cells. *Investigative ophthalmology & visual science,* 53, 8472-8480.

Jun, J. I. and Lau, L. F. (2011) Taking aim at the extracellular matrix: CCN proteins as emerging therapeutic targets. *Nature reviews. Drug discovery,* 10, 945-963.

Kaestel, C. G., Lovato, P., Odum, N., Nissen, M. H. and Ropke, C. (2005) The immune privilege of the eye: human retinal pigment epithelial cells selectively modulate T-cell activation in vitro. *Current eye research,* 30, 375-383.

Kamao, H., Mandai, M., Okamoto, S., Sakai, N., Suga, A., Sugita, S., Kiryu, J. and Takahashi, M. (2014) Characterization of human induced pluripotent stem cell-derived retinal pigment epithelium cell sheets aiming for clinical application. *Stem cell reports,* 2, 205-218.

Kandel, E. R., Schwartz, J. H. and Jessell, T. M. (2000) Principles of Neural Science. In: *Visual processing by the retina.,* pp. 507-522. Mcgraw-Hill Professional.

Karlstetter, M., Ebert, S. and Langmann, T. (2010) Microglia in the healthy and degenerating retina: insights from novel mouse models. *Immunobiology,* 215, 685-691.

Kassen, S. C., Thummel, R., Campochiaro, L. A., Harding, M. J., Bennett, N. A. and Hyde, D. R. (2009) CNTF induces photoreceptor neuroprotection and Muller glial cell proliferation through two different signaling pathways in the adult zebrafish retina. *Experimental eye research,* 88, 1051-1064.

Kastin, A. J., Akerstrom, V. and Pan, W. (2003) Glial cell line-derived neurotrophic factor does not enter normal mouse brain. *Neuroscience letters,* 340, 239-241.

Katahira, T., Nakagiri, S., Terada, K. and Furukawa, T. (2010) Secreted factor FAM3C (ILEI) is involved in retinal laminar formation. *Biochemical and biophysical research communications,* 392, 301-306.

Katsanis, N., Shroyer, N. F., Lewis, R. A., Cavender, J. C., Al-Rajhi, A. A., Jabak, M. and Lupski, J. R. (2001) Fundus albipunctatus and retinitis punctata albescens in a pedigree with an R150Q mutation in RLBP1. *Clinical genetics,* 59, 424-429.

Kaur, J., Mencl, S., Sahaboglu, A., Farinelli, P., van Veen, T., Zrenner, E., Ekstrom, P., Paquet-Durand, F. and Arango-Gonzalez, B. (2011) Calpain and PARP activation during photoreceptor cell death in P23H and S334ter rhodopsin mutant rats. *PloS one,* 6, e22181.

Kayama, M., Nakazawa, T., Thanos, A., Morizane, Y., Murakami, Y., Theodoropoulou, S., Abe, T., Vavvas, D. and Miller, J. W. (2011) Heat shock protein 70 (HSP70) is critical for the photoreceptor stress response after retinal detachment via modulating anti-apoptotic Akt kinase. *The American journal of pathology,* 178, 1080-1091.

Keeler, C. E. (1924) The Inheritance of a Retinal Abnormality in White Mice. *Proceedings of the National Academy of Sciences of the United States of America,* 10, 329-333.

Kennedy, B. N., Li, C., Ortego, J., Coca-Prados, M., Sarthy, V. P. and Crabb, J. W. (2003) CRALBP transcriptional regulation in ciliary epithelial, retinal Muller and retinal pigment epithelial cells. *Experimental eye research,* 76, 257-260.

Khaliq, A., Foreman, D., Ahmed, A., Weich, H., Gregor, Z., McLeod, D. and Boulton, M. (1998) Increased expression of placenta growth factor in proliferative diabetic retinopathy. *Laboratory investigation; a journal of technical methods and pathology,* 78, 109-116.

Khorana, H. G. (1992) Rhodopsin, photoreceptor of the rod cell. An emerging pattern for structure and function. *The Journal of biological chemistry,* 267, 1-4.

Kielczewski, J. L., Hu, P., Shaw, L. C., Li Calzi, S., Mames, R. N., Gardiner, T. A., McFarland, E., Chan-Ling, T. and Grant, M. B. (2011a) Novel protective properties of IGFBP-3 result in enhanced pericyte ensheathment, reduced microglial activation, increased microglial apoptosis, and neuronal protection after ischemic retinal injury. *The American journal of pathology,* 178, 1517-1528.

Kielczewski, J. L., Li Calzi, S., Shaw, L. C. et al. (2011b) Free insulin-like growth factor binding protein-3 (IGFBP-3) reduces retinal vascular permeability in association with a reduction of acid sphingomyelinase (ASMase). *Investigative ophthalmology & visual science,* 52, 8278-8286.

Kim, H. S., Ingermann, A. R., Tsubaki, J., Twigg, S. M., Walker, G. E. and Oh, Y. (2004) Insulin-like growth factor-binding protein 3 induces caspase-dependent apoptosis through a death receptor-mediated pathway in MCF-7 human breast cancer cells. *Cancer research,* 64, 2229-2237.

Kim, J. H., Kim, J. H., Jun, H. O., Yu, Y. S., Min, B. H., Park, K. H. and Kim, K. W. (2010) Protective effect of clusterin from oxidative stress-induced apoptosis in human retinal pigment epithelial cells. *Investigative ophthalmology & visual science,* 51, 561-566.

King, J. L. and Guidry, C. (2012) Vitreous IGFBP-3 effects on Muller cell proliferation and tractional force generation. *Investigative ophthalmology & visual science,* 53, 93-99.

Kirsch, M., Trautmann, N., Ernst, M. and Hofmann, H. D. (2010) Involvement of gp130-associated cytokine signaling in Muller cell activation following optic nerve lesion. *Glia,* 58, 768-779.

Klatt, A. R., Paulsson, M. and Wagener, R. (2002) Expression of matrilins during maturation of mouse skeletal tissues. *Matrix biology : journal of the International Society for Matrix Biology,* 21, 289-296.

Klein, R., Stiller, S. and Gashaw, I. (2012) Epidermal growth factor upregulates endometrial CYR61 expression via activation of the JAK2/STAT3 pathway. *Reproduction, fertility, and development,* 24, 482-489.

Ko, T. H., Fujimoto, J. G., Schuman, J. S. et al. (2005) Comparison of ultrahigh- and standard-resolution optical coherence tomography for imaging macular pathology. *Ophthalmology,* 112, 1922 e1921-1915.

Koch, K. W. and Kaupp, U. B. (1985) Cyclic GMP directly regulates a cation conductance in membranes of bovine rods by a cooperative mechanism. *The Journal of biological chemistry,* 260, 6788-6800.

Kok, S. H., Chang, H. H., Tsai, J. Y., Hung, H. C., Lin, C. Y., Chiang, C. P., Liu, C. M. and Kuo, M. Y. (2010) Expression of Cyr61 (CCN1) in human oral squamous cell carcinoma: An independent marker for poor prognosis. *Head & neck,* 32, 1665-1673.

Kolb, H. (2011) Morphology and Circuitry of Ganglion Cells. In: *Webvision: The Organization of the Retina and Visual System* (H. Kolb, R. Nelson and E. Fernandez eds.). Salt Lake City (UT): University of Utah Health Sciences Center; 1995-.

Kroeger, H., Messah, C., Ahern, K. et al. (2012) Induction of endoplasmic reticulum stress genes, BiP and chop, in genetic and environmental models of retinal degeneration. *Investigative ophthalmology & visual science,* 53, 7590-7599.

Kucharska, J., Del Rio, P., Arango-Gonzalez, B., Gorza, M., Feuchtinger, A., Hauck, S. M. and Ueffing, M. (2014) Cyr61 activates retinal cells and prolongs photoreceptor survival in rd1 mouse model of retinitis pigmentosa. *Journal of neurochemistry*.

Kular, L., Pakradouni, J., Kitabgi, P., Laurent, M. and Martinerie, C. (2011) The CCN family: a new class of inflammation modulators? *Biochimie,* 93, 377-388.

Kumar, M. V., Nagineni, C. N., Chin, M. S., Hooks, J. J. and Detrick, B. (2004) Innate immunity in the retina: Toll-like receptor (TLR) signaling in human retinal pigment epithelial cells. *Journal of neuroimmunology,* 153, 7-15.

Kur, J., Newman, E. A. and Chan-Ling, T. (2012) Cellular and physiological mechanisms underlying blood flow regulation in the retina and choroid in health and disease. *Progress in retinal and eye research,* 31, 377-406.

Kuser-Abali, G., Ozcan, F., Ugurlu, A., Uysal, A., Fuss, S. H. and Bugra-Bilge, K. (2013) SIK2 Is Involved in the Negative Modulation of Insulin-Dependent Muller Cell Survival and implicated in Hyperglycemia Induced Cell Death. *Investigative ophthalmology & visual science*.

Lambooij, A. C., van Wely, K. H., Lindenbergh-Kortleve, D. J., Kuijpers, R. W., Kliffen, M. and Mooy, C. M. (2003) Insulin-like growth factor-I and its receptor in neovascular age-related macular degeneration. *Investigative ophthalmology & visual science,* 44, 2192-2198.

Landers, R. A., Rayborn, M. E., Myers, K. M. and Hollyfield, J. G. (1994) Increased retinal synthesis of heparan sulfate proteoglycan and HNK-1 glycoproteins following photoreceptor degeneration. *Journal of neurochemistry,* 63, 737-750.

Lau, L. F. (2011) CCN1/CYR61: the very model of a modern matricellular protein. *Cellular and molecular life sciences : CMLS,* 68, 3149-3163.

Lau, L. F. and Lam, S. C. (1999) The CCN family of angiogenic regulators: the integrin connection. *Experimental cell research,* 248, 44-57.

Lau, L. F. and Nathans, D. (1987) Expression of a set of growth-related immediate early genes in BALB/c 3T3 cells: coordinate regulation with c-fos or c-myc. *Proceedings of the National Academy of Sciences of the United States of America,* 84, 1182-1186.

LaVail, M. M., Yasumura, D., Matthes, M. T., Lau-Villacorta, C., Unoki, K., Sung, C. H. and Steinberg, R. H. (1998) Protection of mouse photoreceptors by survival factors in retinal degenerations. *Investigative ophthalmology & visual science,* 39, 592-602.

Leask, A. and Abraham, D. J. (2006) All in the CCN family: essential matricellular signaling modulators emerge from the bunker. *Journal of cell science,* 119, 4803-4810.

Lee, E. J., Ji, Y., Zhu, C. L. and Grzywacz, N. M. (2011) Role of Muller cells in cone mosaic rearrangement in a rat model of retinitis pigmentosa. *Glia,* 59, 1107-1117.

Leist, M. and Jaattela, M. (2001) Four deaths and a funeral: from caspases to alternative mechanisms. *Nature reviews. Molecular cell biology,* 2, 589-598.

Leskov, I. B., Klenchin, V. A., Handy, J. W., Whitlock, G. G., Govardovskii, V. I., Bownds, M. D., Lamb, T. D., Pugh, E. N., Jr. and Arshavsky, V. Y. (2000) The gain of rod phototransduction: reconciliation of biochemical and electrophysiological measurements. *Neuron,* 27, 525-537.

Leu, S. J., Lam, S. C. and Lau, L. F. (2002) Pro-angiogenic activities of CYR61 (CCN1) mediated through integrins alphavbeta3 and alpha6beta1 in human umbilical vein endothelial cells. *The Journal of biological chemistry,* 277, 46248-46255.

Lewis, G. P., Erickson, P. A., Guerin, C. J., Anderson, D. H. and Fisher, S. K. (1989) Changes in the expression of specific Muller cell proteins during long-term retinal detachment. *Experimental eye research,* 49, 93-111.

Li, R., Wen, R., Banzon, T., Maminishkis, A. and Miller, S. S. (2011) CNTF mediates neurotrophic factor secretion and fluid absorption in human retinal pigment epithelium. *PloS one,* 6, e23148.

Li, Y., Tao, W., Luo, L., Huang, D., Kauper, K., Stabila, P., Lavail, M. M., Laties, A. M. and Wen, R. (2010) CNTF induces regeneration of cone outer segments in a rat model of retinal degeneration. *PloS one,* 5, e9495.

Li, Z., Dong, X., Liu, H., Chen, X., Shi, H., Fan, Y., Hou, D. and Zhang, X. (2013) Astaxanthin protects ARPE-19 cells from oxidative stress via upregulation of Nrf2-regulated phase II enzymes through activation of PI3K/Akt. *Molecular vision,* 19, 1656-1666.

Li, Z. Y., Possin, D. E. and Milam, A. H. (1995) Histopathology of bone spicule pigmentation in retinitis pigmentosa. *Ophthalmology,* 102, 805-816.

Liang, K. J., Lee, J. E., Wang, Y. D., Ma, W., Fontainhas, A. M., Fariss, R. N. and Wong, W. T. (2009) Regulation of dynamic behavior of retinal microglia by CX3CR1 signaling. *Investigative ophthalmology & visual science,* 50, 4444-4451.

Limb, G. A., Salt, T. E., Munro, P. M., Moss, S. E. and Khaw, P. T. (2002) In vitro characterization of a spontaneously immortalized human Muller cell line (MIO-M1). *Investigative ophthalmology & visual science,* 43, 864-869.

Lin, J., Zhou, Z., Huo, R. et al. (2012) Cyr61 induces IL-6 production by fibroblast-like synoviocytes promoting Th17 differentiation in rheumatoid arthritis. *Journal of immunology,* 188, 5776-5784.

Lin, L. F., Doherty, D. H., Lile, J. D., Bektesh, S. and Collins, F. (1993) GDNF: a glial cell line-derived neurotrophic factor for midbrain dopaminergic neurons. *Science,* 260, 1130-1132.

Lin, M. T., Chang, C. C., Lin, B. R., Yang, H. Y., Chu, C. Y., Wu, M. H. and Kuo, M. L. (2007) Elevated expression of Cyr61 enhances peritoneal dissemination of gastric cancer cells through integrin alpha2beta1. *The Journal of biological chemistry,* 282, 34594-34604.

Lindqvist, N., Liu, Q., Zajadacz, J., Franze, K. and Reichenbach, A. (2010) Retinal glial (Muller) cells: sensing and responding to tissue stretch. *Investigative ophthalmology & visual science,* 51, 1683-1690.

Lipinski, D. M., Singh, M. S. and MacLaren, R. E. (2011) Assessment of cone survival in response to CNTF, GDNF, and VEGF165b in a novel ex vivo model of end-stage retinitis pigmentosa. *Investigative ophthalmology & visual science,* 52, 7340-7346.

Lipton, S. A. and Nicotera, P. (1998) Calcium, free radicals and excitotoxins in neuronal apoptosis. *Cell calcium,* 23, 165-171.

Liu, B., Lee, K. W., Li, H., Ma, L., Lin, G. L., Chandraratna, R. A. and Cohen, P. (2005) Combination therapy of insulin-like growth factor binding protein-3 and retinoid X receptor ligands synergize on prostate cancer cell apoptosis in vitro and in vivo. *Clinical cancer research : an official journal of the American Association for Cancer Research,* 11, 4851-4856.

Liu, C., Li, Y., Peng, M., Laties, A. M. and Wen, R. (1999) Activation of caspase-3 in the retina of transgenic rats with the rhodopsin mutation s334ter during photoreceptor degeneration. *The Journal of neuroscience : the official journal of the Society for Neuroscience,* 19, 4778-4785.

Liu, C., Peng, M., Laties, A. M. and Wen, R. (1998) Preconditioning with bright light evokes a protective response against light damage in the rat retina. *The Journal of neuroscience : the official journal of the Society for Neuroscience,* 18, 1337-1344.

Liu, W. and Rask-Andersen, H. (2014) Immunohistological analysis of neurturin and its receptors in human cochlea. *Auris, nasus, larynx,* 41, 172-178.

Lofqvist, C., Willett, K. L., Aspegren, O., Smith, A. C., Aderman, C. M., Connor, K. M., Chen, J., Hellstrom, A. and Smith, L. E. (2009) Quantification and localization of the IGF/insulin system expression in retinal blood vessels and neurons during oxygen-induced retinopathy in mice. *Investigative ophthalmology & visual science,* 50, 1831-1837.

Lopez, P. F. and Green, W. R. (1992) Peripapillary subretinal neovascularization. A review. *Retina,* 12, 147-171.

Luhmann, U. F., Carvalho, L. S., Robbie, S. J., Cowing, J. A., Duran, Y., Munro, P. M., Bainbridge, J. W. and Ali, R. R. (2013) Ccl2, Cx3cr1 and Ccl2/Cx3cr1 chemokine deficiencies are not sufficient to cause age-related retinal degeneration. *Experimental eye research,* 107, 80-87.

Luna, C., Li, G., Qiu, J., Epstein, D. L. and Gonzalez, P. (2009) Role of miR-29b on the regulation of the extracellular matrix in human trabecular meshwork cells under chronic oxidative stress. *Molecular vision,* 15, 2488-2497.

Luttun, A., Tjwa, M., Moons, L. et al. (2002) Revascularization of ischemic tissues by PlGF treatment, and inhibition of tumor angiogenesis, arthritis and atherosclerosis by anti-Flt1. *Nature medicine,* 8, 831-840.

MacDonald, I. M., Sauve, Y. and Sieving, P. A. (2007) Preventing blindness in retinal disease: ciliary neurotrophic factor intraocular implants. *Canadian journal of ophthalmology. Journal canadien d'ophtalmologie,* 42, 399-402.

Maier, K., Rau, C. R., Storch, M. K. et al. (2004) Ciliary neurotrophic factor protects retinal ganglion cells from secondary cell death during acute autoimmune optic neuritis in rats. *Brain pathology,* 14, 378-387.

Makhoul, M., Bruyns, C., Edimo, W. E., Relvas, L. J., Bazewicz, M., Koch, P., Caspers, L. and Willermain, F. (2012) TNFalpha suppresses IFNgamma-induced MHC class II expression on retinal pigmented epithelial cells cultures. *Acta ophthalmologica,* 90, e38-42.

Malecaze, F., Mascarelli, F., Bugra, K., Fuhrmann, G., Courtois, Y. and Hicks, D. (1993) Fibroblast growth factor receptor deficiency in dystrophic retinal pigmented epithelium. *Journal of cellular physiology,* 154, 631-642.

Malik, A. R., Urbanska, M., Gozdz, A., Swiech, L. J., Nagalski, A., Perycz, M., Blazejczyk, M. and Jaworski, J. (2013) CYR61, a matricellular protein, is needed for dendritic arborization of hippocampal neurons. *The Journal of biological chemistry*.

Mandal, M. N. and Ayyagari, R. (2006) Complement factor H: spatial and temporal expression and localization in the eye. *Investigative ophthalmology & visual science,* 47, 4091-4097.

Mansson, B., Wenglen, C., Morgelin, M., Saxne, T. and Heinegard, D. (2001) Association of chondroadherin with collagen type II. *The Journal of biological chemistry,* 276, 32883-32888.

Marks, C., Belluscio, L. and Ibanez, C. F. (2012) Critical role of GFRalpha1 in the development and function of the main olfactory system. *The Journal of neuroscience : the official journal of the Society for Neuroscience,* 32, 17306-17320.

Marneros, A. G., Keene, D. R., Hansen, U. et al. (2004) Collagen XVIII/endostatin is essential for vision and retinal pigment epithelial function. *The EMBO journal,* 23, 89-99.

Marneros, A. G., She, H., Zambarakji, H., Hashizume, H., Connolly, E. J., Kim, I., Gragoudas, E. S., Miller, J. W. and Olsen, B. R. (2007) Endogenous endostatin inhibits choroidal neovascularization. *FASEB journal : official publication of the Federation of American Societies for Experimental Biology,* 21, 3809-3818.

Marra, C., Gomes Moret, D., de Souza Correa, A., Chagas da Silva, F., Moraes, P., Linden, R. and Sholl-Franco, A. (2011) Protein kinases JAK and ERK mediate protective effect of interleukin-2 upon ganglion cells of the developing rat retina. *Journal of neuroimmunology,* 233, 120-126.

Martinez-Navarrete, G., Seiler, M. J., Aramant, R. B., Fernandez-Sanchez, L., Pinilla, I. and Cuenca, N. (2011) Retinal degeneration in two lines of transgenic S334ter rats. *Experimental eye research,* 92, 227-237.

Mascarelli, F., Raulais, D. and Courtois, Y. (1989) Fibroblast growth factor phosphorylation and receptors in rod outer segments. *The EMBO journal,* 8, 2265-2273.

Matsui, H., Lin, L. R., Singh, D. P., Shinohara, T. and Reddy, V. N. (2001) Lens epithelium-derived growth factor: increased survival and decreased DNA breakage of human RPE cells induced by oxidative stress. *Investigative ophthalmology & visual science,* 42, 2935-2941.

Maw, M. A., Kennedy, B., Knight, A. et al. (1997) Mutation of the gene encoding cellular retinaldehyde-binding protein in autosomal recessive retinitis pigmentosa. *Nature genetics,* 17, 198-200.

McBee, J. K., Palczewski, K., Baehr, W. and Pepperberg, D. R. (2001) Confronting complexity: the interlink of phototransduction and retinoid metabolism in the vertebrate retina. *Progress in retinal and eye research,* 20, 469-529.

McCubrey, J. A., Steelman, L. S., Chappell, W. H. et al. (2012) Mutations and deregulation of Ras/Raf/MEK/ERK and PI3K/PTEN/Akt/mTOR cascades which alter therapy response. *Oncotarget,* 3, 954-987.

McGee Sanftner, L. H., Abel, H., Hauswirth, W. W. and Flannery, J. G. (2001) Glial cell line derived neurotrophic factor delays photoreceptor degeneration in a transgenic rat model of retinitis pigmentosa. *Molecular therapy : the journal of the American Society of Gene Therapy,* 4, 622-629.

McGillem, G. S. and Dacheux, R. F. (1999) Rabbit retinal Muller cells undergo antigenic changes in response to experimentally induced proliferative vitreoretinopathy. *Experimental eye research,* 68, 617-627.

McVicar, C. M., Hamilton, R., Colhoun, L. M., Gardiner, T. A., Brines, M., Cerami, A. and Stitt, A. W. (2011) Intervention with an erythropoietin-derived peptide protects against neuroglial and vascular degeneration during diabetic retinopathy. *Diabetes,* 60, 2995-3005.

Mendes, H. F., van der Spuy, J., Chapple, J. P. and Cheetham, M. E. (2005) Mechanisms of cell death in rhodopsin retinitis pigmentosa: implications for therapy. *Trends in molecular medicine,* 11, 177-185.

Mendez, A., Burns, M. E., Roca, A., Lem, J., Wu, L. W., Simon, M. I., Baylor, D. A. and Chen, J. (2000) Rapid and reproducible deactivation of rhodopsin requires multiple phosphorylation sites. *Neuron,* 28, 153-164.

Menendez, J. A., Vellon, L., Mehmi, I., Teng, P. K., Griggs, D. W. and Lupu, R. (2005) A novel CYR61-triggered 'CYR61-alphavbeta3 integrin loop' regulates breast cancer cell survival and chemosensitivity through activation of ERK1/ERK2 MAPK signaling pathway. *Oncogene,* 24, 761-779.

Ming, M., Li, X., Fan, X., Yang, D., Li, L., Chen, S., Gu, Q. and Le, W. (2009) Retinal pigment epithelial cells secrete neurotrophic factors and synthesize dopamine: possible contribution to therapeutic effects of RPE cell transplantation in Parkinson's disease. *Journal of translational medicine,* 7, 53.

Mitamura, Y., Mitamura-Aizawa, S., Nagasawa, T., Katome, T., Eguchi, H. and Naito, T. (2012) Diagnostic imaging in patients with retinitis pigmentosa. *The journal of medical investigation : JMI,* 59, 1-11.

Mizuno, M., Fujisawa, R. and Kuboki, Y. (1996) Bone chondroadherin promotes attachment of osteoblastic cells to solid-state substrates and shows affinity to collagen. *Calcified tissue international,* 59, 163-167.

Mo, F. E., Muntean, A. G., Chen, C. C., Stolz, D. B., Watkins, S. C. and Lau, L. F. (2002) CYR61 (CCN1) is essential for placental development and vascular integrity. *Molecular and cellular biology,* 22, 8709-8720.

Morimura, H., Berson, E. L. and Dryja, T. P. (1999) Recessive mutations in the RLBP1 gene encoding cellular retinaldehyde-binding protein in a form of retinitis punctata albescens. *Investigative ophthalmology & visual science,* 40, 1000-1004.

Moriondo, A., Pelucchi, B. and Rispoli, G. (2001) Calcium-activated potassium current clamps the dark potential of vertebrate rods. *The European journal of neuroscience,* 14, 19-26.

Moura, L. I., Dias, A. M., Suesca, E., Casadiegos, S., Leal, E. C., Fontanilla, M. R., Carvalho, L., de Sousa, H. C. and Carvalho, E. (2014) Neurotensin-loaded collagen dressings reduce inflammation and improve wound healing in diabetic mice. *Biochimica et biophysica acta,* 1842, 32-43.

Mousa, S. A., Lorelli, W. and Campochiaro, P. A. (1999) Role of hypoxia and extracellular matrix-integrin binding in the modulation of angiogenic growth factors secretion by retinal pigmented epithelial cells. *Journal of cellular biochemistry,* 74, 135-143.

Nakatani, M., Shinohara, Y., Takii, M., Mori, H., Asai, N., Nishimura, S., Furukawa-Hibi, Y., Miyamoto, Y. and Nitta, A. (2011) Periocular injection of in situ hydrogels containing Leu-Ile, an inducer for neurotrophic factors, promotes retinal ganglion cell survival after optic nerve injury. *Experimental eye research,* 93, 873-879.

Nam, T. J., Busby, W. H., Jr., Rees, C. and Clemmons, D. R. (2000) Thrombospondin and osteopontin bind to insulin-like growth factor (IGF)-binding protein-5 leading to an alteration in IGF-I-stimulated cell growth. *Endocrinology,* 141, 1100-1106.

Nandrot, E. F., Kim, Y., Brodie, S. E., Huang, X., Sheppard, D. and Finnemann, S. C. (2004) Loss of synchronized retinal phagocytosis and age-related blindness in mice lacking alphavbeta5 integrin. *The Journal of experimental medicine,* 200, 1539-1545.

Nawrot, M., West, K., Huang, J., Possin, D. E., Bretscher, A., Crabb, J. W. and Saari, J. C. (2004) Cellular retinaldehyde-binding protein interacts with ERM-binding phosphoprotein 50 in retinal pigment epithelium. *Investigative ophthalmology & visual science,* 45, 393-401.

Nelson, C. M., Gorsuch, R. A., Bailey, T. J., Ackerman, K. M., Kassen, S. C. and Hyde, D. R. (2012) Stat3 defines three populations of Muller glia and is required for initiating maximal muller glia proliferation in the regenerating zebrafish retina. *The Journal of comparative neurology,* 520, 4294-4311.

Nelson, R. (2007) Ganglion Cell Physiology. In: *Webvision: The Organization of the Retina and Visual System*, (H. Kolb, R. Nelson and E. Fernandez eds.). Salt Lake City (UT): University of Utah Health Sciences Center; 1995-.

Nentwich, M. M. and Rudolph, G. (2013) Hereditary retinal eye diseases in childhood and youth affecting the central retina. *Oman journal of ophthalmology,* 6, S18-S25.

Newman, E. and Reichenbach, A. (1996) The Muller cell: a functional element of the retina. *Trends in neurosciences,* 19, 307-312.

Newman, E. A. and Zahs, K. R. (1998) Modulation of neuronal activity by glial cells in the retina. *The Journal of neuroscience : the official journal of the Society for Neuroscience,* 18, 4022-4028.

Ni, J., Abrahamson, M., Zhang, M. et al. (1997) Cystatin E is a novel human cysteine proteinase inhibitor with structural resemblance to family 2 cystatins. *The Journal of biological chemistry,* 272, 10853-10858.

Norton, A. W., D'Amours, M. R., Grazio, H. J., Hebert, T. L. and Cote, R. H. (2000) Mechanism of transducin activation of frog rod photoreceptor phosphodiesterase. Allosteric interactiona between the inhibitory gamma subunit and the noncatalytic cGMP-binding sites. *The Journal of biological chemistry,* 275, 38611-38619.

Nosrat, C. A., Tomac, A., Lindqvist, E., Lindskog, S., Humpel, C., Stromberg, I., Ebendal, T., Hoffer, B. J. and Olson, L. (1996) Cellular expression of GDNF mRNA suggests multiple functions inside and outside the nervous system. *Cell and tissue research,* 286, 191-207.

O'Brien, T. P. and Lau, L. F. (1992) Expression of the growth factor-inducible immediate early gene cyr61 correlates with chondrogenesis during mouse embryonic development. *Cell growth & differentiation : the molecular biology journal of the American Association for Cancer Research,* 3, 645-654.

O'Brien, T. P., Yang, G. P., Sanders, L. and Lau, L. F. (1990) Expression of cyr61, a growth factor-inducible immediate-early gene. *Molecular and cellular biology,* 10, 3569-3577.

O'Reilly, M. S., Boehm, T., Shing, Y. et al. (1997) Endostatin: an endogenous inhibitor of angiogenesis and tumor growth. *Cell,* 88, 277-285.

Oh, J. W., Hsi, T. C., Guerrero-Juarez, C. F., Ramos, R. and Plikus, M. V. (2013) Organotypic skin culture. *The Journal of investigative dermatology,* 133, e14.

Ohnaka, M., Miki, K., Gong, Y. Y., Stevens, R., Iwase, T., Hackett, S. F. and Campochiaro, P. A. (2012) Long-term expression of glial cell line-derived neurotrophic factor slows, but does not stop retinal degeneration in a model of retinitis pigmentosa. *Journal of neurochemistry,* 122, 1047-1053.

Omori, H., Hatamochi, A., Koike, M. et al. (2011) Sigmoid colon perforation induced by the vascular type of Ehlers-Danlos syndrome: report of a case. *Surgery today,* 41, 733-736.

Orosz, K. E., Gupta, S., Hassink, M., Abdel-Rahman, M., Moldovan, L., Davidorf, F. H. and Moldovan, N. I. (2004) Delivery of antiangiogenic and antioxidant drugs of ophthalmic interest through a nanoporous inorganic filter. *Molecular vision,* 10, 555-565.

Padgett, L. C., Lui, G. M., Werb, Z. and LaVail, M. M. (1997) Matrix metalloproteinase-2 and tissue inhibitor of metalloproteinase-1 in the retinal pigment epithelium and interphotoreceptor matrix: vectorial secretion and regulation. *Experimental eye research,* 64, 927-938.

Paques, M., Simonutti, M., Roux, M. J., Picaud, S., Levavasseur, E., Bellman, C. and Sahel, J. A. (2006) High resolution fundus imaging by confocal scanning laser ophthalmoscopy in the mouse. *Vision research,* 46, 1336-1345.

Paquet-Durand, F., Azadi, S., Hauck, S. M., Ueffing, M., van Veen, T. and Ekstrom, P. (2006) Calpain is activated in degenerating photoreceptors in the rd1 mouse. *Journal of neurochemistry,* 96, 802-814.

Paquet-Durand, F., Hauck, S. M., van Veen, T., Ueffing, M. and Ekstrom, P. (2009) PKG activity causes photoreceptor cell death in two retinitis pigmentosa models. *Journal of neurochemistry,* 108, 796-810.

Paquet-Durand, F., Sanges, D., McCall, J., Silva, J., van Veen, T., Marigo, V. and Ekstrom, P. (2010) Photoreceptor rescue and toxicity induced by different calpain inhibitors. *Journal of neurochemistry,* 115, 930-940.

Park, J. E., Chen, H. H., Winer, J., Houck, K. A. and Ferrara, N. (1994) Placenta growth factor. Potentiation of vascular endothelial growth factor bioactivity, in vitro and in vivo, and high affinity binding to Flt-1 but not to Flk-1/KDR. *The Journal of biological chemistry,* 269, 25646-25654.

Paulson, O. B. and Newman, E. A. (1987) Does the release of potassium from astrocyte endfeet regulate cerebral blood flow? *Science,* 237, 896-898.

Pawlyk, B. S., Li, T., Scimeca, M. S., Sandberg, M. A. and Berson, E. L. (2002) Absence of photoreceptor rescue with D-cis-diltiazem in the rd mouse. *Investigative ophthalmology & visual science,* 43, 1912-1915.

Pennesi, M. E., Michaels, K. V., Magee, S. S. et al. (2012) Long-term characterization of retinal degeneration in rd1 and rd10 mice using spectral domain optical coherence tomography. *Investigative ophthalmology & visual science,* 53, 4644-4656.

Pennesi, M. E., Nishikawa, S., Matthes, M. T., Yasumura, D. and LaVail, M. M. (2008) The relationship of photoreceptor degeneration to retinal vascular development and loss in mutant rhodopsin transgenic and RCS rats. *Experimental eye research,* 87, 561-570.

Perusek, L. and Maeda, T. (2013) Vitamin A derivatives as treatment options for retinal degenerative diseases. *Nutrients,* 5, 2646-2666.

Peterson, W. M., Wang, Q., Tzekova, R. and Wiegand, S. J. (2000) Ciliary neurotrophic factor and stress stimuli activate the Jak-STAT pathway in retinal neurons and glia. *The Journal of neuroscience : the official journal of the Society for Neuroscience,* 20, 4081-4090.

Pezaris, J. S. and Eskandar, E. N. (2009) Getting signals into the brain: visual prosthetics through thalamic microstimulation. *Neurosurgical focus,* 27, E6.

Pfaffl, M. W. (2001) A new mathematical model for relative quantification in real-time RT-PCR. *Nucleic acids research,* 29, e45.

Pfeiffer, A., Spranger, J., Meyer-Schwickerath, R. and Schatz, H. (1997) Growth factor alterations in advanced diabetic retinopathy: a possible role of blood retina barrier breakdown. *Diabetes,* 46 Suppl 2, S26-30.

Pittler, S. J. and Baehr, W. (1991) Identification of a nonsense mutation in the rod photoreceptor cGMP phosphodiesterase beta-subunit gene of the rd mouse. *Proceedings of the National Academy of Sciences of the United States of America,* 88, 8322-8326.

Poitry-Yamate, C. L., Poitry, S. and Tsacopoulos, M. (1995) Lactate released by Muller glial cells is metabolized by photoreceptors from mammalian retina. *The Journal of neuroscience : the official journal of the Society for Neuroscience,* 15, 5179-5191.

Popovic, P., Jarc-Vidmar, M. and Hawlina, M. (2005) Abnormal fundus autofluorescence in relation to retinal function in patients with retinitis pigmentosa. *Graefe's archive for clinical and experimental ophthalmology = Albrecht von Graefes Archiv fur klinische und experimentelle Ophthalmologie,* 243, 1018-1027.

Portera-Cailliau, C., Sung, C. H., Nathans, J. and Adler, R. (1994) Apoptotic photoreceptor cell death in mouse models of retinitis pigmentosa. *Proceedings of the National Academy of Sciences of the United States of America,* 91, 974-978.

Pulukuri, S. M., Gorantla, B., Knost, J. A. and Rao, J. S. (2009) Frequent loss of cystatin E/M expression implicated in the progression of prostate cancer. *Oncogene,* 28, 2829-2838.

Qiao, X., Lu, J. Y. and Hofmann, S. L. (2007) Gene expression profiling in a mouse model of infantile neuronal ceroid lipofuscinosis reveals upregulation of immediate early genes and mediators of the inflammatory response. *BMC neuroscience,* 8, 95.

Qiu, J., Ai, L., Ramachandran, C. et al. (2008) Invasion suppressor cystatin E/M (CST6): high-level cell type-specific expression in normal brain and epigenetic silencing in gliomas. *Laboratory investigation; a journal of technical methods and pathology,* 88, 910-925.

Quan, T., He, T., Shao, Y., Lin, L., Kang, S., Voorhees, J. J. and Fisher, G. J. (2006) Elevated cysteine-rich 61 mediates aberrant collagen homeostasis in chronologically aged and photoaged human skin. *The American journal of pathology,* 169, 482-490.

Rakheja, D., Narayan, S. B. and Bennett, M. J. (2007) Juvenile neuronal ceroid-lipofuscinosis (Batten disease): a brief review and update. *Current molecular medicine,* 7, 603-608.

Ray, A., Sun, G. J., Chan, L., Grzywacz, N. M., Weiland, J. and Lee, E. J. (2010) Morphological alterations in retinal neurons in the S334ter-line3 transgenic rat. *Cell and tissue research,* 339, 481-491.

Rayssac, A., Neveu, C., Pucelle, M., Van den Berghe, L., Prado-Lourenco, L., Arnal, J. F., Chaufour, X. and Prats, A. C. (2009) IRES-based vector coexpressing FGF2 and Cyr61 provides synergistic and safe therapeutics of lower limb ischemia. *Molecular therapy : the journal of the American Society of Gene Therapy,* 17, 2010-2019.

Reichenbach, A. and Bringmann, A. (2013) New functions of Muller cells. *Glia,* 61, 651-678.

Reichenbach, A., Fuchs, U., Kasper, M., el-Hifnawi, E. and Eckstein, A. K. (1995) Hepatic retinopathy: morphological features of retinal glial (Muller) cells accompanying hepatic failure. *Acta neuropathologica,* 90, 273-281.

Reichenbach, A., Stolzenburg, J. U., Eberhardt, W., Chao, T. I., Dettmer, D. and Hertz, L. (1993) What do retinal muller (glial) cells do for their neuronal 'small siblings'? *Journal of chemical neuroanatomy,* 6, 201-213.

Rhee, K. D., Nusinowitz, S., Chao, K., Yu, F., Bok, D. and Yang, X. J. (2013) CNTF-mediated protection of photoreceptors requires initial activation of the cytokine receptor gp130 in Muller glial cells. *Proceedings of the National Academy of Sciences of the United States of America,* 110, E4520-4529.

Richardson, M. R., Segu, Z. M., Price, M. O., Lai, X., Witzmann, F. A., Mechref, Y., Yoder, M. C. and Price, F. W. (2010) Alterations in the aqueous humor proteome in patients with Fuchs endothelial corneal dystrophy. *Molecular vision,* 16, 2376-2383.

Rios-Munoz, W., Soto, I., Duprey-Diaz, M. V., Blagburn, J. and Blanco, R. E. (2005) Fibroblast growth factor 2 applied to the optic nerve after axotomy increases Bcl-2 and decreases Bax in ganglion cells by activating the extracellular signal-regulated kinase signaling pathway. *Journal of neurochemistry,* 93, 1422-1433.

Ritter, M. R., Aguilar, E., Banin, E., Scheppke, L., Uusitalo-Jarvinen, H. and Friedlander, M. (2005) Three-dimensional in vivo imaging of the mouse intraocular vasculature during development and disease. *Investigative ophthalmology & visual science,* 46, 3021-3026.

Roberts, P. J. and Der, C. J. (2007) Targeting the Raf-MEK-ERK mitogen-activated protein kinase cascade for the treatment of cancer. *Oncogene,* 26, 3291-3310.

Robson, A. G., Saihan, Z., Jenkins, S. A., Fitzke, F. W., Bird, A. C., Webster, A. R. and Holder, G. E. (2006) Functional characterisation and serial imaging of abnormal fundus autofluorescence in patients with retinitis pigmentosa and normal visual acuity. *The British journal of ophthalmology,* 90, 472-479.

Roskoski, R., Jr. (2012) ERK1/2 MAP kinases: structure, function, and regulation. *Pharmacological research : the official journal of the Italian Pharmacological Society,* 66, 105-143.

Rothermel, A., Volpert, K., Schlichting, R., Huhn, J., Stotz-Reimers, M., Robitzki, A. A. and Layer, P. G. (2004) Spatial and temporal expression patterns of GDNF family

receptor alpha4 in the developing chicken retina. *Gene expression patterns : GEP,* 4, 59-63.
Saari, J. C., Bredberg, L. and Garwin, G. G. (1982) Identification of the endogenous retinoids associated with three cellular retinoid-binding proteins from bovine retina and retinal pigment epithelium. *The Journal of biological chemistry,* 257, 13329-13333.
Saari, J. C., Huang, J., Possin, D. E., Fariss, R. N., Leonard, J., Garwin, G. G., Crabb, J. W. and Milam, A. H. (1997) Cellular retinaldehyde-binding protein is expressed by oligodendrocytes in optic nerve and brain. *Glia,* 21, 259-268.
Saari, J. C., Nawrot, M., Kennedy, B. N., Garwin, G. G., Hurley, J. B., Huang, J., Possin, D. E. and Crabb, J. W. (2001) Visual cycle impairment in cellular retinaldehyde binding protein (CRALBP) knockout mice results in delayed dark adaptation. *Neuron,* 29, 739-748.
Sabile, A. A., Arlt, M. J., Muff, R. et al. (2012) Cyr61 expression in osteosarcoma indicates poor prognosis and promotes intratibial growth and lung metastasis in mice. *Journal of bone and mineral research : the official journal of the American Society for Bone and Mineral Research,* 27, 58-67.
Saito, T., Abe, T., Wakusawa, R., Sato, H., Asai, H., Tokita-Ishikawa, Y. and Nishida, K. (2009) TrkB-T1 receptors on Muller cells play critical role in brain-derived neurotrophic factor-mediated photoreceptor protection against phototoxicity. *Current eye research,* 34, 580-588.
Sakamoto, T. and Khorana, H. G. (1995) Structure and function in rhodopsin: the fate of opsin formed upon the decay of light-activated metarhodopsin II in vitro. *Proceedings of the National Academy of Sciences of the United States of America,* 92, 249-253.
Sakamoto, Y. R., Nakajima, T. R., Fukiage, C. R., Sakai, O. R., Yoshida, Y. R., Azuma, M. R. and Shearer, T. R. (2000) Involvement of calpain isoforms in ischemia-reperfusion injury in rat retina. *Current eye research,* 21, 571-580.
Samardzija, M., Wariwoda, H., Imsand, C., Huber, P., Heynen, S. R., Gubler, A. and Grimm, C. (2012) Activation of survival pathways in the degenerating retina of rd10 mice. *Experimental eye research,* 99, 17-26.
Sandberg, M. A., Brockhurst, R. J., Gaudio, A. R. and Berson, E. L. (2005) The association between visual acuity and central retinal thickness in retinitis pigmentosa. *Investigative ophthalmology & visual science,* 46, 3349-3354.
Sandberg, M. A., Weigel-DiFranco, C., Dryja, T. P. and Berson, E. L. (1995) Clinical expression correlates with location of rhodopsin mutation in dominant retinitis pigmentosa. *Investigative ophthalmology & visual science,* 36, 1934-1942.
Sanges, D., Comitato, A., Tammaro, R. and Marigo, V. (2006) Apoptosis in retinal degeneration involves cross-talk between apoptosis-inducing factor (AIF) and caspase-12 and is blocked by calpain inhibitors. *Proceedings of the National Academy of Sciences of the United States of America,* 103, 17366-17371.
Sanyal, S. and Bal, A. K. (1973) Comparative light and electron microscopic study of retinal histogenesis in normal and rd mutant mice. *Zeitschrift fur Anatomie und Entwicklungsgeschichte,* 142, 219-238.
Sarbassov, D. D., Guertin, D. A., Ali, S. M. and Sabatini, D. M. (2005) Phosphorylation and regulation of Akt/PKB by the rictor-mTOR complex. *Science,* 307, 1098-1101.
Sariola, H. and Saarma, M. (2003) Novel functions and signalling pathways for GDNF. *Journal of cell science,* 116, 3855-3862.

Savchenko, A., Kraft, T. W., Molokanova, E. and Kramer, R. H. (2001) Growth factors regulate phototransduction in retinal rods by modulating cyclic nucleotide-gated channels through dephosphorylation of a specific tyrosine residue. *Proceedings of the National Academy of Sciences of the United States of America,* 98, 5880-5885.

Schallenberg, M., Charalambous, P. and Thanos, S. (2012) GM-CSF protects rat photoreceptors from death by activating the SRC-dependent signalling and elevating anti-apoptotic factors and neurotrophins. *Graefe's archive for clinical and experimental ophthalmology = Albrecht von Graefes Archiv fur klinische und experimentelle Ophthalmologie,* 250, 699-712.

Seiler, M. J. and Aramant, R. B. (2012) Cell replacement and visual restoration by retinal sheet transplants. *Progress in retinal and eye research,* 31, 661-687.

Seiler, M. J., Thomas, B. B., Chen, Z., Wu, R., Sadda, S. R. and Aramant, R. B. (2008) Retinal transplants restore visual responses: trans-synaptic tracing from visually responsive sites labels transplant neurons. *The European journal of neuroscience,* 28, 208-220.

Seitz, R., Hackl, S., Seibuchner, T., Tamm, E. R. and Ohlmann, A. (2010) Norrin mediates neuroprotective effects on retinal ganglion cells via activation of the Wnt/beta-catenin signaling pathway and the induction of neuroprotective growth factors in Muller cells. *The Journal of neuroscience : the official journal of the Society for Neuroscience,* 30, 5998-6010.

Shadrach, K. G., Rayborn, M. E., Hollyfield, J. G. and Bonilha, V. L. (2013) DJ-1-dependent regulation of oxidative stress in the retinal pigment epithelium (RPE). *PloS one,* 8, e67983.

Sheedlo, H. J., Jaynes, D., Bolan, A. L. and Turner, J. E. (1995) Mullerian glia in dystrophic rodent retinas: an immunocytochemical analysis. *Brain research. Developmental brain research,* 85, 171-180.

Shih, S. C., Ju, M., Liu, N. and Smith, L. E. (2003) Selective stimulation of VEGFR-1 prevents oxygen-induced retinal vascular degeneration in retinopathy of prematurity. *The Journal of clinical investigation,* 112, 50-57.

Shun, C. T., Lin, S. K., Hong, C. Y., Huang, H. M. and Liu, C. M. (2011) Hypoxia induces cysteine-rich 61, vascular endothelial growth factor, and interleukin-8 expressions in human nasal polyp fibroblasts: An implication of neutrophils in the pathogenesis of nasal polyposis. *American journal of rhinology & allergy,* 25, 15-18.

Silverman, M. D., Zamora, D. O., Pan, Y., Texeira, P. V., Baek, S. H., Planck, S. R. and Rosenbaum, J. T. (2003) Constitutive and inflammatory mediator-regulated fractalkine expression in human ocular tissues and cultured cells. *Investigative ophthalmology & visual science,* 44, 1608-1615.

Simpson, D. A., Murphy, G. M., Bhaduri, T., Gardiner, T. A., Archer, D. B. and Stitt, A. W. (1999) Expression of the VEGF gene family during retinal vaso-obliteration and hypoxia. *Biochemical and biophysical research communications,* 262, 333-340.

Slomiany, M. G. and Rosenzweig, S. A. (2004) Autocrine effects of IGF-I-induced VEGF and IGFBP-3 secretion in retinal pigment epithelial cell line ARPE-19. *American journal of physiology. Cell physiology,* 287, C746-753.

Smith, R., Johansen, H. T., Nilsen, H., Haugen, M. H., Pettersen, S. J., Maelandsmo, G. M., Abrahamson, M. and Solberg, R. (2012) Intra- and extracellular regulation of activity and processing of legumain by cystatin E/M. *Biochimie,* 94, 2590-2599.

Steindl-Kuscher, K., Boulton, M. E., Haas, P., Dossenbach-Glaninger, A., Feichtinger, H. and Binder, S. (2011) Epidermal growth factor: the driving force in initiation of

RPE cell proliferation. *Graefe's archive for clinical and experimental ophthalmology = Albrecht von Graefes Archiv fur klinische und experimentelle Ophthalmologie,* 249, 1195-1200.

Stepkowski, S. M., Chen, W., Ross, J. A., Nagy, Z. S. and Kirken, R. A. (2008) STAT3: an important regulator of multiple cytokine functions. *Transplantation,* 85, 1372-1377.

Stevens, E. R., Esguerra, M., Kim, P. M., Newman, E. A., Snyder, S. H., Zahs, K. R. and Miller, R. F. (2003) D-serine and serine racemase are present in the vertebrate retina and contribute to the physiological activation of NMDA receptors. *Proceedings of the National Academy of Sciences of the United States of America,* 100, 6789-6794.

Sung, C. H., Davenport, C. M., Hennessey, J. C. et al. (1991) Rhodopsin mutations in autosomal dominant retinitis pigmentosa. *Proceedings of the National Academy of Sciences of the United States of America,* 88, 6481-6485.

Sung, C. H., Davenport, C. M. and Nathans, J. (1993) Rhodopsin mutations responsible for autosomal dominant retinitis pigmentosa. Clustering of functional classes along the polypeptide chain. *The Journal of biological chemistry,* 268, 26645-26649.

Sureshbabu, A., Okajima, H., Yamanaka, D. et al. (2012) IGFBP5 induces cell adhesion, increases cell survival and inhibits cell migration in MCF-7 human breast cancer cells. *Journal of cell science,* 125, 1693-1705.

Szalai, E., Felszeghy, S., Hegyi, Z., Modis, L., Jr., Berta, A. and Kaarniranta, K. (2012) Fibrillin-2, tenascin-C, matrilin-2, and matrilin-4 are strongly expressed in the epithelium of human granular and lattice type I corneal dystrophies. *Molecular vision,* 18, 1927-1936.

Takano, Y., Ohguro, H., Dezawa, M. et al. (2004) Study of drug effects of calcium channel blockers on retinal degeneration of rd mouse. *Biochemical and biophysical research communications,* 313, 1015-1022.

Takeda, M., Takamiya, A., Yoshida, A. and Kiyama, H. (2002) Extracellular signal-regulated kinase activation predominantly in Muller cells of retina with endotoxin-induced uveitis. *Investigative ophthalmology & visual science,* 43, 907-911.

Tan, T. W., Yang, W. H., Lin, Y. T., Hsu, S. F., Li, T. M., Kao, S. T., Chen, W. C., Fong, Y. C. and Tang, C. H. (2009) Cyr61 increases migration and MMP-13 expression via alphavbeta3 integrin, FAK, ERK and AP-1-dependent pathway in human chondrosarcoma cells. *Carcinogenesis,* 30, 258-268.

Tang, Q. L., Fan, S., Li, H. G., Chen, W. L., Shen, X. M., Yuan, X. P., Chang, S. H. and Song, Y. (2011) Expression of Cyr61 in primary salivary adenoid cystic carcinoma and its relation to Ki-67 and prognosis. *Oral oncology,* 47, 365-370.

Tasheva, E. S., Ke, A., Deng, Y., Jun, C., Takemoto, L. J., Koester, A. and Conrad, G. W. (2004) Differentially expressed genes in the lens of mimecan-null mice. *Molecular vision,* 10, 403-416.

Tatar, O., Shinoda, K., Adam, A., Eckert, T., Eckardt, C., Lucke, K., Deuter, C., Bartz-Schmidt, K. U. and Grisanti, S. (2007) Effect of verteporfin photodynamic therapy on endostatin and angiogenesis in human choroidal neovascular membranes. *The British journal of ophthalmology,* 91, 166-173.

Tatar, O., Shinoda, K., Adam, A., Rohrbach, J. M., Lucke, K., Henke-Fahle, S., Bartz-Schmidt, K. U. and Grisanti, S. (2006) Expression of endostatin in human choroidal neovascular membranes secondary to age-related macular degeneration. *Experimental eye research,* 83, 329-338.

Tatar, O., Shinoda, K., Kaiserling, E. et al. (2008) Early effects of triamcinolone on vascular endothelial growth factor and endostatin in human choroidal neovascularization. *Archives of ophthalmology,* 126, 193-199.

Tawara, A. and Inomata, H. (1987) Histological study on transient ocular hypertension after laser iridotomy in rabbits. *Graefe's archive for clinical and experimental ophthalmology = Albrecht von Graefes Archiv fur klinische und experimentelle Ophthalmologie,* 225, 114-122.

Tawara, A., Varner, H. H. and Hollyfield, J. G. (1989) Proteoglycans in the mouse interphotoreceptor matrix. II. Origin and development of proteoglycans. *Experimental eye research,* 48, 815-839.

Thanos, C. and Emerich, D. (2005) Delivery of neurotrophic factors and therapeutic proteins for retinal diseases. *Expert opinion on biological therapy,* 5, 1443-1452.

Todorovic, V., Chen, C. C., Hay, N. and Lau, L. F. (2005) The matrix protein CCN1 (CYR61) induces apoptosis in fibroblasts. *The Journal of cell biology,* 171, 559-568.

Touchard, E., Heiduschka, P., Berdugo, M., Kowalczuk, L., Bigey, P., Chahory, S., Gandolphe, C., Jeanny, J. C. and Behar-Cohen, F. (2012) Non-viral gene therapy for GDNF production in RCS rat: the crucial role of the plasmid dose. *Gene therapy,* 19, 886-898.

Tout, S., Chan-Ling, T., Hollander, H. and Stone, J. (1993) The role of Muller cells in the formation of the blood-retinal barrier. *Neuroscience,* 55, 291-301.

Tsacopoulos, M. and Magistretti, P. J. (1996) Metabolic coupling between glia and neurons. *The Journal of neuroscience : the official journal of the Society for Neuroscience,* 16, 877-885.

Tsao, Y. P., Ho, T. C., Chen, S. L. and Cheng, H. C. (2006) Pigment epithelium-derived factor inhibits oxidative stress-induced cell death by activation of extracellular signal-regulated kinases in cultured retinal pigment epithelial cells. *Life sciences,* 79, 545-550.

Van Hooser, J. P., Aleman, T. S., He, Y. G., Cideciyan, A. V., Kuksa, V., Pittler, S. J., Stone, E. M., Jacobson, S. G. and Palczewski, K. (2000) Rapid restoration of visual pigment and function with oral retinoid in a mouse model of childhood blindness. *Proceedings of the National Academy of Sciences of the United States of America,* 97, 8623-8628.

van Soest, S., Westerveld, A., de Jong, P. T., Bleeker-Wagemakers, E. M. and Bergen, A. A. (1999) Retinitis pigmentosa: defined from a molecular point of view. *Survey of ophthalmology,* 43, 321-334.

Veena, M. S., Lee, G., Keppler, D., Mendonca, M. S., Redpath, J. L., Stanbridge, E. J., Wilczynski, S. P. and Srivatsan, E. S. (2008) Inactivation of the cystatin E/M tumor suppressor gene in cervical cancer. *Genes, chromosomes & cancer,* 47, 740-754.

Vlachantoni, D., Bramall, A. N., Murphy, M. P. et al. (2011) Evidence of severe mitochondrial oxidative stress and a protective effect of low oxygen in mouse models of inherited photoreceptor degeneration. *Human molecular genetics,* 20, 322-335.

Wagener, R., Kobbe, B. and Paulsson, M. (1998) Matrilin-4, a new member of the matrilin family of extracellular matrix proteins. *FEBS letters,* 436, 123-127.

Wen, R., Song, Y., Kjellstrom, S. et al. (2006) Regulation of rod phototransduction machinery by ciliary neurotrophic factor. *The Journal of neuroscience : the official journal of the Society for Neuroscience,* 26, 13523-13530.

Wen, R., Song, Y., Liu, Y., Li, Y., Zhao, L. and Laties, A. M. (2008) CNTF negatively regulates the phototransduction machinery in rod photoreceptors: implication for light-induced photostasis plasticity. *Advances in experimental medicine and biology,* 613, 407-413.

Wen, R., Tao, W., Li, Y. and Sieving, P. A. (2012) CNTF and retina. *Progress in retinal and eye research,* 31, 136-151.

Willbold, E., Berger, J., Reinicke, M. and Wolburg, H. (1997) On the role of Muller glia cells in histogenesis: only retinal spheroids, but not tectal, telencephalic and cerebellar spheroids develop histotypical patterns. *Journal fur Hirnforschung,* 38, 383-396.

Wright, A. F., Chakarova, C. F., Abd El-Aziz, M. M. and Bhattacharya, S. S. (2010) Photoreceptor degeneration: genetic and mechanistic dissection of a complex trait. *Nature reviews. Genetics,* 11, 273-284.

Xia, X., Li, Y., Huang, D., Wang, Z., Luo, L., Song, Y., Zhao, L. and Wen, R. (2011) Oncostatin M protects rod and cone photoreceptors and promotes regeneration of cone outer segment in a rat model of retinal degeneration. *PloS one,* 6, e18282.

Xu, H., Yang, J. N., Li, X. K., Zheng, Q., Zhao, W., Su, Z. J. and Huang, Y. D. (2008) Retina protective effect of acidic fibroblast growth factor after canceling its mitogenic activity. *Journal of ocular pharmacology and therapeutics : the official journal of the Association for Ocular Pharmacology and Therapeutics,* 24, 445-451.

Yang, G. P. and Lau, L. F. (1991) Cyr61, product of a growth factor-inducible immediate early gene, is associated with the extracellular matrix and the cell surface. *Cell growth & differentiation : the molecular biology journal of the American Association for Cancer Research,* 2, 351-357.

Yang, J. and Guan, Y. (2013) Family with sequence similarity 3 gene family and nonalcoholic fatty liver disease. *Journal of gastroenterology and hepatology,* 28 Suppl 1, 105-111.

Yang, L. P., Wu, L. M., Guo, X. J. and Tso, M. O. (2007) Activation of endoplasmic reticulum stress in degenerating photoreceptors of the rd1 mouse. *Investigative ophthalmology & visual science,* 48, 5191-5198.

Yang, Y., Mohand-Said, S., Danan, A., Simonutti, M., Fontaine, V., Clerin, E., Picaud, S., Leveillard, T. and Sahel, J. A. (2009) Functional cone rescue by RdCVF protein in a dominant model of retinitis pigmentosa. *Molecular therapy : the journal of the American Society of Gene Therapy,* 17, 787-795.

Yao, Y. G., Yang, H. S., Cao, Z., Danielsson, J. and Duh, E. J. (2005) Upregulation of placental growth factor by vascular endothelial growth factor via a post-transcriptional mechanism. *FEBS letters,* 579, 1227-1234.

Yoshida, Y., Togi, K., Matsumae, H. et al. (2007) CCN1 protects cardiac myocytes from oxidative stress via beta1 integrin-Akt pathway. *Biochemical and biophysical research communications,* 355, 611-618.

You, J. J., Yang, C. H., Chen, M. S. and Yang, C. M. (2009) Cysteine-rich 61, a member of the CCN family, as a factor involved in the pathogenesis of proliferative diabetic retinopathy. *Investigative ophthalmology & visual science,* 50, 3447-3455.

You, J. J., Yang, C. M., Chen, M. S. and Yang, C. H. (2010) Regulation of Cyr61/CCN1 expression by hypoxia through cooperation of c-Jun/AP-1 and HIF-1alpha in retinal vascular endothelial cells. *Experimental eye research,* 91, 825-836.

You, J. J., Yang, C. M., Chen, M. S. and Yang, C. H. (2012) Elevation of angiogenic factor Cysteine-rich 61 levels in vitreous of patients with proliferative diabetic retinopathy. *Retina,* 32, 103-111.

Yu, T., Scully, S., Yu, Y., Fox, G. M., Jing, S. and Zhou, R. (1998) Expression of GDNF family receptor components during development: implications in the mechanisms of interaction. *The Journal of neuroscience : the official journal of the Society for Neuroscience,* 18, 4684-4696.

Yu, Y., Gao, Y., Wang, H. et al. (2008) The matrix protein CCN1 (CYR61) promotes proliferation, migration and tube formation of endothelial progenitor cells. *Experimental cell research,* 314, 3198-3208.

Yuan, X., Hua, X. and Wilhelmus, K. R. (2010) Expression of small leucine-rich proteoglycans during experimental fungal keratitis. *Cornea,* 29, 674-679.

Yun, S. P., Lee, S. J., Jung, Y. H. and Han, H. J. (2014) Galectin-1 stimulates motility of human umbilical cord blood-derived mesenchymal stem cells by downregulation of smad2/3-dependent collagen 3/5 and upregulation of NF-kappaB-dependent fibronectin/laminin 5 expression. *Cell death & disease,* 5, e1049.

Zeiss, C. J. and Johnson, E. A. (2004) Proliferation of microglia, but not photoreceptors, in the outer nuclear layer of the rd-1 mouse. *Investigative ophthalmology & visual science,* 45, 971-976.

Zeiss, C. J., Neal, J. and Johnson, E. A. (2004) Caspase-3 in postnatal retinal development and degeneration. *Investigative ophthalmology & visual science,* 45, 964-970.

Zeng, H. Y., Zhu, X. A., Zhang, C., Yang, L. P., Wu, L. M. and Tso, M. O. (2005) Identification of sequential events and factors associated with microglial activation, migration, and cytotoxicity in retinal degeneration in rd mice. *Investigative ophthalmology & visual science,* 46, 2992-2999.

Zhang, M., Mo, X., Fang, Y., Guo, W., Wu, J., Zhang, S. and Huang, Q. (2009) Rescue of photoreceptors by BDNF gene transfer using in vivo electroporation in the RCS rat of retinitis pigmentosa. *Current eye research,* 34, 791-799.

Zhang, M., Xu, G., Liu, W., Ni, Y. and Zhou, W. (2012a) Role of fractalkine/CX3CR1 interaction in light-induced photoreceptor degeneration through regulating retinal microglial activation and migration. *PloS one,* 7, e35446.

Zhang, N. L., Samadani, E. E. and Frank, R. N. (1993) Mitogenesis and retinal pigment epithelial cell antigen expression in the rat after krypton laser photocoagulation. *Investigative ophthalmology & visual science,* 34, 2412-2424.

Zhang, Q., Guy, K., Pagadala, J. et al. (2012b) Compound 49b prevents diabetes-induced apoptosis through increased IGFBP-3 levels. *Investigative ophthalmology & visual science,* 53, 3004-3013.

Zhang, Q., Soderland, C. and Steinle, J. J. (2013) Regulation of retinal endothelial cell apoptosis through activation of the IGFBP-3 receptor. *Apoptosis : an international journal on programmed cell death,* 18, 361-368.

Zhang, R., Hrushesky, W. J., Wood, P. A., Lee, S. H., Hunt, R. C. and Jahng, W. J. (2010) Melatonin reprogrammes proteomic profile in light-exposed retina in vivo. *International journal of biological macromolecules,* 47, 255-260.

Zhang, X., Ding, L., Diao, Z., Yan, G., Sun, H. and Hu, Y. (2012c) CYR61 modulates the vascular endothelial growth factor C expression of decidual NK cells via PI3K/AKT pathway. *American journal of reproductive immunology,* 67, 216-223.

Zhao, B., Cai, J. and Boulton, M. (2004) Expression of placenta growth factor is regulated by both VEGF and hyperglycaemia via VEGFR-2. *Microvascular research,* 68, 239-246.

Zhao, L., Ma, W., Fariss, R. N. and Wong, W. T. (2009) Retinal vascular repair and neovascularization are not dependent on CX3CR1 signaling in a model of ischemic retinopathy. *Experimental eye research,* 88, 1004-1013.

Zhou, D., Herrick, D. J., Rosenbloom, J. and Chaqour, B. (2005) Cyr61 mediates the expression of VEGF, alphav-integrin, and alpha-actin genes through cytoskeletally based mechanotransduction mechanisms in bladder smooth muscle cells. *Journal of applied physiology,* 98, 2344-2354.

Zhu, C. L., Ji, Y., Lee, E. J. and Grzywacz, N. M. (2013) Spatiotemporal pattern of rod degeneration in the S334ter-line-3 rat model of retinitis pigmentosa. *Cell and tissue research,* 351, 29-40.

Zhu, X., Sun, Y., Wang, Z., Cui, W., Peng, Y. and Li, R. (2012) Expression of glial cell line-derived neurotrophic factor and its receptors in cultured retinal Muller cells under high glucose circumstance. *Anatomical record,* 295, 532-539.

Zhu, Y., Xu, G., Patel, A. et al. (2002) Cloning, expression, and initial characterization of a novel cytokine-like gene family. *Genomics,* 80, 144-150.

Zou, Y., Zhang, H., Li, H., Chen, H., Song, W. and Wang, Y. (2012) Strain-dependent production of interleukin-17/interferon-gamma and matrix remodeling-associated genes in experimental Candida albicans keratitis. *Molecular vision,* 18, 1215-1225.

Zrenner, E., Bartz-Schmidt, K. U., Benav, H. et al. (2011) Subretinal electronic chips allow blind patients to read letters and combine them to words. *Proceedings. Biological sciences / The Royal Society,* 278, 1489-1497.

Zwickl, H., Traxler, E., Staettner, S., Parzefall, W., Grasl-Kraupp, B., Karner, J., Schulte-Hermann, R. and Gerner, C. (2005) A novel technique to specifically analyze the secretome of cells and tissues. *Electrophoresis,* 26, 2779-2785.

VI. ANNEXES

1. Index of figures

2. Index of tables

3. Publications and presentations

3.1 Peer Reviewed Publications

- Kucharska, J., del Rio, P., Arango-Gonzales, B., Gorza, M., Feuchtinger, A., Hauck, S.M. and Ueffing, M. (2014) Cyr61 activates retinal cells and prolongs photoreceptor survival in rd1 mouse model of retinitis pigmentosa. *Journal of Neurochemistry,* Accepted Article, doi: 10.1111/jnc.12704
- Sielska, M., Przanowski, P., Wylot, B., Gabrusiewicz, K., Maleszewska, M., Kijewska, M., Zawadzka, M., Kucharska, J., Vinnakota, K., Kettenmann, H., Kotulska, K., Grajkowska, W., Kaminska, B. (2013) Distinct roles of CSF family cytokines in macrophage infiltration and activation in glioma progression and injury response. *The Journal of Pathology,* 230, 310-321.
- Sobierajska, K., Glos, J., Daborowska, J., Kucharska, J., Bregier, C., Fabczak, S. and Fabczak, H. (2010) Visualization of the interaction between Gbetagamma and tubulin during light-induced cell elongation of Blepharisma japonicum. *Photochemical & photobiological sciences: Official journal of the European Photochemistry Association and the European Society for Photobiology*, 9, 1101-1110.
- Tyburczy, M. E., Kotulska, K., Pokarowski, P., Mieczkowski, J., Kucharska, J., Grajkowska, W., Roszkowski, M., Jozwiak, S. and Kaminska, B. (2010) Novel proteins regulated by mTOR in subependymal giant cell astrocytomas of patients with tuberous sclerosis complex and new therapeutic implications. *The American Journal of Pathology,* 176, 1878-1890.

3.2 Oral presentations

- EduGlia Final Meeting, Lepizig, Germany: Cyr61 activates retinal cells and prolongs photoreceptor survival in retinitis pigmentosa mouse model, July 2013.
- Young Researcher Vision Camp 2013, Castle Wildenstein, Germany: Cyr61 activates retinal cells and prolongs photoreceptor survival in retinitis pigmentosa mouse model, June 2013.
- 3rd Edu-GLIA Annual Meeting, Margaux, France: Cyr61 promotes photoreceptor survival in porcine and rd1 mouse animal experimental models, August 2012.
- 2nd EduGlia Annual Meeting, Särö, Sweden: Müller glial cells: Novel neuroprotective signalling in the retina, June 2011.

3.3 Poster presentations

- XI European Meeting on Glial Cells in Health and Disease Berlin, Germany: Kucharska J, del Rio P, Arango-Gonzales B, Gorza M, Feuchtinger A, Hauck SM and Ueffing M. GDNF induces secretion of Cyr61 from retinal Müller glial cells - a novel neuroprotective factor in retinal degeneration, July 2013.
- RNA Quality EMBO Workshop, Vienna, Austria: M. Dziembowska, A. Janusz, J. Milek, J. Kucharska, L. Kaczmarek MMP-9 mRNA is transported to the dendrites in neuronal RNP granules, May 2010.
- 2nd Congress of Contemporary Oncology of the series Cancer – the challenge of the 21st century, Personalized Oncology; Poznan, Poland: M. Sielska, K. Gabrusiewicz, J. Kucharska, M. Zawadzka, E. Kwiatkowska, D. Kowalczyk, A.

Ellert-Miklaszewska, B. Kaminska [Acumulation of resident and peripheral macrophages in glioma and their role in glioblastoma development.], April 2010.

- Tumour Microenvironment: Progression, Therapy and Prevention; Versailles, France: M. Sielska, K. Gabrusiewicz, E. Kwiatkowska, D. Kowalczyk, A. Ellert-Miklaszewska, J. Kucharska, B. Kaminska Bone marrow-derived macrophages and microglia cells in glioma pathogenesis, October 2009.
- V National Conference Junior Research Workers of Gastrointestinal Tract Physiology; Lublin, Poland: K. Bialkowska, M. Grabowska, J. Kucharska, A. Kotunia, A. Jankowska, J. Wolinski, Z. Gajewska, G. Kulasek, R. Zabielski (2007) [Influence of bioactive substances on intestine brush border enzymatic activities in neonatal piglets.], May 2007.

4. Acknowledgements

Time flies by very fast and it feels like just yesterday that I packed my suitcase and left my home in Warsaw to start a new chapter of my life in Munich. During the time of my work in Germany I had great luck to meet many wonderful people. Here I would like to extend special thanks:

To Prof. Dr. Marius Ueffing for giving me the opportunity to work on my PhD at his laboratory on a topic so close to clinical applications. I am very grateful for his support and involvement to help me develop on the professional level.

To Prof. Dr. Robert Feil thanks to whose kindness and help I could present my thesis at the Mathematisch-Naturwissenschaftliche Fakultät.

To Dr. Stefanie Hauck, Dr. Blanca Arango-Gonzales and Dr. Patricia del Rio for their trust and sharing their data for the Cyr61 validation with me, which became one of the foundations of the presented doctoral thesis. I am also thankful for their support during my work and revisions of the Cyr61 article.

To Dr. Phillip Holroyd, Dr. Yilmaz Niyaz, Dr. Wolf Malkusch, Dr. Eva Simbürger, and all colleagues at Zeiss GmbH in Munich for their professional support with technical issues and the very friendly working atmosphere. Especially, I would like to thank to Dr. Horst Wolf, who always had time to discuss trouble points of my project as well as my professional development with me. I want also to thank him for the unrestrained access to the best microscopic equipment, which resulted in beautiful retinal pictures, sample of which can be seen in this thesis.

To all members of the Marie Curie Research Training Network "EduGlia": The organizers for the possibility to participate in international meetings and the unique opportunity to learn directly from the best scientists during seminars and informal discussions. I send my special thanks to the participants for the time we spent together in great atmosphere and with a lot of support.

To my colleagues from the Research Unit Protein Science for the great atmosphere and sharing their professional knowledge with me. Especially I thank Dr. Matteo Gorza for the stimulating scientific discussions and willingly shared laboratory experience; Jenifer Behler and Nicole Senninger for their help during experiments and friendship; Dr. Alice Ly, Dr. Juliane Merl and Dr. Markus Priller, each of them always took time to answer my questions.

To Dr. Anette Feuchtinger for her great help with the revisions of the Cyr61 article and data analysis of Cyr61 *in vivo* examination.

I would like to thank all my friends from Poland and Germany, particularly: Sophia Bardehle, Jasmin Hirche, Ania Ćmoch, Kasia Beme, Kasia Jedynak-Chołuj, Magdalena Tyburczy and Małgorzata Kozłowska, who always had time and good advices for me during these three years of very intense work.

I would like to give my special thanks to my wonderful and supportive boyfriend, Alexander Schäfer, especially for scratching photoreceptors with me, but also for having time for discussions over my results and revising this thesis.

At the end I would like to thank the people from whom it all started - my Parents, the best I could have, and my brother, for all the love and support they have given me throughout my life.